DESIGN, SIMULATION, CONSTRUCTION AND PERFORMANCE EVALUATION OF A SOLAR OVEN

BY

MUHAMMED BABA ABDULLAHI

DEPARTMENT OF MECHANICAL ENGINEERING
FACULTY OF ENGINEERING
AHMADU BELLO UNIVERSITY, ZARIA
NIGERIA

JULY 2015

DESIGN, SIMULATION, CONSTRUCTION AND PERFORMANCE EVALUATION OF A SOLAR OVEN

BY

Muhammed Baba ABDULLAHI, B. Eng(MechEngrr) 2009

M.Sc/ENG/2217/2010-2011

A THESIS SUBMITTED TO THE SCHOOL OF POSTGRADUATE STUDIES, AHMADU BELLO UNIVERSITY, ZARIA

IN PARTIAL FULFILLMENT OF THE REQUIREMENTS FOR THE AWARD OF A MASTER OF SCIENCE DEGREE IN MECHANICAL ENGINEERING

DEPARTMENT OF MECHANICAL ENGINEERING
FACULTY OF ENGINEERING
AHMADU BELLO UNIVERSITY, ZARIA
NIGERIA

JULY, 2015

DECLARATION

I declare that the work in this thesis entitled '**Design, simulation, construction and performance evaluation of a solar oven**' has been carried out by me in the **Department of Mechanical Engineering** under the supervision of Dr G.Y Pam, and Dr F.O Anafi. The information derived from the literature has been duly acknowledged in the text and a list of references provided. No part of this dissertation was previously presented for another degree or diploma in this or any other institution.

MUHAMMED BABA ABDULLAHI ……. ……....

Signature Date

CERTIFICATION

This thesis entitled 'DESIGN, SIMULATION, CONSTRUCTION AND PERFORMANCE EVALUATION OF A SOLAR OVEN'by MUHAMMED BABA ABDULLAHImeets the regulations governing the award of the degree of **Master of Science** in **Mechanical Engineering** of **Ahmadu Bello University,** and is approved for its contribution to knowledge and literary presentation.

Dr. G.Y Pam _____ _____ _____
(Chairman, Supervisory Committee) Signature Date

Dr. F.O. Anafi _____ _____
(Member, Supervisory Committee) Signature Date

Dr. M.Dauda _____ _____
(Head of Department) Signature Date

Prof. A. Z. Hassan_____ _____
(Dean, School of Postgraduate Studies) Signature Date

ACKNOWLEDGEMENTS

I would like to thank my major supervisor Dr.G.Y. Pam for his support, guidance, endurance and providing many of the ideas related to this research.

My appreciation also goes to my minor supervisor Dr. F.O Anafi and the entire staff of Department of Mechanical Engineering.

Thanks Dad and Mom for your support and encouragement in all my work, also to my brothers and sisters for their various contributions. To my friends and colleagues:Zwalnan Johnson, Yusuf Bello, Ahmed Ibrahim, Peter,Aminu Musa, Sa'ad Musa, Abubakar, Rabiu Musa and many others, thanks for yoursupport throughout the course of this work. Special thanks go to Sayyid Bashir Sheik Tahir Usman for his prayers and words of encouragement.

To my wife and children in appreciation for the patience, understanding and love you have all given me. May Almighty Allah reward you all.

Abstract

A solar ovenis a device that converts solar energy into useful heat in a confined space (oven chamber) which can be utilised for cooking and baking purposes.The oven consists of plane reflectors to concentrate the solar radiation on the collector.The heat gain is maximum if the collector and reflectors are continuously adjusted such that the incidence angle of the reflected and direct radiations are minimised. In practise, it is always difficult to manually track the movement of the sun and the use of trackers can be very expensive. As such, an analytical model was developed to evaluate the optimum monthly collector and reflector tilts for maximum output hen employing the single axis tracking mode. The operation of the different components of the oven was modelled using TRNSYS, Microsoft Excel and EES programs alongside solar data for Zaria. Optimisation of the design was carried out based onweather conditions prevalent on the average day of the design month i.e. the month with the least solar radiation. The tilt angles of collector and reflectors required for the optimum collection of solar irradiation for each month were obtained from the simulation results of the oven model carried out for 12 months of the year. The optimum collector area and insulation thickness were also obtained through parametric studies by varying the aforementioned parameters until a stagnation temperature of 100□C was obtained for the average day of the design month. The simulation results for the design with different collector areas and insulation thickness show that an area of 0.49m^2 and thickness of 0.12m yields a stagnation temperature of 100□C. However, the stagnation temperature achieved was insensitive to larger values of the design parameters.

Table of Contents

LIST OF FIGURES

LIST OF TABLES

LIST OF APPENDICES

NOMENCLATURE

A_a Aperure area of cavity collector (m^2)

A_i Inner surface area of cavity area (m^2)

A_{sb} Area of side and bottom of oven chamber (m^2)

A_c Collector area (m^2)

A_{pt} Base area of pot (m^2)

A_{spt} Area of sides of pot (m^2)

A_{w-pt} Area of pot in contact with water (m^2)

a Length of collector (m)

C_w Specific heat capacity of water (kJ/kgk)

d Depth of collector (m)

f_{rc1} Exchange factor of collector and reflector R1

f_{rc2} Exchange factor of collector and reflector R2

h_1 Convection heat transfer coefficient of air to glass cover

h_2 Convection heat transfer coefficient of air to base of collector

h_3 Convection heat transfer coefficient of air to sides of collector

h_r Radiation heat transfer coefficient

h_{pt} Convection heat transfer coefficient of air to pot

h_t Convection heat transfer coefficient of air to tray

h_w Wind Convection coefficient

h_{rca} Radiation heat transfer coefficient from glass cover to air

I_b Beam radiation on a horizontal surface (W/m^2)

I_{bc} Beam component of solar radiation on collector (W/m^2)

I_{br1} Beam radiation reflected from R1 (W/m^2)

I_{br2} Beam radiation reflected from R2 (W/m^2)

I_{dc} Diffuse component of solar radiation on collector (W/m^2)

I_d Diffuse radiation on a horizontal surface (W/m^2)

I_r Reflected radiation (W/m^2)

I_T Global radiation (W/m^2)

I_τ Transmitted radiation (W/m^2)

I_{bT} Beam radiation on tilted surface (W/m^2)

I_{dT} Diffuse radiation on tilted surface (W/m^2)

K_a Thermal conductivity of air (kJ/h m ^{o}C)

K_{pt} Thermal conductivity of pot (kJ/h m ^{o}C)

M Mass of water (kg)

Nu_1 Nusselt number of air on horizontal sides

Nu_2 Nusselt number of air on vertical sides

P_c Cooking power (Watt)

P_s Standardised cooking power (Watt)

Q_a Absorbed energy (W/m^2)

q_u Useful energy gain (J/m^2)

R_b Geometrical ratio

Ra_1 Rayleigh number of air on horizontal sides

Ra_2 Rayleigh number of air on vertical sides

S_c Shading factor of reflectors R1 and R2 on collector

S_{rc1} Shading factor of reflectors R1 on collector

S_{rc2} Shading factor of reflectors R2 on collector

T_1 Initial temperature of water (C)

T_2 Final temperature of water (C)

T_a Ambient temperature (C)

T_c Temperature of glass cover (C)

T_d Temperature difference (C)

T_{io} Temperature of air in the oven (C)

T_p Temperature of pot (C)

T_w Temperature of water (C)

t_{pt} Thickness of pot (m)

U_{sb} Side and bottom loss coefficient (kJ/m^{2}hr.k)

U_t Top loss coefficient (kJ/m^{2}hr.k)

V_w Wind speed (m/s)

Greek Symbols

θ_i Angle of incidence of beam radiation

θ_z Zenith angle of the sun

θ_{r1} Angle of incidence of beam radiation on reflector R1

θ_{r2} Angle of incidence of beam radiation on reflector R2

θ_{rc1} Incidence angle of solar radiation reflected from reflector R1

θ_{rc2} Incidence angle of solar radiation reflected from reflector R2

β Angle of inclination

β_c Tilt angle of collector

β_{r1} Tilt angle of reflector R1

β_{r2} Tilt angle of reflector R2

γ Solar azimuth angle

γ_s Surface azimuth angle

δ Angle of declination of the sun

φ Angle of latitude

ω Hour angle

ρ Reflectivity

ε_c Emittance of glass cover

τ Transmisivity of glass cover

τ_d Transmitance of glazing for diffuse radiation

α_i Absorptance for diffuse radiation

α_{eff} Effective absorptance

$(\tau\alpha)_{bc}$ Transmittance – absorptance product of beam radiation

$(\tau\alpha)_{dc}$ Transmittance – absorptance product of diffuse radiation

$(\tau\alpha)_{rc1}$ Transmittance – absorptance product of radiation reflected from R1

$(\tau\alpha)_{rc2}$ Transmittance – absorptance product of radiation reflected from R2

CHAPTER ONE

INTRODUCTION

1.1 Background

Energy is the focal point of all human activities; it is the basis of industrial civilization. Without energy, modern life would cease to exist. In the past, the demand for energy sources was minimal because it was primarily used for cooking and local production. But as time went on, population increase and technological advancement led to more demand for energy. The major sources of energy are the conventional sources, which include: fossil fuels, and nuclear fuels. Fossil fuels, which include petroleum, coal, and natural gas, provide most of the energy need of modern industrial society. Other uses are found in the transportation, residential heating, and electric-power generation. Nuclear fuels are used to generate electricity, but it is utilised mainly in the developed countries due to high level of supervision and maintenance required. The non-conventional (renewable) sources of energy include: hydroelectric power, solar energy, wind energy, biomass, ocean thermal energy, tidal energy, and geothermal energy, but the potential of these sources is still underutilised because they are much more expensive to harness than energy derived from fossil fuels. Hydroelectric power requires a large capital investment, so it is often uneconomical for a region where coal or oil is cheap. As such, they contribute a little percentage to the massive energy requirement of the world population. However, the fear of depletion of fossil fuels due to the fast rate of consumption has provoked further development of these alternative energy sources, such as solar energy.

Household energy need is one of the biggest issues in the daily lives of people around the world. The most important energy-consuming activities in most households are cooking, lighting

and use of electrical appliances. Cooking accounts for a staggering 91 percent of household energy consumption, lighting uses up to 6 percent and the remaining 3 percent can be attributed to the use of basic electrical appliances such as televisions and pressing irons (Temilade, 2008). Cooking is an activity that must be carried out almost on a daily basis for the sustenance of life. An enormous amount of energy is thus expended regularly on cooking. Cooking may be classified in four major categories based on the required range of temperature, viz. baking (85-90°C), boiling (100 to 130°C), frying (200 to 250°C) and roasting (more than 300°C).

The primary household energy carriers are fuel wood, kerosene, electricity and liquefied petroleum gas (LPG). In Nigeria, Fuelwood is the most widely used, supplying over 80 percent of household energy, while less than 20 percent is supplied by the other sources and complemented by small quantities of coal and charcoal (Temilade, 2008). Fuelwood is often collected from the local environment in rural areas or purchased through markets in urban areas. Renewable energy alternatives include biogas, which is used for household heating, cooking and lighting, as well as agricultural and industrial activities.

Solar radiation presents an alternative energy source for a variety of applications. Solar radiation has been identified as the largest renewable resource on earth. The maximum intensity of solar radiation at the earth's surface is about 1.2kW/m^2, but it is encountered only near the equator on clear days at noon. Under these ideal conditions, the total energy received is from 6 - 8 kWh/m^2 per day (Abdulrahim*et al*., 2011). Its intensity varies according to season, geographical location, and orientation of the collector. Solar energy is not available continuously because of the day/night cycle and cloud cover.

Solar cooking offers an effective method of utilising solar energy for meeting a considerable demand for cooking energy and hence, protecting the environment. Fortunately,

Nigeria is among the twenty one countries with the highest potential for solar cooking (www.solarcooking.wikia.com). Nigeria lies within a high sunshine belt and thus, has an enormous solar energy potential. The mean annual average of total solar radiation varies from about 3.5 $kWhm^{-2}day^{-1}$ in the coastal latitudes to about 7 $kWhm^{-2}day^{-1}$ along the semi arid areas in the far North(Sambo, 2009). The country receives an average solar radiation at the level of about 19.8 MJm^{-2} day^{-1}. Average sunshine hours are estimated at 6hrs per day. Solar radiation is fairly well distributed. The minimum average is about 3.55 $kWhm^{-2}day^{-1}$ in Katsina in January and 3.4 $kWhm^{-2}day^{-1}$ for Calabar in August and the maximum average is 8.0 $kWhm^{-2}day^{-1}$ for Nguru in May (Sambo, 2009).

1.2 Statement of the Problem

Cooking is a major necessity for people all over the world. The problem arises when cooking fuel is either scarce or highly expensive. Around the globe, hundreds of millions of people have limited access to cooking fuels (www.solarcookers.org). In situations where electricity and gas are not affordable, charcoal and fuel wood are the major substitutes and even charcoal can be very expensive. So fuel wood is the cheapest alternative left. Families either have to walk for hours to collect cooking wood, or spend the little money they have on fuel, leaving less money to buy food.

The problems related to the use of biomass as an energy source have been an issue of concern for more than three decades. The traditional stoves commonly used for burning biomass have long been found to be highly inefficient and to emit copious quantities of smoke due to the incomplete combustion of fuels. This inefficiency has also consequences on the environment, since intense collection of fuel wood has resulted into deforestation in highly populated areas. The

use of such fuels has also adversely affected health. Fires release gasses into the air. This smoke, filled with particulates, is bad for the environment, but it is even worse for the people who are breathing that air. When people use open fires to cook indoors, they end up inhaling micro particles that can cause all sorts of health problems, including both lung and heart disease. Every year, the smoke from open fires and traditional stoves kills 1.5 million people (www.solarcookers.org).

Production and consumption of almost any type of energy have environmental impacts. Harvesting of fuel wood, in particular, contributes to deforestation, soil erosion, and desertification. In Nigeria, harvesting of fuel wood contributes to deforestation at a rate of about 400,000 hectares per year. If this trend continues the country's forest resources could be completely depleted by 2020 (Oleg and Ralph, 1999).

For the rural and urban poor, connection to the electricity supply is often prohibitively expensive or unavailable, even though the price of electricity itself may be low enough to encourage a switch from other fuels. As at the year 2003, less than 45% of the Nigerian population had access to electric power (Suleiman, 2011).

1.3 The Present Work

The present work focuses on designing, simulating and constructing a solar oven that can augment conventional ovens in rural areas. The oven consists of plane reflectors to concentrate the solar radiation on the collector. The oven box is rotated about the vertical axis in order to track the movement of the sun (east to west). Oven inclination is also adjusted monthly to ensure optimum collection of solar radiation. Much emphasis was laid on the materials with suitable properties needed to give high temperatures required for most cooking operations as well as

rigidity needed to keep the assembly in place in case of wind. Numerical simulation of the design model was carried out using transient system simulation programme (TRNSYS), Engineering equation solver (EES) and Microsoft excel to obtain optimum design parameters which would yield acceptable performance. The solar oven was then fabricated and finally subjected to experimental tests to validate the results obtained from the simulation.

1.4 Aim and Objectives

The aim of the present work is to design, simulate, construct and test an optimized solar box oven equipped with two plane reflectors that would be technically efficient, user friendly and cost effective in Zaria, Nigeria.

The specific objectives of the work are:

i. Select appropriate materials (bearing in mind cost, availability and durability) for the various parts of the solar oven.

ii. To study the influence of the following parameters on the solar oven's performance:

- Collector slope
- Angular orientation of the reflectors
- Area of collector
- Insulator thickness

iii. Simulate its performance and validate it with experimental results from a test.

iv. Estimate the cost of a prototype of the system.

1.5 Justification of the Work

i. The energy supply mix in Nigeria is presently dominated by oil and gas. In spite of a considerable solar resource in the country, it is still underdeveloped (Etiosa*et al*., 2008). Solarenergy contributes very little to Nigeria's energy mix as it is currently at the early stage of development. Energy/electricity insufficiency in Nigeria can be alleviated through exploitation of the enormous renewable resources available to the country.

ii. It is normally estimated that areas of the world lying between latitudes 35°N and 35°S of the equator and which have at least 2000 hours of bright sunshine per year are ideal for the utilisation of the sun's energy. Nigeria, located between latitudes 4°N and 14°N of the equator is very much within this area (Abdulrahim*et al*., 2011). A modest estimate of the solar energy potential in Nigeria with 5% device efficiency is put at 15×10^{14} kJ of useful energy annually. This translates to about 258.62 million barrels of oil equivalent or 4×10^{5}GWh of electricity production annually (Sambo, 2009).

iii. With the high cost of cooking fuels in Nigeria and the epileptic supply of electricity, majority of Nigerians are left with no option but to use fuel wood for cooking. The health and environmental hazards associated with this practice cannot be over emphasized. As such, solar cooking would provide an alternative to reduce total dependence on fuel wood.

iv. The use of solar energy for cooking will have a great impact in reducing electricity consumption. This energy saving could be used for other activities.

CHAPTER TWO

LITERATURE REVIEW

2.1 Preamble

Solar cooker is a device that cooks food using only solar radiation and can save conventional fuels to a significant amount. It is the simplest, safest, most convenient way to cook food without consuming fuels or heating up the kitchen. It however, supplements the cooking fuel and cannot replace it in total. In recent times, rigorous studies were carried out on the method of utilisation of solar energy. Solar cookers like box type and concentrator type have offered important tools for these studies. Efforts have been specially geared towards the design, development and testing of these devices around the globe. Out of these types of solar cookers, the box type and the parabolic solar cookers, which are simpler in terms of operation and fabrication, have been so far studied extensively within the West African sub-region. Temperatures of between 80°C–100°C have been achieved in most cases (www.solarcookers.org).

2.2 Solar Radiation

The sun radiates energy approximately as a blackbody (perfect absorber and emitter of radiation at all wavelengths) at an effective temperature of 6000 K(Duffie and Beckman, 2001). It showers the atmosphere and the earth surface with an enormous quantity of electromagnetic energy. The total amount of energy emitted by the sun and received at the extremity of the earth's atmosphere is constant – 1367 W/m^2 (Duffie and Beckman, 2001).

2.3 Applications of Solar Radiation

Solar energy (radiant light and heat from the sun) has been harnessed by humans since ancient times using a range of technologies. Solar energy technologies include solar heating, solar drying, solar still, solar photovoltaic, solar thermal electricity and solar architecture, which can make considerable contributions to solving some of the most urgent energy problems (www.iea.org, 2012).

Solar technologies are broadly characterised as either passive or active, depending on the way they capture, convert and distribute solar energy. Active solar techniques include the use of photovoltaic panels and solar thermal collectors to harness the energy. Passive solar techniques include orienting a building to the Sun, selecting materials with favourable thermal mass or light dispersing properties, and designing spaces that naturally circulate air. Active solar technologies increase the supply of energy and are considered supply side technologies, while passive solar technologies reduce the need for alternative resources and are generally considered demand side technologies.

2.3.1 Solar power applications

Solar power is the conversion of sunlight into electricity. Sunlight can be converted directly into electricity using photovoltaic (PV), or indirectly with concentrated solar power (CSP) devices.

- Photovoltaic Cell (PV): A solar cell or photovoltaic cell is a device that converts light into electric current using the photoelectric effect. Solar cells produce direct current (DC) power, which fluctuates with the intensity of the irradiated light. This usually

requires conversion to certain desired voltages or alternating current (AC), which requires the use of inverters. Multiple solar cells are connected inside the modules. Modules are wired together to form arrays, then tied to an inverter, which produces power with the desired voltage, and frequency/phase.

- Concentrating Solar Power (CSP): CSP systems use lenses or mirrors and tracking systems to focus sunlight onto a small area. The concentrated heat is then used as a heat source for a conventional power plant. A wide range of concentrating technologies exists; the most developed are the parabolic trough, the concentrating linear Fresnel reflector, the Stirling dish and the solar power tower. Various techniques are used to track the Sun and focus light. In all of these systems a working fluid is heated by the concentrated sunlight, and is then used for power generation or energy storage.

2.3.2 Solar thermal applications

- Solar Hot Water Systems: Use sunlight to heat water. In low geographical latitudes (below 40 degrees) from 60 to 70% of the domestic hot water use with temperatures up to 60 °C can be provided by solar heating systems (www.iea.org). The most common types of solar water heaters are evacuated tube collectors and glazed flat plate collectors generally used for domestic hot water. Unglazed plastic collectors are used mainly to heat swimming pools (www.iea.org). In order to heat water using solar energy, a collector, often fastened to a roof or a wall facing the sun, heats a working fluid that is either pumped (active system) or driven by natural convection (passive system) through it. The collector could be made of a simple glass-topped insulated box with a flat solar absorber made of sheet metal, attached to copper pipes and dark-coloured, or a set of

metal tubes surrounded by an evacuated (near vacuum) glass cylinder. For industrial purposes, a parabolic mirror can concentrate sunlight on the tubes.

- Solar Still: A solar still is a low-tech way of distilling water, powered by the heat of the sun. Two basic types of solar stills are box and pit stills. In a solar still, impure water is contained outside the collector, where it is evaporated by sunlight shining through clear plastic. The pure water vapour (and any other included volatile solvent) condenses on the cool inside plastic surface and drips down from the weighted low point, where it is collected and removed.
- Solar Dryer: Solar dryers are mechanised methods of using solar radiation to dry agricultural crops that excludes the traditional method of open to sun or air drying. Different types of solar crop dryers produced by many agencies include solar dryer for grains such as maize, rice, beans, vegetable, pepper, melon, and root crops.

2.3.3 Solar powered cooling systems

Solar powered cooling has become very attractive during the last twenty years, since the amount of solar radiation and cooling loads both reach peak levels in the same season. It is to this end that there has been technological advancement to utilise this low grade energy to attain cooling of buildings for industrial applications, thermal comfort, thereby achieving energy savings. The solar cooling system is generally comprised of three sub systems: the solar energy conversion system, refrigeration system and cooling load. The appropriate cycle in each application depends on the cooling demand, power, and temperature levels of the refrigerated object, as well as the environment.

2.4 Solar Cookers

A solar cooker or solar oven is a device which uses the energy of sunlight to heat food or drink to cook or sterilise it. High-tech versions, for example electric ovens powered by solar cells, are possible, and have some advantages such as being able to work in diffuse light. However at present, they are very unusual because they are expensive. The vast majority of solar cookers presently in use are relatively cheap, low-tech devices, because they use no fuel and cost nothing to operate. It takes several successive steps to transmit and convert solar energy from its reception to the point of actually heating food. Depending on the type of solar cooker being used, those steps differ from case to case.

2.4.1 Solar box oven

A solar box oven basically consists of a black painted metallic tray and is usually covered with a double glass window. It is fixed in an insulated outer casing. The incoming radiation falls onto the double glass lid and passes through it to strike the blackened interior of the oven box. The glass covers while transmitting radiation of short wave length which forms a major part of the solar spectrum is almost opaque to long wave radiation emitted within the box. Thus, the temperature of the box rises until a balance is reached between the heat absorbed and heat lost by the exposed surface. A plane reflecting mirror of about the same size as the aperture area can be used to augment the solar radiation on the aperture. The reflector is set in such a way as to reflect the radiation falling on it to the box oven aperture. A simple setup of a solar box oven is shown in Figure 2.1.

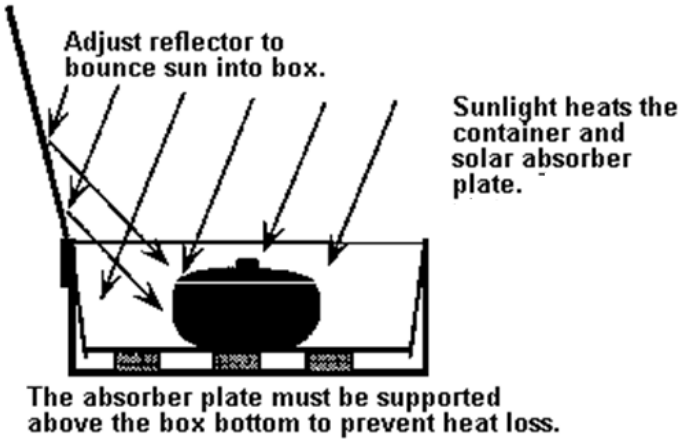

Figure 2.1: Side view of a box type solar cooker. Source: www.solarcooking.org, 2012

2.4.2 Parabolic cookers

This type of cooker consists of a reflector with parabolic shape. Reflector cookers exploit only the radiation that impinges directly onto the reflecting mirrors, which redirect it toward the cooking pot as shown in Figure 2.2. The dark-coloured bottom and sides of the pot absorb the radiation and transfer the heat to the food. The concentrated radiation has a higher power density and is therefore able to generate higher temperatures and temperature gradients at and within the pot. While that does make for faster cooking, it also makes the food more susceptible to burning than would be the case in a solar box oven.

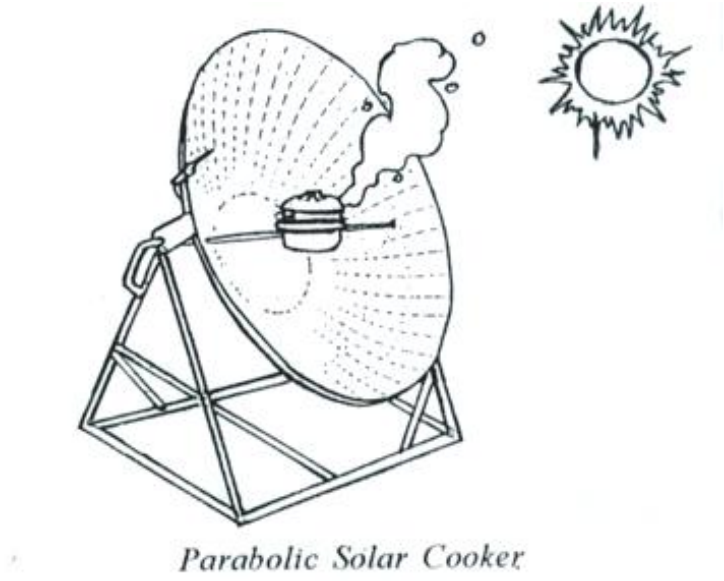

Figure 2.2: A parabolic solar cooker. Source:www.panasia.org, 2012

2.4.3 Panel cookers

Panel cookers are flat reflective panels which focus the sunlight onto a cooking vessel without the inner box in box cookers. Panel cookers are the easiest and least costly to make, requiring just four reflective panels and a cooking vessel, but they are unstable in high winds and do not retain as much heat when the sun is hidden behind clouds. Figure 2.3 shows a panel cooker with a dark cooking vessel wrapped in a plastic oven bag.

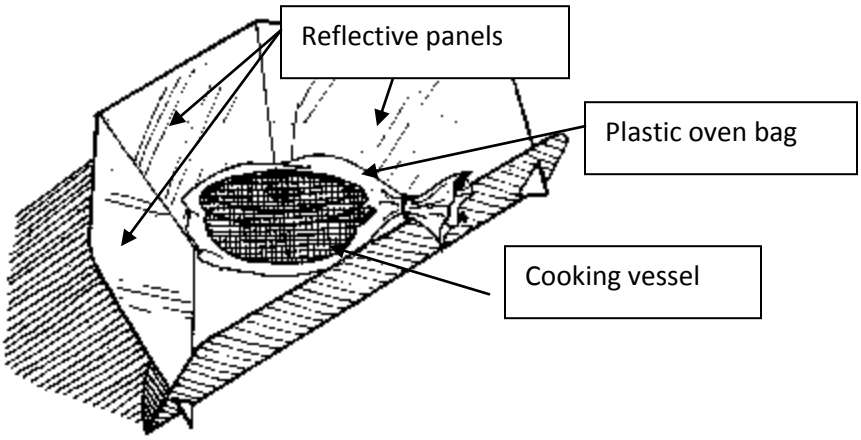

Figure 2.3: Sketch of a panel solar cooker. Source: www.solarcooking.org, 2012

2.4.4 Heat-accumulating solar cookers

Heat-accumulating solar cookers store heat in a solid or liquid medium. In a cooking box equipped for heat storage, the process of heating up the storage mass can be exactly the same as for heating food: radiation absorption, thermal radiation, convection, heat conduction. The food (in a pot in or on the heat store) gets most of its heat by conduction and radiation from the heat store. The more advanced types of heat-accumulating solar cookers have very elaborate heat transfer mechanisms. They collect solar energy not directly in the cooking containment, but in highly efficient tube/flat-plate collectors. The heat is transferred at a relatively high temperature to the heat store by heat pipes or a thermal oil loop; in the former case a solid store is used, and in the latter case the heat is stored in a volume of liquid serving as an integral part of the collecting cycle.

2.5 Historical Background of Solar Cookers

The contemporary solar cooking movement began in earnest in mid 19th century. In the late 1950s, the M.I.T.(Massachusetts Institute of Technology) scientist, Maria Telkes, interest on solar cooking occurred in the context of her professional activities in the housing field, particularly in using solar thermal energy to heat buildings. That interest led her to construct a classic box cooker, an insulated box of plywood with an inclined top of two layers of glass (with a small airspace between them) and four large flared reflectors. The design is used, in infinite variations, to the present day. George Lof, a former director of the Industrial Research Institute at the University of Denver, Colorado, was also an early pioneer of solar-powered technology, including solar cooking. In the 1950's, he experimented with a parabolic solar cooker design that he dubbed the "Umbroiler" because of its umbrella-like structure. He marketed the design, but it was a commercial failure for the times.

After that period, the years of the latter half of the 20th century show a number of individuals and groups experimenting with, demonstrating the potential, and conducting small and large projects using solar cooking devices. As early as 1955, a group of individuals in Phoenix organised themselves into an Association for Applied Solar Energy and held their first conference. Ultimately the group was the foundation of the American Solar Energy Society and its international counterpart, the International Solar Energy Society. Growing fuel wood and other energy shortages, coupled with expanding populations in China and India, encouraged governmental research on alternatives in the 1970s, with China holding its first seminar on solar cooking in 1973. China began distribution of subsidized cookers in 1981. Additional drive for investigating the potential of solar energy came from the oil shocks of that era, with considerable

experimentation in both Europe and the United States as well as in Asia. The ULOG group in Switzerland and EG Solar in Germany, as well as Solar Cookers International in the United States, originated in the 1987. The founding of Solar Cookers International was the beginning of an effort to link solar cooking promoters everywhere in the networking sense, since its intent was largely educational and networking. Also in 1980, an Arizona woman, Barbara Kerr, with other colleagues, continued to develop solar cooker models, to test their efficiency, to experiment with various materials, and to promote the technology. In 1980, Barbara Kerr and a neighbour, Sherry Cole, designed a cardboard box cooker "kit" that could be largely built by a customer, and was highly valued by those who purchased one. This work of these two women inspired the formation of Solar Cookers International. A few years later, the organization, again with the technical assistance of Barbara Kerr, pioneered the introduction of a different type of cooking device, the panel cooker, a hybrid between box and parabolic. This invention was a breakthrough, as it was less expensive and thus able to serve the needs of the world's poorest inhabitants.

2.6 Review of Past Works

Dasin*et al.*, (2011) designed and simulated a parabolic dish solar cooker which could be used for boiling water and cooking. A simulation model was used to predict the temperature of the various parts of the cooker. The simulation results were compared with experimental results and they yielded similar outputs. An average instantaneous efficiency of 84% was obtained for beam radiation of 650W/m^2.

Ekechukwu (2001) designed a box type solar cooker with a plane reflector. Aluminum plate absorber and fibre glass wool insulation were used. Experiments were carried out in Nsukka. Test results showed stagnation absorber plate temperatures of 138°C with reflector and 119°C

without reflector. Boiling times for 1kg of water were 60 min and 70 min with and without reflectors, respectively.

Taura and Musa (2012) constructed a solar cooker with single glazing for use in the city of Kano. A temperature of 90°C was achieved during rainy season and 100°C during dry season. The efficiency of the cooker was 31.57%.

Fayadh (2011) investigated the thermal performance of a solar cooker with reflector. Figure of merit F_1 and F_2 methods were employed. Efficiencies obtained fell within the international standard test range of 0.12 and 0.4 respectively.

Huseyn*et al.,* (2010) evaluated the efficiency of a solar cooker using both exergy and energy analysis. They found that exergy efficiency measure is more significant than that of energy, as such exergy analysis should be considered in the evaluation of solar cookers.

Nahar (2009) carried out the design and construction of a large size non tracking solar cooker. Stagnation temperatures of up to 118.5°C were achieved. The efficiency was found to be 27.5%.

Abdulrahim*et al*., (2011) developed and tested a solar tracking bi-focal collector system. Two paraboloids, each having an aperture area of 1.53 m^2 with concentration ratio of 22 were used. The tracking mode adopted in their work was the mechanical clockwork system using chains and sprockets. Performance evaluation of the developed solar collector revealed that a maximum outlet flow water temperature of 78°C was achieved in the month of September in Maiduguri environment.

Balogun (2006) carried out design and construction of a solar box oven comprising of reflectors glazing layers and absorber plate. Plywood was used as box frame. Experimental results yielded an oven air temperature of218 C under no load and 142 C with 1.1kg mass of cake.

Gwani(2010) constructed a solar cooker with adjustable reflectors at the sides. Fabrication was carried out using locally available materials that satisfy the necessary requirements. Temperatures as high as 97 C for cooker chamber were obtained.

Ogunwole (2006) designed, and constructed a solar cooker. The solar cooker was made of a casing and an absorber. The absorber was a square base pot, blackened with smoke, and it was made of stainless steel. The casing was made of two boxes to minimize heat loss. Aluminium foil was used as reflectors. The test involved cooking and it was observed that rice took 1 hour 45 minutes, beans took 2 hours 30 minutes, and yam took 1 hour 30 minutes. An average temperature of 100 ^{o}C was obtained from the collector for an ambient temperature of 34 ^{o}C.

Kimambo (2007) carried out a comprehensive study involving theoretical review, development work, experimental testing on six different types of solar cookers. The cookers were the sun stove box cooker, wooden box cooker, panel cooker, reflector cooker with unpolished aluminium reflectors, reflector cooker with polished aluminium reflectors and reflector cooker with glass mirror reflectors. Results obtained indicated that many of the cookers could be used to cook food for households in areas with medium and high insolation, with appropriate selection of the type and specification of the cookers, based on the measured insolation data of the location.

Ishan*et al.*, (2007) modelled a box type solar cooker employing non-tracking planar reflectors which was designed and fabricated. Its thermal performance was investigated experimentally. The cooking power of the laboratory model was found to be 25-50% higher than

that of the conventional cooker in various pre-specified test conditions. It was also concluded that the solar cooker utilising non-tracking reflectors provides increased heat collection and faster cooking, compared to the conventional box type solar cooker.

2.7 Theoretical Background

Solar radiation reaching the earth surface is comprised of beam and diffuse radiation. Diffuse radiation is due to the scattering of sunlight by the atmosphere, while beam radiation is the unaffected part. The beam component forms a larger part of the total radiation.

Solar cookers with reflectors convert both the beam and diffuse components of solar radiation into thermal energy through the following processes:

i. Reflection
ii. Transmission
iii. Absorption

2.7.1 Incident radiation

In order to determine the incident beam radiation on a surface of arbitrary orientation, it is necessary to evaluate the geometrical ratio, R_b, given by (Duffie and Beckman, 2001):

$$R_b = \frac{\cos\theta_i}{\cos\theta_z} \qquad (2.1)$$

Where: θ_i is the angle of incidence of beam radiation relative to the normal of asurface

$\theta_z$is the zenith angle of the sun

$\cos\theta_i$and$\cos\theta_z$are evaluated as follows (Duffie and Beckman, 2001):

$$\cos\theta_i = \cos\theta_z \cos\beta + \sin\theta_z \sin\beta \cos(\gamma_s - \gamma) \quad (2.2)$$
$$\cos\theta_z = \sin\delta \sin\varphi + \cos\delta \cos\varphi \cos\omega \quad (2.3)$$

Where: β is the inclination of the surface

$\gamma_s$is the surface azimuth angle

$\gamma$is the azimuth angle

$\delta$is the declination

$\varphi$is the latitude of the location

ωhour angle

The beam and diffuse radiation on a tilted surface are then given by (Duffie and Beckman, 2001):

$$\dot{I_{bT}} = \dot{I_b} R_b \quad (2.4)$$
$$\dot{I_{dT}} = \dot{I_d} \frac{(1+\cos\beta)}{2} \quad (2.5)$$

Where: $\dot{I_b}$ is the beam radiation on a horizontal surface (W/m^2)

$\dot{I_d}$is the diffuse radiation (W/m^2)

2.7.2 Reflection of radiation

Plane reflectors are used to increase the amount of radiation flux onto the aperture of the oven box. When sun ray strikes a specular reflecting surface, the angle of incidence is equal to the angle of reflection. Reflectivity is the ratio of the reflected energy to the incident energy.

The intensity of reflected radiation is given as (Pejack, 2003):

$$\dot{I_r} = \rho . \dot{I_{bT}} \quad (2.6)$$

Where: $\dot{I_r}$ is the reflected radiation, (W/m^2)

$\dot{I_{bT}}$is the incident beam radiation on a tilted surface (W/m^2)

$\rho$is the reflectivity

2.7.3 Transmission of radiation

The direct and reflected radiations incident on glazing is transmitted into the oven chamber. When solar radiation is transmitted through the glazing, some part of the radiation is reflected at the surface, absorbed within the glazing, while the remaining is transmitted (Pejack, 2003).

$$\dot{I_\tau} = \tau\left(\dot{I_T} + \dot{I_r}\right) \quad (2.7)$$

Where: $\dot{I_\tau}$ is the transmitted radiation, (W/m^2)

$\dot{I_T}$is the global radiation, (W/m^2)

$\tau$is the transmissivity

2.7.4 Absorption

When solar radiation is incident on an opaque surface, part of it is reflected, and the rest is absorbed. The absorbed radiation manifests as a heat input at the surface. The fraction of the incident radiation that is absorbed is termed absorptance, α.

The effective absorptance of a cavity receiver in a direct-gain passive solar heating application like a solar oven is given by (Duffie and Beckman, 2001):

$$\alpha_{eff} = \frac{\alpha_i}{\alpha_i + (1-\alpha_i)\tau_d \frac{A_a}{A_i}} \quad (2.8)$$

Where:

$\alpha_i$is the absorptance for diffuse radiation of the inner surface of cavity.

$\tau_d$is the transmittance of the glazing for isotropic diffuse solar radiation.

$A_a$is the area of aperture (m^2).

$A_i$is the area of the inside cavity (m^2).

The energy absorbed in the solar oven chamber can therefore be expressed as:

$$Q_a = \alpha_{eff} \dot{I}_\tau \qquad (2.9)$$

2.8 Performance Evaluation of Solar Oven

Although there are many test procedures for thermal rating of flat plate collectors in different countries of which the most widely accepted and used is ASHRAE standard, yet there is no universal standard test procedure for solar cookers (Garg and Prakash, 2000). There are many standards which have been proposed by different organisations for testing and evaluating solar cookers. One of such standards is the ASAE (American Society of Agricultural Engineers) standard known as ASAE S580. The standard was initiated by the tests standard committee at the third world conference on solar cooking held in India in 1997. It was developed by the ASAE solar energy committee (SE-414) march, 2012 and approved by ASAE structures and environment division standards committee January 2003. This standard is intended to (ASAE, 2003):

i. Promote uniformity and consistency in the terms and units used to describe, test, rate and evaluate solar cookers, solar cooker components and solar cooker operation.

ii. Provide a common format for presentation and interpretation of test results to facilitate communication.

iii. Provide single measure of performance so that consumers may compare different designs when selecting a solar cooker.

2.8.1 Test protocol

The average temperature inside a container of water is measured and averaged over ten minute intervals. Ambient temperature and normal irradiance are also measured and recorded. The primary figure of merit used in the ASAE standard is the cooking power, P_c, defined by (ASAE, 2003).

$$P_c = \frac{T_2 - T_1}{600} M C_w \qquad (2.12)$$

Where:

P_c is the cooking power (Watts)

T_2 is the final temperature (°C)

T_1 is the initial temperature (°C)

M is the mass of water (kg)

C_w is the specific heat of water (kJ/kgk)

The cooking power is normalised for solar radiation of 700W/m^2 as (ASAE S580, 2003):

$$P_s = P_c \left(\frac{700}{I_{av}}\right) \qquad (2.13)$$

Ambient temperature for each interval is subtracted from the average cooking vessel contents temperature for each corresponding interval.

$$T_d = T_w - T_a \quad (2.14)$$

Where:

T_d is the temperature difference

T_w is the water temperature

T_a is the ambient air temperature

The standardised cooking power, P_s, is plotted against temperature difference T_d, for each time interval.

A linear regression of the plotted points are used to find the relationship between cooking power and temperature in terms of intercept a(W) and slope b(W/°C) given as (ASAE S580, 2003):

$$P_s = a + bT_d \quad (2.15)$$

The coefficient of determination (r^2) or proportion of variation in cooking power can then be attributed to the relationship found by regression and should be higher than 0.75 or specially noted. The value for standardised cooking power is computed for temperature difference T_d of 50°C using the regression relationship (ASAE S580, 2003).

CHAPTER THREE

MATERIALS AND METHODS

A solar oven was designed, simulated, fabricated using an optimised model and tested in the study. The test was carried out in the Mechanical Engineering Workshop of Ahmadu Bello University, Zaria.

3.1 Description of Solar Oven System

The solar oven was designed to achieve heating by direct exposure to solar radiation. The system consists of the following components as shown in Figure 3.1; reflectors, cavity collector and inverted T-frame support. The design is such that the collector and the reflectors can be adjusted to track the movement of the sun.

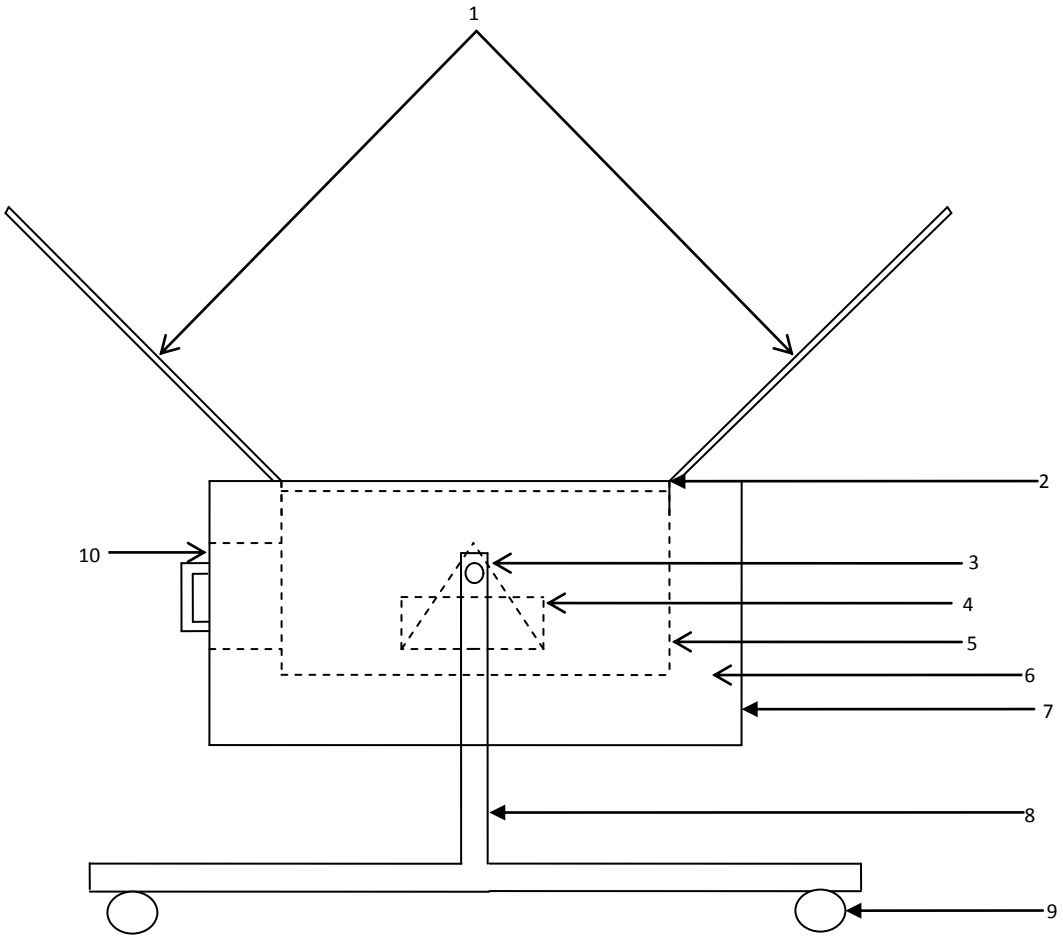

Figure 3.1 Schematic representation of the solar oven

KEY

1- Reflectors	6- Insulation
2- Glazing	7- Outer casing
3- Leveling tray	8- Inverted T-frame
4- Pot	9- Rollers
5- Oven chamber (absorber)	10- Door

3.2 Materials

In order to construct an effective solar oven, the choice of materials has to be given considerable thought. The materials chosen must be structurally sound, able to withstand high temperatures, safe, and effective with regard to the capture of solar energy and retention of heat. Finally, cost has to be considered in order to make it affordable for the target population.

3.2.1 Reflectors

Concentrating solar collectors require the use of reflective surfaces to direct the beam component of solar radiation onto a receiver. This requires surfaces of high specular reflectance for radiation in the solar spectrum (Duffie and Beckman, 2001).

Specular surfaces are usually metals or metallic coatings on smooth substrates. Specular surfaces can also be applied to transparent substrates including glass or plastic. Back silvered glass can have excellent specular reflectance, and if the reflective coatings are adequately protected, durability is excellent. Typical values of specular reflectance of surfaces for solar radiation are shown in Table 3.1.

Back silvered low-reflectance glass is considered due to its high reflectance and low cost.

Table 3.1: Normal specular solar reflectance of surfaces(Duffie and Beckman, 2001)

Surface	**Reflectance**
Back-silvered low-reflectance glass	0.94
Electroplated silver, new	0.96
High-purity Al, new clean	0.91
Sputtered aluminium optical reflector	0.89
Brytal processed aluminium, high purity	0.89
Back silvered water white plate glass, new clean	0.88
Al, SiO coating, clean	0.87
Aluminium foil, 99.5% pure	0.86
Back aluminized 3M acrylic, new	0.86

3.2.2 Glazing

Glazings are transparent covers used to prevent heat loss by convection from the collector. The properties of glazing materials that have been considered for solar collector covers are given in Table 3.2.

Table 3.2 Average refractive indexof some coversin the solar spectrum (Mahavar*et al.*, 2012)

Glaze material	**Refractive index**	**Extinction coefficient (m^{-1})**	**Density (kg/m^3)**	**Thickness (mm)**
Glass	1.52	15	2450	3.94
Polymethyl methacrylate (PMMC)	1.49	0.05	1172	2.75
Polycarbonate (PC)	1.58	0.05	1177	2.9

From Table 3.2, it can be seen that PMMC and PC have favourable properties required for effective solar radiation collection, but glass is considered because it is cheaper and withstands high temperatures.

3.2.3 Insulation

The material property that governs the ability of a material to conduct heat is the thermal conductivity. For effective insulation, low thermal conductivities are desired. Other properties that determine the suitability of insulators for solar oven application are rigidity and thermal stability. Table 3.3 gives typical values of thermal conductivity for various insulation materials. Saw dust was considered, due to low thermal conductivity, low cost and availability.

Table 3.3: Thermal conductivities of various insulating materials (Pejack, 2003)

Material	**Thermal conductivity (W/m□C)**
Air	0.03
Foam(polyurethane)	0.03
Fibre glass	0.04
Corkboard	0.04
Felt Wool	0.05
Cotton	0.06
Saw dust	0.06
Paper	0.18
Wood	0.1 – 0.2
Sand	0.3

3.2.4 Casing

Galvanized iron, steel, aluminium, wood and fibre sheet are commonly used casing materials. These materials have very good weather stability as well as durability, but these differ in cost and weight. Properties of some casing materials are shown in Table 3.4. Hard board was chosen for the casing due to its low conductivity, density and cost.

Table 3.4: Properties of casing materials(Mahavar et al., 2012)

Material	**Thermal conductivity (W/mK)**	**Density (kg/m^3)**	**Thickness (m)**
Fibre sheet	0.048	240	0.002
Galvanized iron	59	7880	0.00088
Aluminium	228	2700	0.00071
Stainless steel	15.6	7913	0.00046
Hard board	0.15	730	0.0025

3.3 Solar Data

Global solar radiation measurements are required for the design, optimisation and prediction of the performance of solar energy systems (Sanusi*et al.*, 2011). Metrological data of the city, where the test was carried out (Zaria) was used. This data include: solar radiation, wind speed, ambient temperature, and number of sunshine hours.

Solar radiation measurements are often available in form of daily and hourly radiation on a horizontal surface. Hourly radiation on a horizontal surface can be generated from the TMY (typical meteorological year) data using TRNSYS simulation software.

A TMY data is a collation of selected weather data for a specific location, generated from a data bank much longer than a year in duration. It is specially selected so that it presents the range of weather phenomena for the location in question, while still giving annual averages that are consistent with the long-term averages for the location.

3.4 Design Theory

The design model of the solar box oven was based on the following assumptions:

i. Specular reflection takes place from the reflectors.

ii. The absorber includes the blackened interior walls of the insulated box.

iii. Adjustment is constantly made so that surface azimuth is always equal to solar azimuth.

iv. The transmittance of the glazing is a function of the angle of incidence.

v. The air mass in the oven is constant and only acts as a medium for convective heat transport.

vi. The collector and reflector have the same area.

vii. The temperatures of the side walls and base of the oven chamber are equal.

3.4.1Tracking mode

Collectors can be continuously adjusted in prescribed ways to minimise the angle of incidence of beam radiation on their surfaces and thus maximise the incident beam radiation.

The collector azimuth and tilt angles can be adjusted periodically to maximise the radiation incident on the collector. The tracking method employed is that for a surface at a fixed slope and variable azimuth, rotating about a vertical axis as depicted in Fig 3.2. In this case the beam radiation is maximised when solar azimuth is equal to surface azimuth.

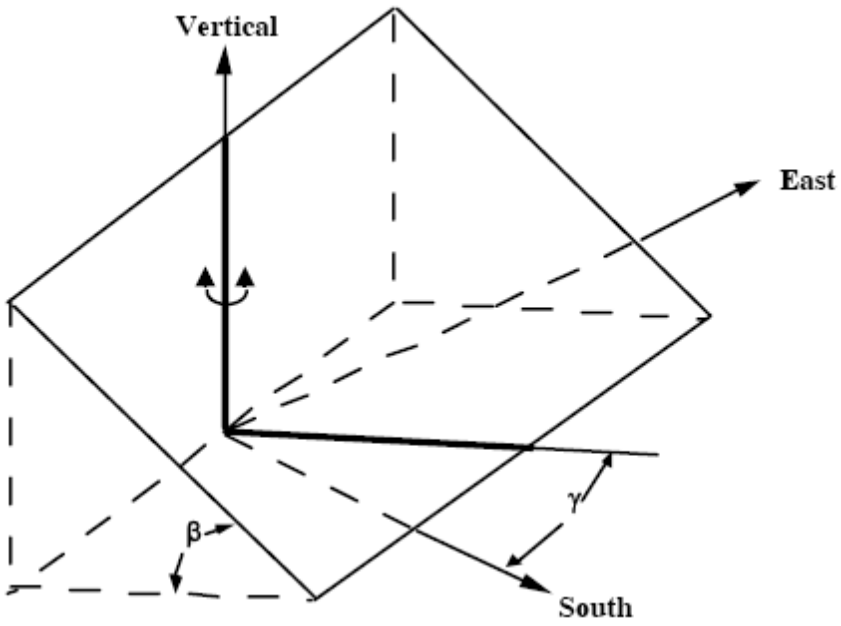

Figure 3.2: Tracking mode of collector surface (TRNSYS 16 – Mathematical Reference,2007)

The energy absorbed by a solar collector depends on the angle of incidence of the direct and reflected radiation on the collector surface. The geometric relationship between the plane of the collector, reflectors and the position of the sun can be described in terms of several angles as shown in Figure 3.3.

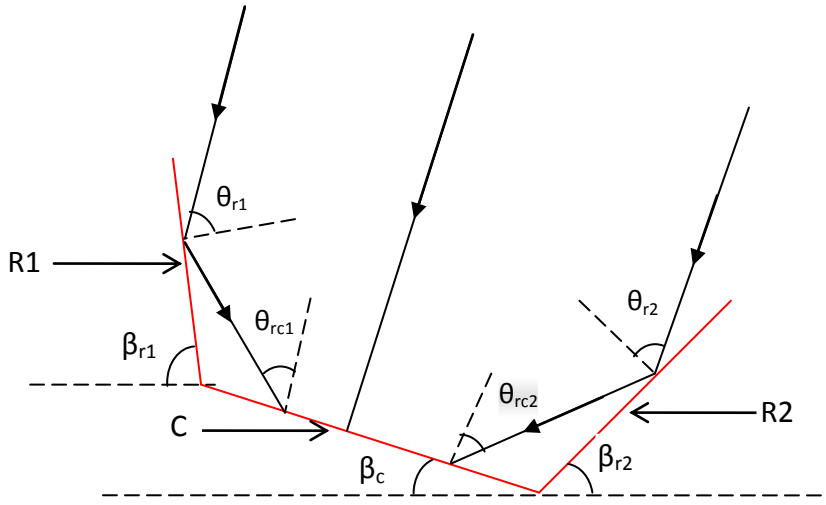

Figure 3.3: A schematic representation of the radiation incident on the collector-reflector assembly.

The collector and reflectors are denoted as C, R_1, and R_2 respectively.

3.4.2 Angle of incidence of reflected radiation

The reflectors are more effective when the solar incidence angle increases with the position of the sun and becomes less effective when the incidence angle on the reflector surface decreases. The expressions for the angles of incidence on the collector for the reflected rays are (Rakesh*et al*,. 1994):

$$cos\theta_{rc1} = -u_1 sin\beta_c cos\gamma_s - v_1 sin\beta_c cos\gamma_s - w_1 cos\beta_c \quad (3.1)$$

$$cos\theta_{rc2} = -u_2 sin\beta_c cos\gamma_s - v_2 sin\beta_c cos\gamma_s - w_2 cos\beta_c \quad (3.1)$$

Where:

$$u_1 = -sin\theta_z cos\gamma + 2cos\theta_{r1} sin\beta_{r1} cos\gamma_s \quad (3.3)$$

$$u_2 = -sin\theta_z cos\gamma - 2cos\theta_{r2} sin\beta_{r2} cos\gamma_s \quad (3.4)$$

$$v_1 = -sin\theta_z sin\gamma + 2cos\theta_{r1} sin\beta_{r1} sin\gamma_s \quad (3.5)$$

$$v_2 = -sin\theta_z sin\gamma - 2cos\theta_{r2} sin\beta_{r2} sin\gamma_s \quad (3.6)$$

$$w_1 = -cos\theta_z + 2cos\theta_{r1} cos\beta_{r1} \quad (3.7)$$

$$w_2 = -cos\theta_z + 2cos\theta_{r2} cos\beta_{r2} \quad (3.8)$$

Where:

$\beta_{r1}$is the tilt angle of reflector R1.

$\beta_{r2}$is the tilt angle of reflector R2.

$\beta_c$is the collector tilt angle.

$\theta_{r1}$is the angle of incidence of solar radiation on R1.

$\theta_{r2}$is the angle of incidence of solar radiation on R2.

3.4.3 Exchange and shading factors

If e_1 and e_2 are the position vectors of the points on the incident solar rays after reflection, then (Rakesh*et al*,. 1994):

$$\bar{e}_1 = e_{x1}\bar{\imath} + e_{y1}\bar{\jmath} + e_{z1}\bar{k} \quad (3.9)$$

$$\bar{e}_2 = e_{x2}\bar{\imath} + e_{y2}\bar{\jmath} + e_{z2}\bar{k} \quad (3.10)$$

Where:

$$e_{x1} = -(a/2)sin\gamma_s - acos\beta_{r1} cos\gamma_s + C_{e1} u_1 \quad (3.11)$$

$$e_{y1} = -(a/2)sin\gamma_s - acos\beta_{r1} cos\gamma_s + C_{e1} v_1 \quad (3.12)$$

$$e_{z1} = asin\beta_{r1} cos\gamma_s + C_{e1} w_1 \quad (3.13)$$

$$e_{x2} = -(a/2)sin\gamma_s - acos\beta_{r2} cos\gamma_s + C_{e2} u_2 \quad (3.14)$$

$$e_{y2} = -(a/2)sin\gamma_s - acos\beta_{r2}cos\gamma_s + C_{e2}v_2 \quad (3.15)$$

$$e_{z2} = asin\beta_{r2} + C_{e2}w_2 \quad (3.16)$$

$$C_{e1} = asin(\beta_{r1} - \beta_c)/cos\theta_{rc1} \quad (3.17)$$

$$C_{e2} = asin(\beta_{r2} + \beta_c)/cos\theta_{rc2} \quad (3.18)$$

Where:

$a$is the length of collector.

Expressions for the exchange factors with respect to different regions of the reflectors are given in Tables 3.5 and 3.6

Table 3.5: Exchange factors with specified boundary conditions between the reflector R-1 and the collector for six different regions (Rakesh*et al,.* 1994).

Region	**Boundary conditions**	**Exchange factors (f_{rc1})**
1	$R_1 \geq 0$, $S_1 < -0.5$ $(R_1+S_1W_1) < 0.5W_1$	$0.5R_1/W_1(0.5-S_1)$
2	$R_1 > W_1$, $S_1 \leq 0.5$ $(R_1+S_1W_1) \geq 0.5W_1$	$0.5[2-(0.5-S_1)W_1/R_1]$
3	$-0.5 \leq S_1 \leq 0.5$ $0 \leq R_1 \leq W_1$	$0.5(1.5+S_1)R_1/W_1$
4	$S_1 > 0.5$, $R_1 \geq W_1$ $(R_1-S_1W_1) > 0.5W_1$	$0.5[2-(S_1-0.5)W_1/R_1]$
5	$0.5 < S_1 \leq 1.5$ $0 \leq R_1 < W_1$	$0.5R_1(2.5-S_1)/W_1$
6	$S_1 > 0.5$, $R_1 \geq 0$ $(R_1-S_1W_1) < 0.5W_1$	$0.5R_1/W_1(S_1-0.5)$

Where S_1, R_1 and W_1 are given by (Rakesh*et al,.* 1994):

$$S_1 = -(e_{x1}/a)sin\gamma + (e_{y1}/a)cos\gamma \quad (3.19)$$

$$R_1 = (e_{x1}/a)cos\gamma + (e_{y1}/a)sin\gamma \quad (3.20)$$

$$W_1 = cos\beta_c \quad (3.21)$$

Table 3.6: Exchange factors with specified boundary conditions between the reflector R-2 and the collector for six different regions (Rakesh*et al,*. 1994).

Region	**Boundary conditions**	**Exchange factors (f_{rc2})**
1	$R_2 \leq 0$, $S_2 < -0.5$ $(R_2+S_2W_2) > 0.5W_1$	$0.5R_2/W_2(0.5-S_2)$
2	$R_2 < W_2$, $S_2 \leq 0.5$ $(R_2+S_2W_2) < 0.5W_2$	$0.5[2-(0.5-S_2)W_2/R_2]$
3	$-0.5 \leq S_2 \leq 0.5$ $0 \geq R_2 > W_2$	$0.5(1.5+S_2)R_2/W_2$
4	$S_2 > 0.5$, $R_2 \leq W_2$ $(R_2-S_2W_2) < -0.5W_2$	$0.5[2-(S_2-0.5)W_2/R_2]$
5	$0.5 < S_2 \leq 1.5$ $0 \geq R_2 > W_2$	$0.5R_2(2.5-S_2)/W_2$
6	$S_2 > 0.5$, $R_2 \leq 0$ $(R_2-S_2W_2) > -0.5W_1$	$0.5R_2/W_2(S_2-0.5)$

Where S_2, R_2 and W_2 are given by (Rakesh*et al,*. 1994):

$$S_2 = -(e_{x2}/a)sin\gamma + (e_{y2}/a)cos\gamma \quad (3.22)$$

$$R_2 = (e_{x2}/a)cos\gamma - (e_{y2}/a)sin\gamma \quad (3.23)$$

$$W_2 = cos\beta_c \quad (3.24)$$

Shading of reflectors on collector is also calculated in the same fashion. In this case, the incoming beam radiation passing from points on the reflector to the collector is considered. The position vectors of points for which the incoming beams are incident on the collector are (Rakesh*et al,*. 1994):

$$\vec{e}_1 = e_{x1}\bar{\imath} + e_{y1}\bar{\jmath} + e_{z1}\bar{k} \quad (3.25)$$

$$\vec{e}_2 = e_{x2}\bar{\imath} + e_{y2}\bar{\jmath} + e_{z2}\bar{k} \quad (3.26)$$

Where:

$$e_{x1}^{`} = -(a/2)sin\gamma_s - a\,cos\beta_{r1}cos\gamma_s - C_{e1}^{`}sin\theta_z cos\gamma_s \quad (3.27)$$

$$e_{y1}^{`} = -(a/2)sin\gamma_s - a\,cos\beta_{r1}sin\gamma_s - C_{e1}^{`}sin\theta_z cos\gamma_s \quad (3.28)$$

$$e_{z1}^{`} = a\,sin\beta_{r1} - C_{e1}^{`}cos\theta_z \quad (3.29)$$

$$e_{x2}^{`} = -(a/2)sin\gamma_s - a\,cos\beta_{r2}cos\gamma_s - C_{e2}^{`}sin\theta_z cos\gamma_s \quad (3.30)$$

$$e_{y2}^{`} = -(a/2)sin\gamma_s - a\,cos\beta_{r2}cos\gamma_s - C_{e2}^{`}sin\theta_z cos\gamma_s \quad (3.31)$$

$$e_{z2}^{`} = a\,sin\beta_{r2} - C_{e2}^{`}cos\theta_z \quad (3.32)$$

$$C_{e1}^{`} = a\sin(S_{r1} - S_c)\,/cos\theta_c \quad (3.33)$$

$$C_{e2}^{`} = a\sin(S_{r2} + S_c)\,/cos\theta_c \quad (3.34)$$

Expressions for the shading factors with respect to different regions of the reflectors are obtained using Tables 3.7 and 3.8

Table 3.7: Shading factors with specified boundary conditions between the reflector R-1 and the collector for six different regions (Rakesh*et al*,. 1994).

Region	**Boundary conditions**	**Shading factors (S_{rc1})**
1	$R_1 \geq 0$, $S_1 < -0.5$ $(R_1 + S_1 W_1) < 0.5W_1$	$0.5R_1/W_1(0.5-S_1)$
2	$R_1 > W_1$, $S_1 \leq 0.5$ $(R_1 + S_1 W_1) \geq 0.5W_1$	$0.5[2-(0.5-S_1)W_1/R_1]$
3	$-0.5 \leq S_1 \leq 0.5$ $0 \leq R_1 \leq W_1$	$0.5(1.5+S_1)R_1/W_1$
4	$S_1 > 0.5$, $R_1 \geq W_1$ $(R_1 - S_1 W_1) > 0.5W_1$	$0.5[2-(S_1-0.5)W_1/R_1]$
5	$0.5 < S_1 \leq 1.5$ $0 \leq R_1 < W_1$	$0.5R_1(2.5-S_1)/W_1$
6	$S_1 > 0.5$, $R_1 \geq 0$ $(R_1 - S_1 W_1) < 0.5W_1$	$0.5R_1/W_1(S_1-0.5)$

Where S_1, R_1 and W_1 are given by (Rakesh*et al*,. 1994):

$$\grave{S}_1 = -(\grave{e}_{x1}/a)sin\gamma + (\grave{e}_{y1}/a)cos\gamma \quad (3.35)$$

$$\grave{R}_1 = (\grave{e}_{x1}/a)cos\gamma + (\grave{e}_{y1}/a)sin\gamma \quad (3.36)$$

$$W_1 = cos\beta_c \quad (3.37)$$

Table 3.8: Shading factors with specified boundary conditions between the reflector R-2 and the collector for six different regions (Rakesh*et al*,. 1994).

Region	**Boundary conditions**	**Shading factors (S_{rc2})**
1	$R\square_2 \leq 0$, $S\square_2 < -0.5$ $(R\square_2 + S\square_2 W_2) > 0.5W_1$	$0.5R\square_2/W_2(0.5-S\square_2)$
2	$R\square_2 < W_2$, $S\square_2 \leq 0.5$ $(R\square_2 + S\square_2 W_2) < 0.5W_2$	$0.5[2-(0.5-S\square_2)W_2/R\square_2]$
3	$-0.5 \leq S\square_2 \leq 0.5$ $0 \geq R\square_2 > W_2$	$0.5(1.5+S\square_2)R\square_2/W_2$
4	$S\square_2 > 0.5$, $R\square_2 \leq W_2$ $(R\square_2 - S\square_2 W_2) < -0.5W_2$	$0.5[2-(S\square_2-0.5)W_2/R\square_2]$
5	$0.5 < S\square_2 \leq 1.5$ $0 \geq R\square_2 > W_2$	$0.5R\square_2(2.5-S\square_2)/W_2$
6	$S\square_2 > 0.5$, $R\square_2 \leq 0$ $(R_2 - S_2W_2) > -0.5W_1$	$0.5R\square_2/W_2(S\square_2-0.5)$

Where $S\square_2$, $R\square_2$ and W_2 are given by (Rakesh et al,. 1994):

$$\grave{S}_2 = -(\grave{e}_{x2}/a)sin\gamma + (\grave{e}_{y2}/a)cos\gamma \quad (3.38)$$

$$\grave{R}_2 = (\grave{e}_{x2}/a)cos\gamma - (\grave{e}_{y2}/a)sin\gamma \quad (3.39)$$

$$W_2 = cos\beta_c \quad (3.40)$$

3.4.4 Energy absorbed by collector

The total radiation on the collector is given by the sum of the radiation directly incident on the collector and the reflected radiation from the reflectors R_1 and R_2. The absorbed energy is then given as (Rakesh*et al*,. 1994):

$$Q_a = (1 - S_c)\{(\tau\alpha)_{bc}I_{bc} + (\tau\alpha)_{dc}I_{dc} + \rho[(\tau\alpha)_{rc1}I_{br1}f_{rc1}\cos\theta_{rc1} + (\tau\alpha)_{rc2}I_{br2}f_{rc2}\cos\theta_{rc2}]\} \quad (3.41)$$

$$S_c = S_{rc1} + S_{rc2} \quad (3.42)$$

Where:

$S_c$is the shading factor of the reflectors R1 and R2 on collector.

$I_{bc}$is the beam component of radiation on collector (W/m^2)

$I_{dc}$is the diffuse component of radiation on collector (W/m^2)

$I_{br1}$is the radiation reflected from reflector R1 (W/m^2)

$I_{br2}$is the radiation reflected from reflector R2 (W/m^2)

$(\tau\alpha)$is the transmittance absorptance product.

3.4.5 Heat balance equations

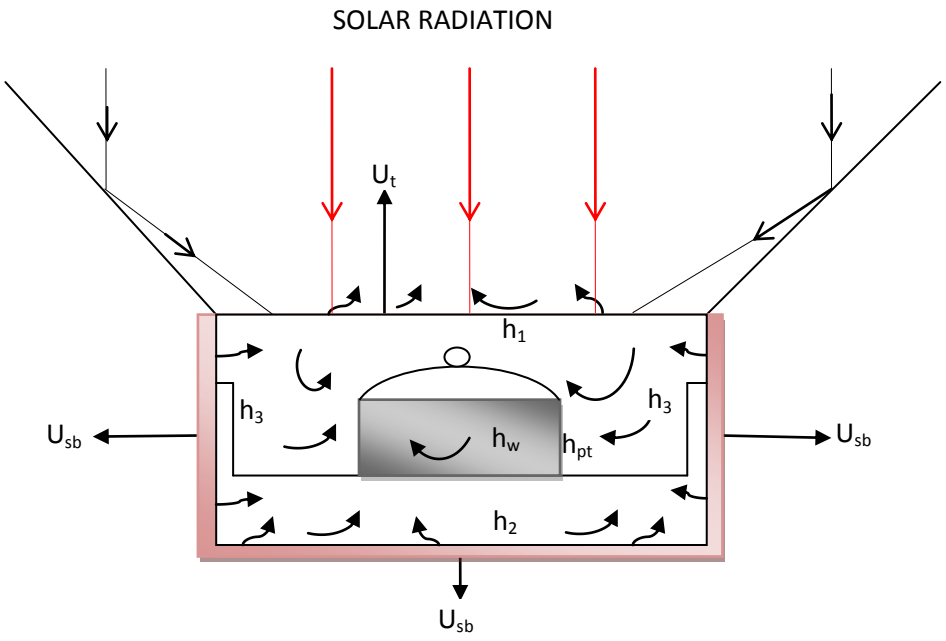

Figure3.4: Physical model of solar oven with plane reflectors

The physical model postulated for the solar oven is shown in Figure 3.4. The oven cavity is heated by the radiation transmitted through the glazing. Heat is transferred from the side and bottom walls of the oven chamber at temperature,T_p, to the ambient air at T_a through the side and bottom loss coefficient U_{sb}, to the air in the oven chamber at temperature T_{io}, through the convection coefficients h_2 and h_3, to glazingat temperature T_c, through the linearised radiation heat transfer coefficient h_r. Heat is transferred to the cover glass from the air in the oven chamber through the heat transfer coefficient h_1, to the pot through the heat transfer coefficient h_{pt}, and finally to the water at temperature T_w,through the heat transfer coefficient h_{wt}. Energy is lost from the glazing to the ambient air through the combined convection and radiation coefficient U_t.

Energy balances carried out under steady state on the glazing, oven walls, air in the oven chamber, tray, pot and water yield the following equations (Duffie and Beckman, 2001):

Glazing: $U_t(T_a - T_c) + h_r(T_p - T_c) + h_1(T_{io} - T_c) = 0$ (3.43)

Oven walls: $A_c Q_a + U_{sb}A_{sb}(T_a - T_p) + \{A_c h_2 + (A_{sb} - A_c)h_3\}(T_{io} - T_p) + h_r A_c(T_c - T_p) = 0$ (3.44)

Air in oven chamber: $h_1 A_c(T_c - T_{io}) + \{A_c h_2 + (A_{sb} - A_c)h_3\}(T_p - T_{io}) = 0$(3.45)

Tray: $A_t h_t(T_{io} - T_t) + \frac{A_{pt}K_{pt}}{t_{pt}}(T_{pt} - T_t) = 0$ (3.46)

Pot: $\frac{A_{pt}K_{pt}}{t_{pt}}(T_{pt} - T_t) + A_{spt}(T_{io} - T_{pt}) + A_{w-pt}h_{wt}(T_{wt} - T_{pt}) = 0$ (3.47)

Water: $A_{w-pt}h_{wt}(T_{pt} - T_{wt}) = q_u$(3.48)

$$q_u = \frac{MC_w\Delta T_{wt}}{t} \quad (3.49)$$

Where:

$$U_t = h_w + h_{rca} \quad (3.50)$$

$$h_w = 2.8 + 3V_w \quad (3.51)$$

$$h_{rca} = \varepsilon_c \delta \left(T_c{}^2 + T_a{}^2\right)(T_c + T_a) \quad (3.52)$$

$$h_1 = \frac{Nu_1 K_a}{a} \quad (3.53)$$

$$Nu_1 = 0.27 Ra_1{}^{\frac{1}{3}} \quad (3.54)$$

$$h_2 = \frac{Nu_2 K_a}{a} \quad (3.55)$$

$$Nu_2 = 0.27 Ra_2{}^{\frac{1}{3}} \quad (3.56)$$

$$h_3 = \frac{Nu_1 K_a}{d} \quad (3.57)$$

$T_{io}$is the temperature of oven chamber(□C)

Nu is the Nusselt number.

Ra is the Rayleigh number

K_a is the thermal conductivity of air (W/mk)

3.5Solar Oven Model and Optimisation

Simulation is very essential in the design of any solar device. TRNSYS (Transient System Simulation), EES (engineering equation solver) and Microsoft excel were used to model and simulate the operation of the system.

TRNSYS consists of many subroutines that model subsystem components. It also has the capability of interconnecting system components in any desired manner. Each component is represented as a box, which requires a number of constant parameters and time dependent inputs and produces time dependent outputs. A given output can however be used as an input to any number of other components. When a flow diagram is drawn in TRNSYS, a deck file is created

containing information on all the components of the system, weather data file and the output format. TRNSYS also has a provision for calling external programs like Microsoft excel, EES (engineering equation solver) and so on.

3.5.1 Thermal system modelling

The system model consists of different components with inputs and outputs. The model shown in the TRNSYS simulation studio evaluates the average power absorbed by the solar oven within the time interval specified in the control cards. The model with the TRNSYS components and all interconnections are shown in Figure 3.5. The solar thermal system consists of weather data, reflectors and collector.

a. Weather data

   TRNSYS type109-tmy2 component was used to model the weather data. This component reads weather data at regular intervals from a data file, converts and processes the solar radiation data to obtain tilted surface radiation and other solar angle geometries for the collector surface.

b. Plane Reflectors

   The type 62 EXCEL component of TRNSYS was used to model the concentration of radiation by the reflectors. This TRNSYS type implements a link with Microsoft excel. The exchange and shading factors of the reflectors as well as the angle of incidence of the reflected radiation were evaluated using the input values from TMY weather component. The result output was sent through the link to the equations component.

c. The collector

   The collector was modelled as a macro which consists of the type 35b and the equations components. The type 35b component calculates the transmissivities of the

glazing for the incident and reflected radiation. Equation 3.41 was modelled in the equations component which calculates the solar energy absorbed per metre square of the collector. The parameters required for the model are given in Table 3.9. The type 55 periodic integrator component was used to calculate the integral of the energy absorbed in the collector within a specified period of time. Type 25c printer component was finally used to display the results at the end of each time interval.

Table 3.9: Simulation parameters for solar oven box model

Parameter	**Value**
Number of glazing	1
Extinction coefficient of glazing	0.037
Refractive index	1.526
Absorbtivity	0.9
Reflectivity	0.9
Collector depth	0.3m

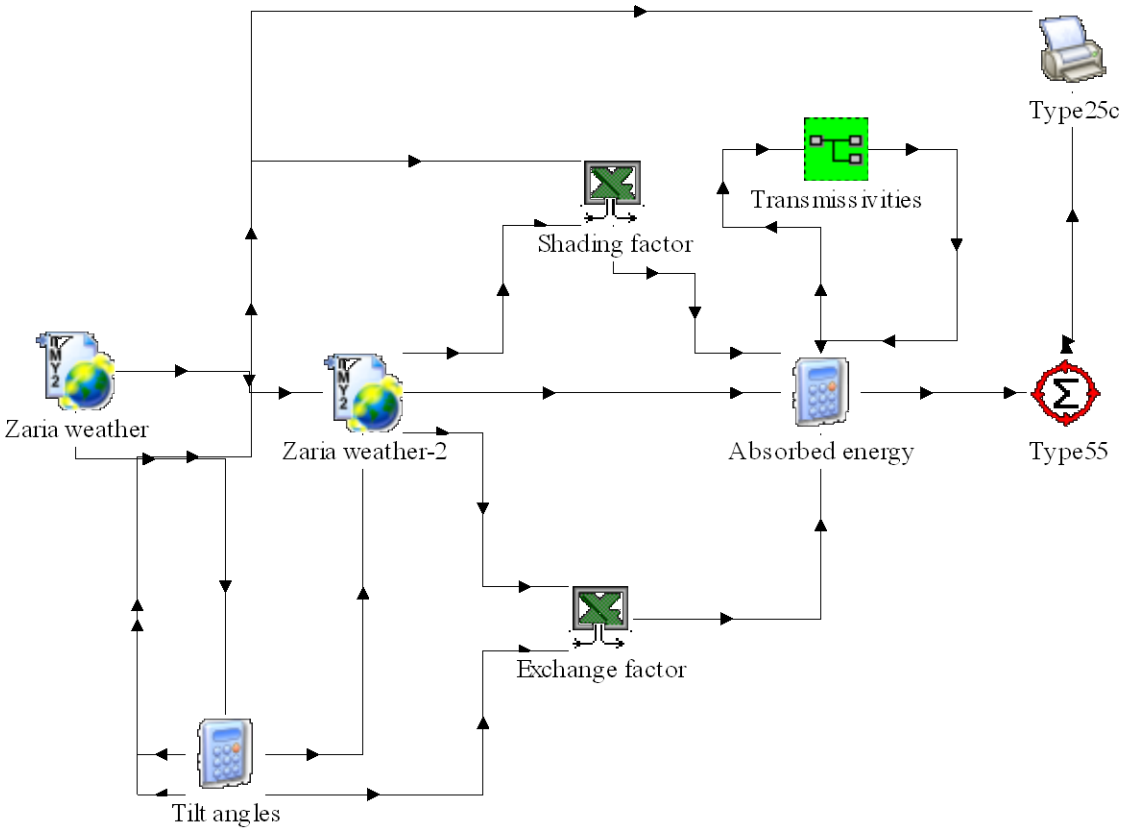

Figure 3.5: Trnsys studio model of solar oven.

3.5.2 Determination ofmonthlyoptimum collector slope

The TRNSYS model used to determine the collector tilt angle required for optimum interception of solar radiation is shown in Figure 3.6. Type109 weather component evaluates the solar radiation incident on the surface with tilt angle specified in the equations component. The type 55 component integrates and calculates the average radiation incident on the surface for the period specified in the control card.

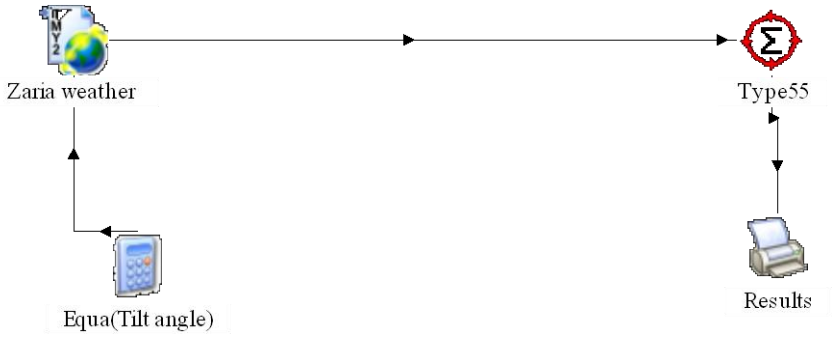

Figure 3.6Trnsys studio model for determining monthly optimum tilt angle

The Trnedit program was used to create a parametric table with tilt angles varying from 0-50 degrees using the TRNSYS deck file shown in appendix A. Trnedit evaluates the monthly average solar radiation incident on the surface for each tilt angle from 8a.m to 3p.m for the whole month.

3.5.3 Determination of Monthly Optimum Tilt Angles of Reflectors R_1 and R_2

Trnedit was used to edit the deck files for the TRNSYS model shown in figure 3.15. A parametric table was created with both reflectors set at a number of varying tilt angle combinations. The average power absorbed by the solar oven model for various combination of reflector tilt angles (β_{r1} and β_{r2}) within each month of the year was obtained.

3.5.4 Determination of Design month

The design month is the month with the lowest solar irradiance when the least system performance is expected. The weather condition for the recommended average day for the month was utilized. The recommended average day for each month of the year is given in Table 3.10 (Duffie and Beckman, 2001).

Table 3.10: Recommended Average Days for months and Values of n_i (Day of theYear) by months

Month	**Date**	**n_i**	**Hours**
January	17	17	384 – 408
February	16	47	1104 – 1128
March	16	75	1824 – 1848
April	15	105	2496 – 2520
May	15	135	3216 – 3240
June	11	162	3864 – 3888
July	17	198	4728 – 4752
August	16	228	5448 – 5472
September	15	258	6168 – 6192
October	15	288	6888 – 6912
November	14	318	7608 – 7632
December	10	344	8256 – 8280

3.5.5 Determination of optimum collector area and insulation thickness

The economic problem in solar system design is to find the lowest cost system. In principle, the problem is a multivariable one, with all of the components in the system and the system configuration having some effect on the thermal performance and thus on cost (Duffie and Beckman, 2001). The optimisation process in this work was carried out using weather data for Zaria, based on a minimum oven temperature of 100 degree Celsius. The subsequent sizing of collector area and insulation thickness was such that a stagnation temperature of 100 C was attained in the average day of the design month. The flow chart of the optimisation process is shown in appendix A.

3.5.6 Temperature calculations

The transfer of heat generated in the solar oven was modelled using engineering equation solver (EES).

With the collector and reflector tilt angles set at optimum values obtained for the design month, the average energy absorbed was evaluated using TRNSYS at a time step of one minute. These values were used in the EES model (appendix D) to calculate the temperature of the lumped system as a function of time for six different areas and insulation thicknesses. The table value function and parametric table were employed in solving the differential equation numerically using Euler's method. The parametric table calculates the temperature of the oven at the end of each minute.

3.6 Production of Oven Components

The assembly and working drawing of the solar oven are shown in appendix C.The system was constructed in Ahmadu Bello University (A.B.U) Zaria Mechanical Engineering Department workshop based on theoptimumsystem dimensions obtained.

3.6.1 Insulated oven box

The inner and outer casing of the oven compartment was fabricated with plywood of thickness 0.015m. The dimension for the inner casing is 0.7m x 0.7m x0.3m, while the outer casing has dimension 0.9m x 0.9m x0.45m. A 0.6m x 0.2m rectangular opening was cut on one side of each box to serve as a door. A 0.1m x 0.1m hard wood was nailed along the top of the inner sides of the outer casing. The inner casing was then nailed to the hard wood at a distance of 0.05m from the top after which the sides of the door were sealed with plywood. The whole

assembly was turned upside down after which the space was filled with saw dust and then finally covered with 0.9m x 0.9m plywood.

3.6.2 Absorber

Aluminium roofing sheet was flattened and used to fabricate a 0.7m x 0.7m x 0.3m box with 0.6m x 0.2m rectangular opening on one side. It was then inserted in the oven box and nailed at the sides using 2mm nails.

3.6.3 Level tray

The level tray consists of a 0.6m x 0.2m angle bar frame with a steel plate of the same dimension welded to the bottom of the frame. The tray is suspended from pivots through 0.1m flat bars welded at right angles to the midpoint of the sides of the tray.

3.6.4 Glazing

White tempered glass of thickness 4mm and dimension 0.73m x 0.73m was placed on top of the inner box. The space at the sides was sealed with silicone sealant.

3.6.5 Reflectors

Two 3mm thick, silver plated mirrors, 0.7m x 0.7m in dimension were each mounted on 0.7m x 0.9m plywood with the aid of clips. Each reflector was hinged by the opposite sides of the oven box. The reflectors were held at the sides using flat bars, with one end permanently fixed to the midpoint of the adjacent side on the collector and the other end sliding on the 3mm hole along the angle bar screwed to the plywood. A butterfly screw was used to tighten the flat bar to the angle bar when the reflector was at the desired position.

3.6.6 Door

Aluminium sheet was used to fabricate an open box with dimension 0.6m x 0.2m x 0.1m. It was filled with sawdust and then covered with plywood of dimension 0.7m x 0.3m. Two cupboard handles were finally screwed to the plywood cover.

3.6.7 Support frame

The oven box was suspended from an inverted T-frame with rollers welded to the base for easy movement. The oven box was rotated about the horizontal axis and the inclination can be adjusted using a link which has one end fixed to the frame and the other end to the side of the oven box. A butterfly screw was used to tighten the link to the oven when the oven is at the desired inclination.

3.7 Simulation of Solar Oven Chamber Temperature

The solar oven model was simulated using Zaria solar data for 3rd and5th April. The stagnation temperature of the oven was simulated from 9:00am to 3:00pm on 3rd April, while simulation with 1.5kg of water as load was carried out for 5th April.

The tilt angles of the collector and reflectors were set to the optimum values obtained for the month of April as given in Tables 3.10 and 3.11 respectively, in the equations component of the TRNSYS environment. The model evaluates the energy absorbed in the oven chamber at intervals of one minute as specified in the control cards. These values were used in the EES model to calculate the temperatures of the glazing, oven chamber and water after every time step of one minute. The cooking power, standardised cooking power and temperature difference were also evaluated at these intervals. When the temperature of water reached 90 C, the oven chamber was reloaded and simulation restarted.

3.8 Experimental Setup

The system was setup as shown in appendix C. One end of each of the three thermocouples was attached to the glazing, levelling tray and pot. A pyranometer was placed on the collector with its plane parallel to the plane of the collector. The anemometer was mounted on the same level as the solar oven. The reflectors R1 and R2 were tilted at 85□ and 30□ respectively, which are the optimum tilt angles for the month of April.

3.9 Test Procedure

Tests were conducted to determine the performance of the solar oven based on the ASAE S580 standard.

The test was carried out on 3rd and 5th April 2014, at the Department of Mechanical Engineering workshop, Ahmadu Bello University, Zaria. The objective of the test was to obtain the continuous measurement of the system performance. In doing this, a consistent procedure was followed.

The surface azimuth was adjusted every ten minutes to make up for the change in solar azimuth. Temperature, solar radiation, and wind velocity readings were recorded every ten minutes as required. On the first day, the temperatures of the oven chamber, glazing and ambient air were recorded from 9:00am to 3:00pm with no load. On the second day, the system was setup with 1.5 kg of water in the pot. The pot was emptied and refilled when the temperature of water reached 90□C. This procedure was repeated three times in order to obtain an average value of the performance coefficient.

3.10 Error Analysis

The root mean square error (R.M.S) was used to determine the level of deviation of the predicted result from the actual result. The R.M.S measures the quality of fit between the actual data and the predicted model (Julien *et al.*, 2013).

The RMSE of a model prediction with respect to the estimated variable X_{model} is defined as the square root of the mean squared error (Neil, 2010).

$$RMSE = \sqrt{\frac{\sum_{i=1}^{n}(X_{obs,i} - X_{model,i})^2}{n}} \qquad (3.57)$$

Where:

X_{obs} is observed values

X_{model} is modelled values

The lower the Mean Absolute Error or the Bias Percentage value, the better the performance of the model (Neil, 2010).

Furthermore, the Nash-Sutcliffe Coefficient of Efficiency (NSE) defined as follows:

$$NSE = 1 - \frac{\sum_{i=1}^{n}(X_{obs,i} - X_{model})^2}{\sum_{i=1}^{n}(X_{obs,i} - \overline{X_{obs}})^2}, \qquad (3.58)$$

Where:

X_{obs} is observed value

X_{model} is modelled value

NSE is generally used to quantitatively describe the accuracy of model outputs. Nash-Sutcliffe efficiencies can range from -∞ to 1. An efficiency of 1 (NSE = 1) corresponds to a

perfect match between model and observations. An efficiency of 0 indicates that the model predictions are as accurate as the mean of the observed data, whereas an efficiency less than zero ($-\infty < E < 0$) occurs when the observed mean is a better predictor than the model (Julien *et al.*, 2013).

Equations 3.62 and 3.63 were modelled in EES and used to determine the RMSE and NSE values of the results obtained from the experiments and simulations. The model is shown in appendix E.

CHAPTER FOUR

RESULTS AND DISCUSSUION

4.1Optimisation of Design Parameters

4.1.1 Monthly optimum collector slope

Figures 4.1 and 4.2 show simulated average monthly solar radiation incident on surfaces at different tilt angles for each month of the year in Zaria. The tilt angle at which the highest average radiation value is observed is the optimum collector slope for the month. The optimum collector tilt angles for each month is summarised in table 4.1.

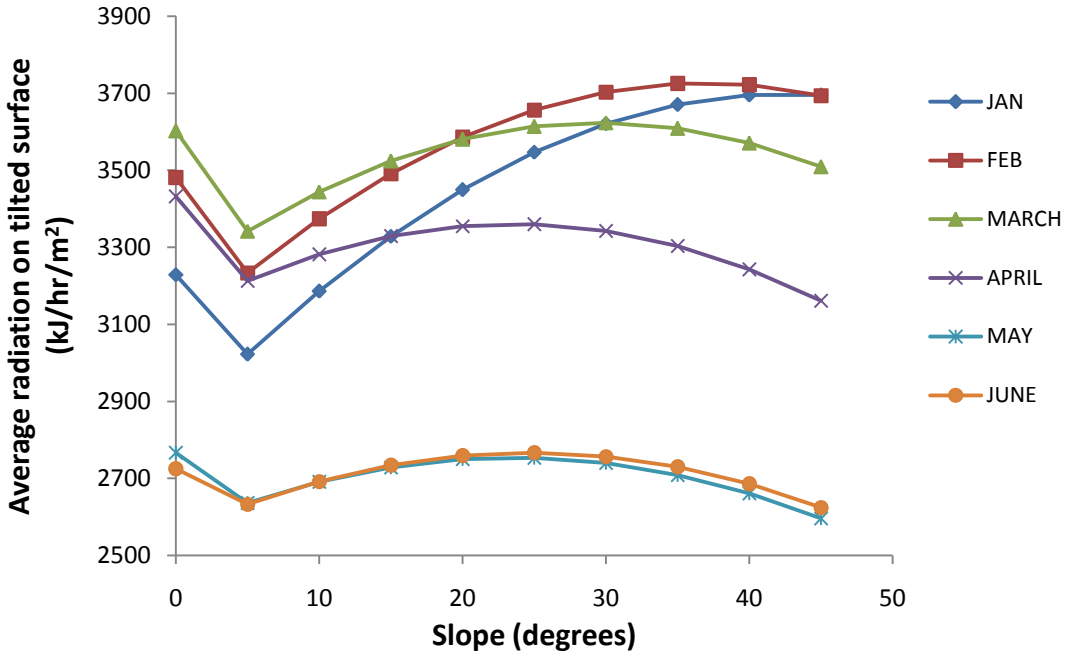

Figure 4.1: Variation of the average radiation incident on tilted surface for different values of tilt angles (β_c) for the months of January to June.

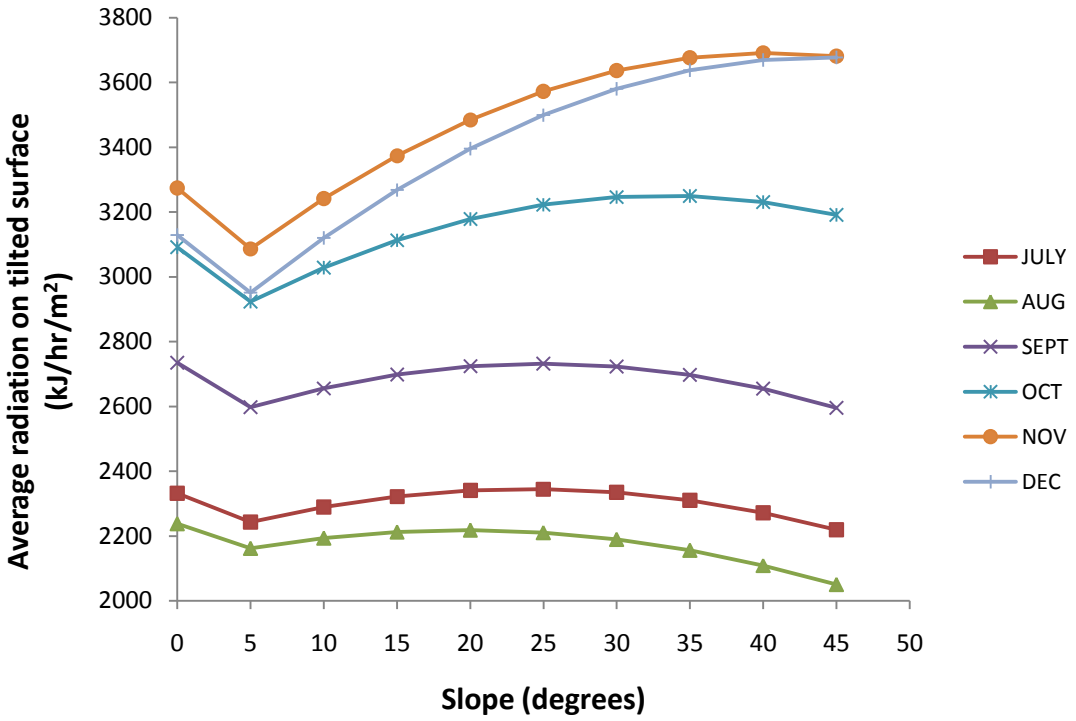

Figure 4.2: Variation of the average radiation incident on tilted surface for different values of tilt angles (β_c) for the months of July to December.

Table 4.1: Monthly optimum tilt angles of collector

Month	Slope (°)
January	45
February	35
March	30
April	0
May	0
June	25
July	25
August	0
September	0
October	35
November	40
December	45

4.1.2 Monthly optimum tilt angles of reflectors, R_1 and R_2

The monthly average absorbed solar radiation was simulated as a function of reflector tilt angles (β_{r1} and β_{r2}). The results plotted for each month of the year are shown in figures 4.3 through 4.14.

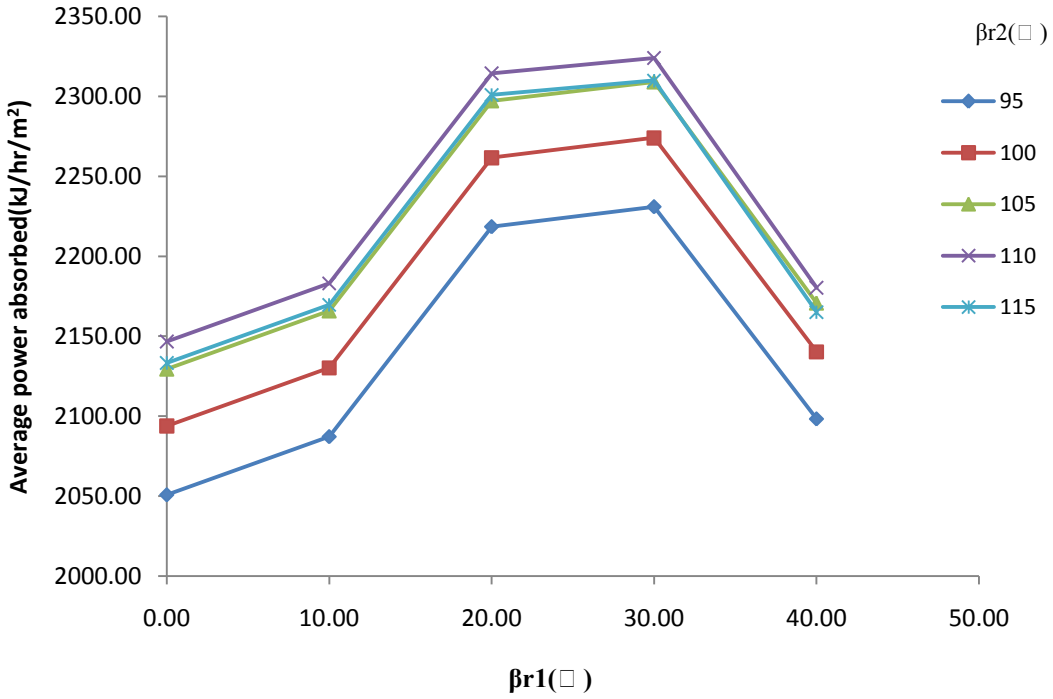

Figure 4.3: Variation of average power absorbed by the solar oven with β_{r2} for different values of β_{r1} for the month of January.

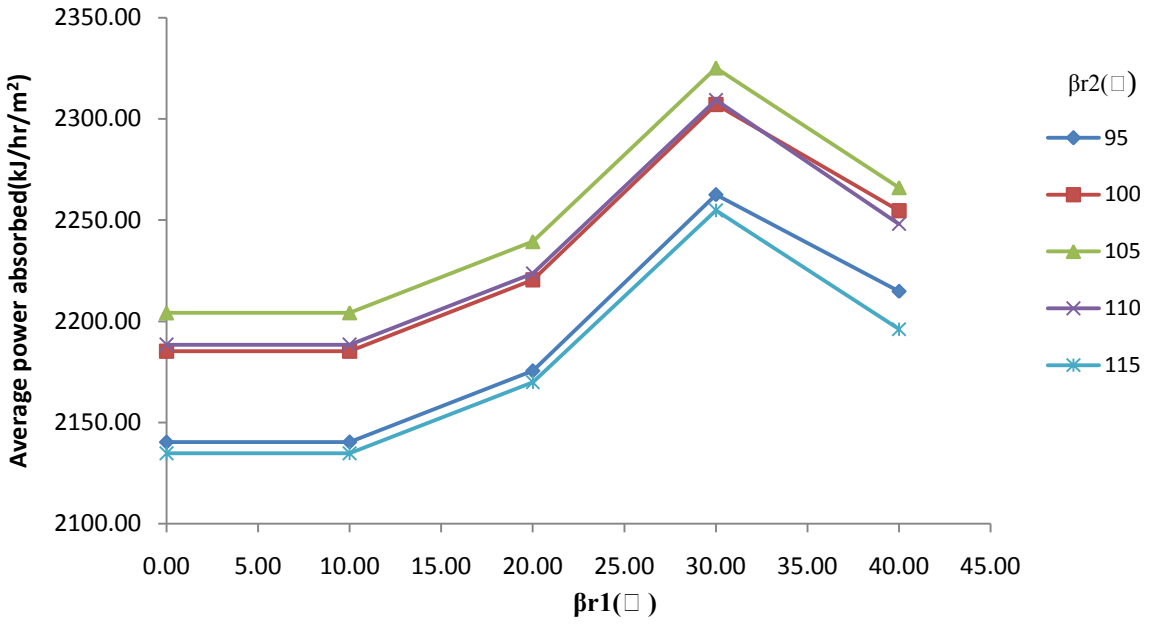

Figure 4.4: Variation of average power absorbed by the solar oven with β_{r2} for different values of β_{r1} for the month of February.

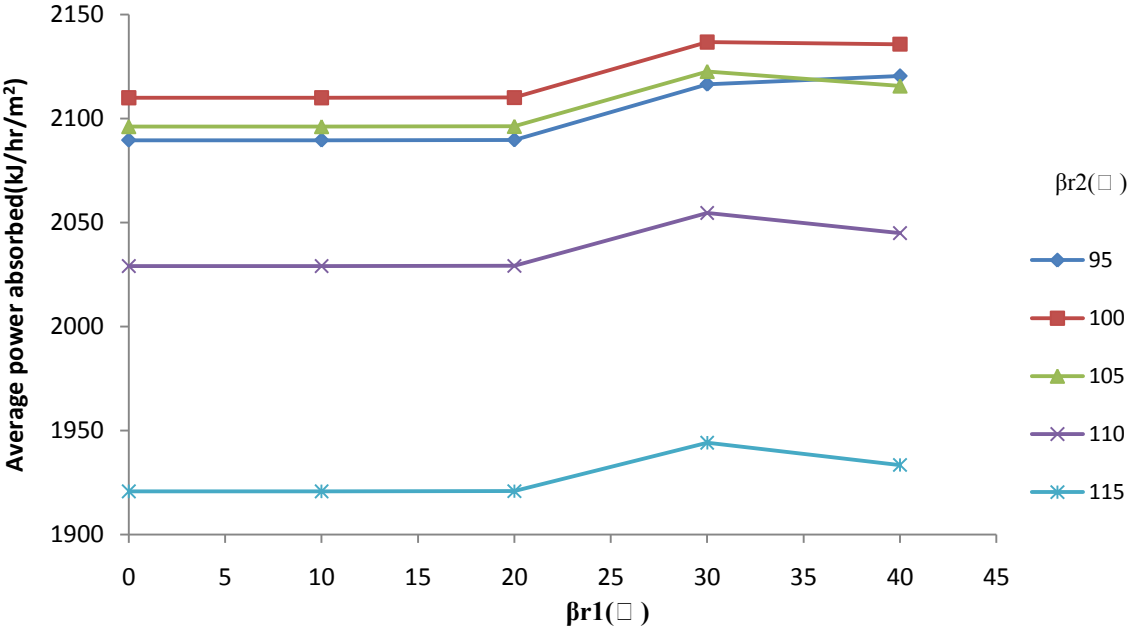

Figure 4.5: Variation of average power absorbed by the solar oven with β_{r2} for different values of β_{r1} for the month of March.

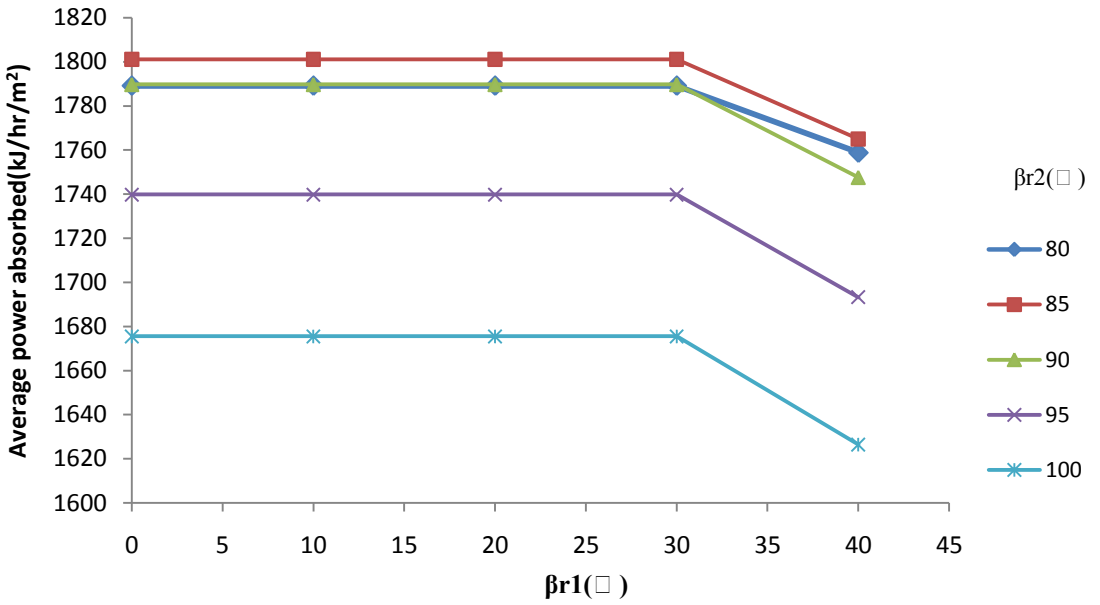

Figure 4.6: Variation of average power absorbed by the solar oven with β_{r2} for different values of β_{r1} for the month of April.

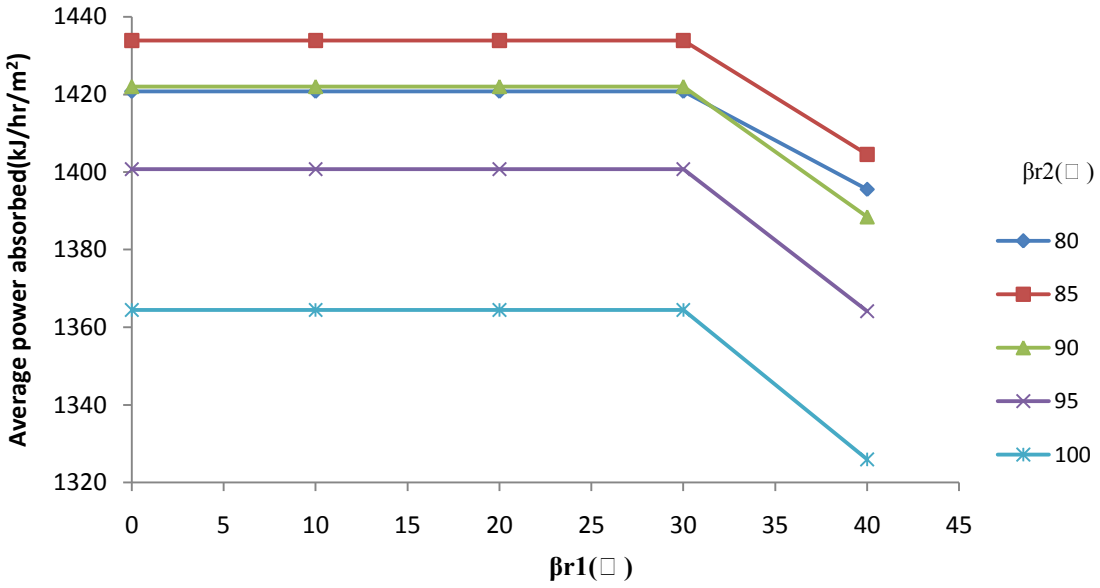

Figure 4.7:Variation of average power absorbed by the solar oven with β_{r2} for different values of β_{r1} for the month of May.

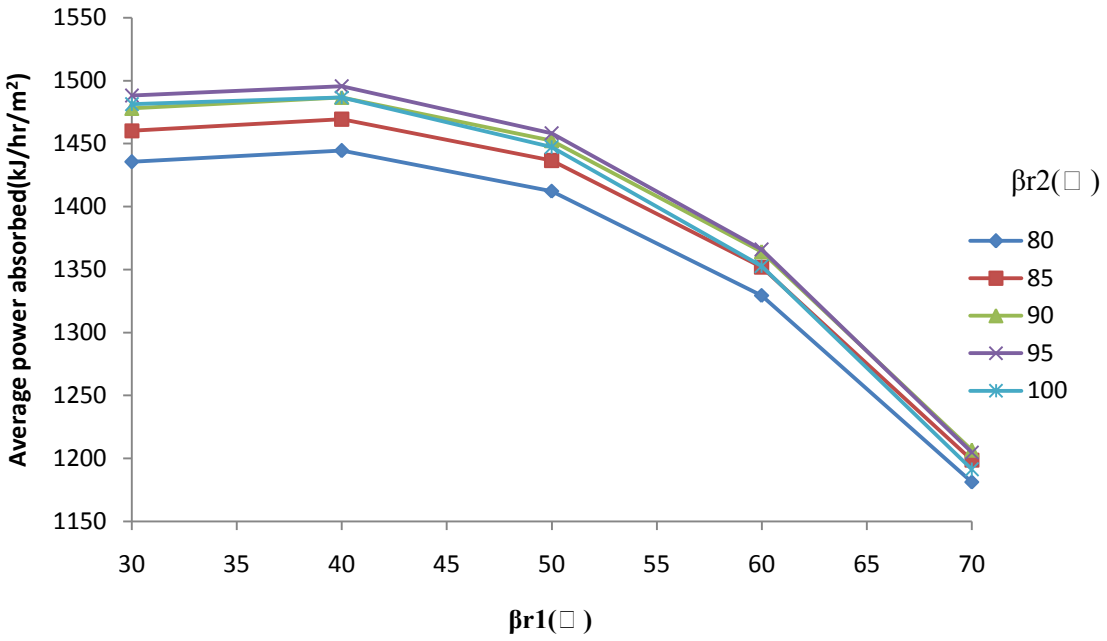

Figure 4.8: Variation of average power absorbed by the solar oven with β_{r2} for different values of β_{r1} for the month of June.

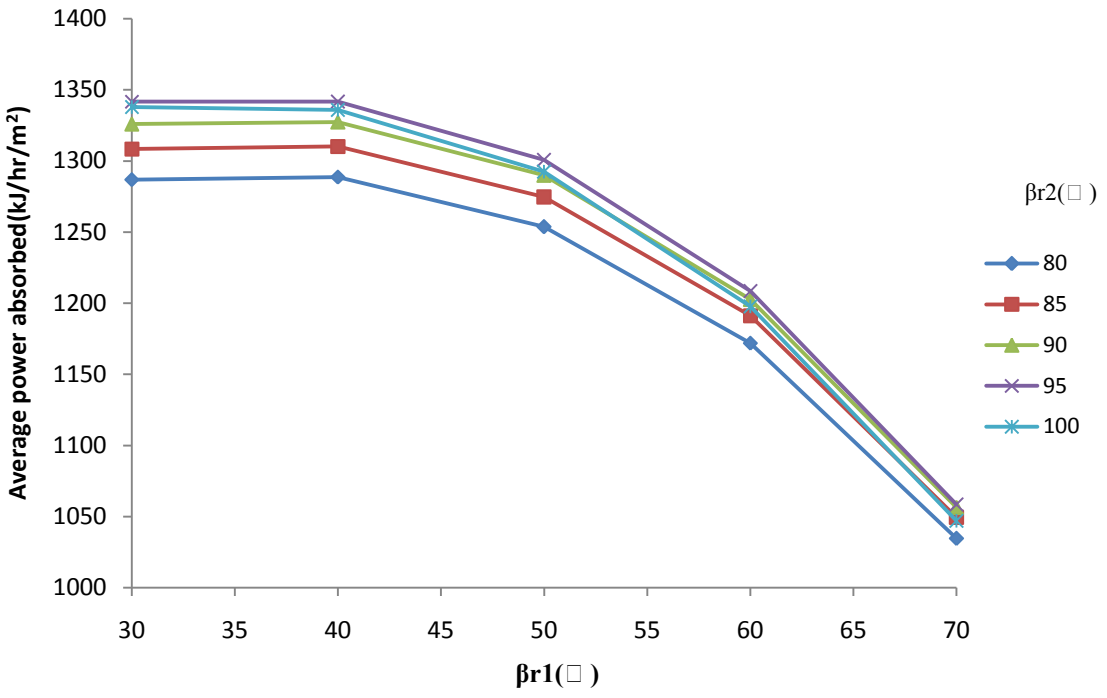

Figure 4.9: Variation of average power absorbed by the solar oven with β_{r2} for different values of β_{r1} for the month of July.

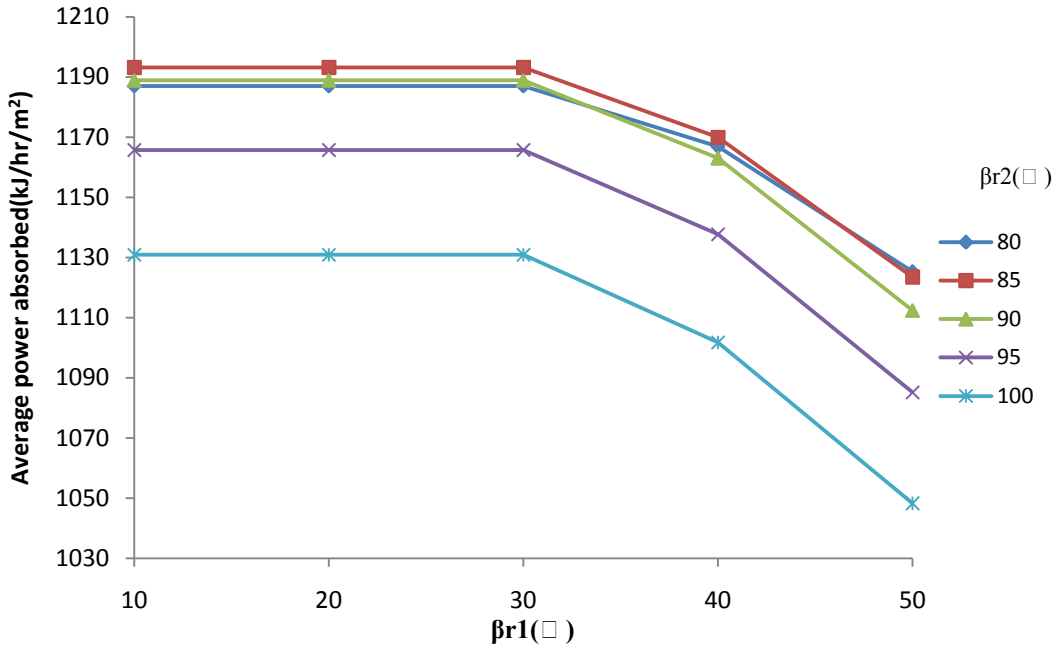

Figure 4.10: Variation of average power absorbed by the solar oven with β_{r2} for different values of β_{r1} for the month of August.

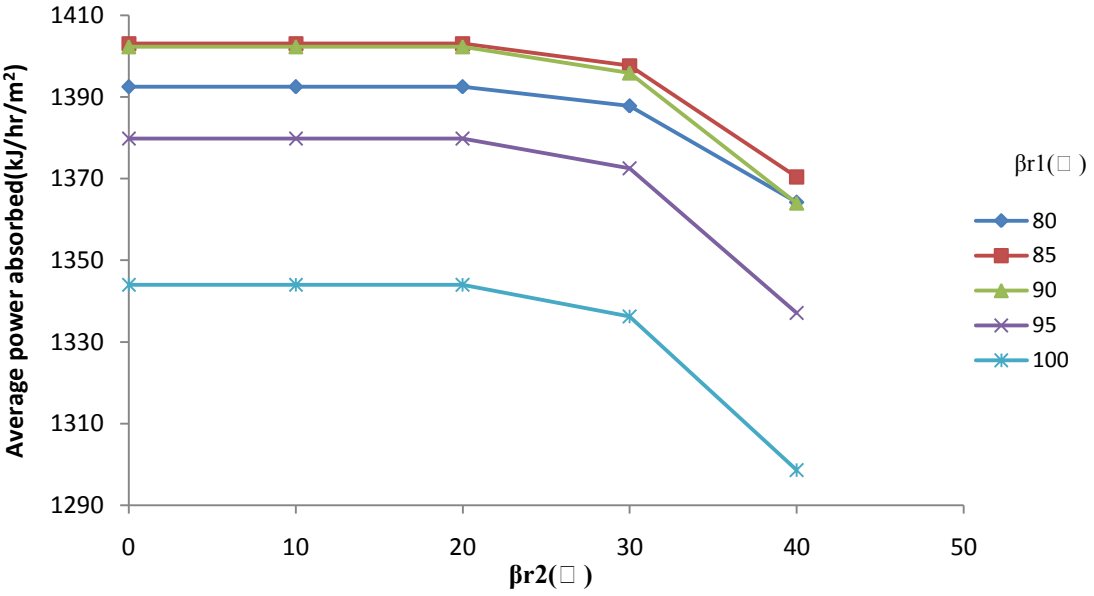

Figure 4.11: Variation of average power absorbed by the solar oven with β_{r2} for different values of β_{r1} for the month of September.

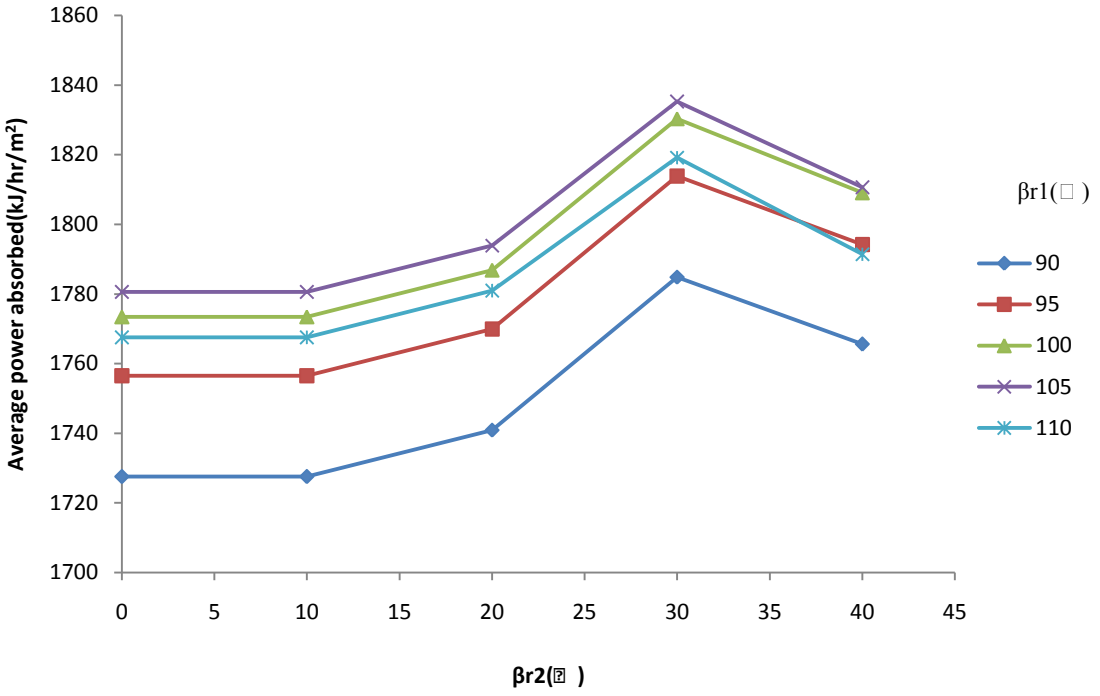

Figure 4.12: Variation of average power absorbed by the solar oven with β_{r2} for different values of β_{r1} for the month of October.

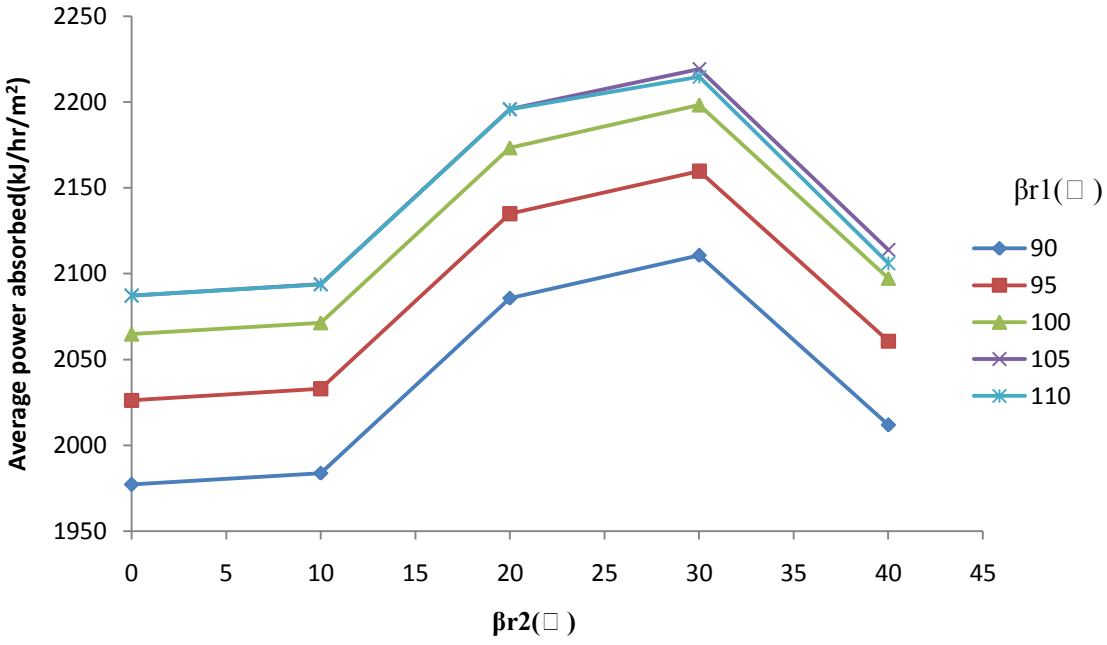

Figure 4.13: Variation of average power absorbed by the solar oven with β_{r2} for different values of β_{r1} for the month of November.

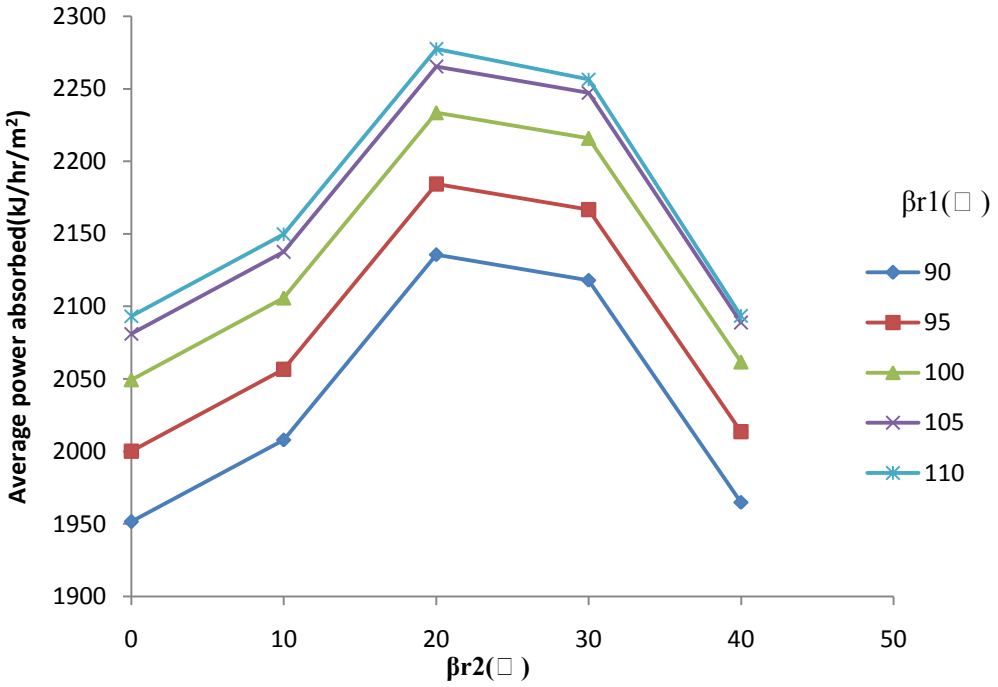

Figure 4.14: Variation of average power absorbed by the solar oven with β_{r2} for different values of β_{r1} for the month of December.

From Figures 4.3 to 4.14, the optimum tilts for reflectors R1 and R2 for each month of the year are obtained. This is summarised in Table 4.2.

Table 4.2: Optimum monthly tilts of reflectors R1 and R2

Month	**β_{r1} (degrees)**	**β_{r2} (degrees)**
January	30	110
February	30	105
March	30	100
April	30	85
May	30	85
June	40	95
July	30	95
August	10	85
September	85	0
October	105	30
November	105	30
December	110	20

4.1.3 Design month

From Figures 4.1 and 4.2, it is observed that August has the lowest monthly average solar irradiance which makes it the design month. The weather condition for the recommended average day for the month of August (16th August) was utilized.

Figure 4.15 presents the incident solar radiation on a horizontal surface and ambient temperature on16th August (5448-5472hrs) in Zaria.It can be observed that there is steady increase in solar radiation intensity from 12 noon (5460hrs) until it reaches its peak at about 3 p.m. (5463hrs), from then it decreases gradually till 8p.m (5468hrs) when the sun sets. The solar oven model was simulated within this time interval (12noon-3:00p.m).

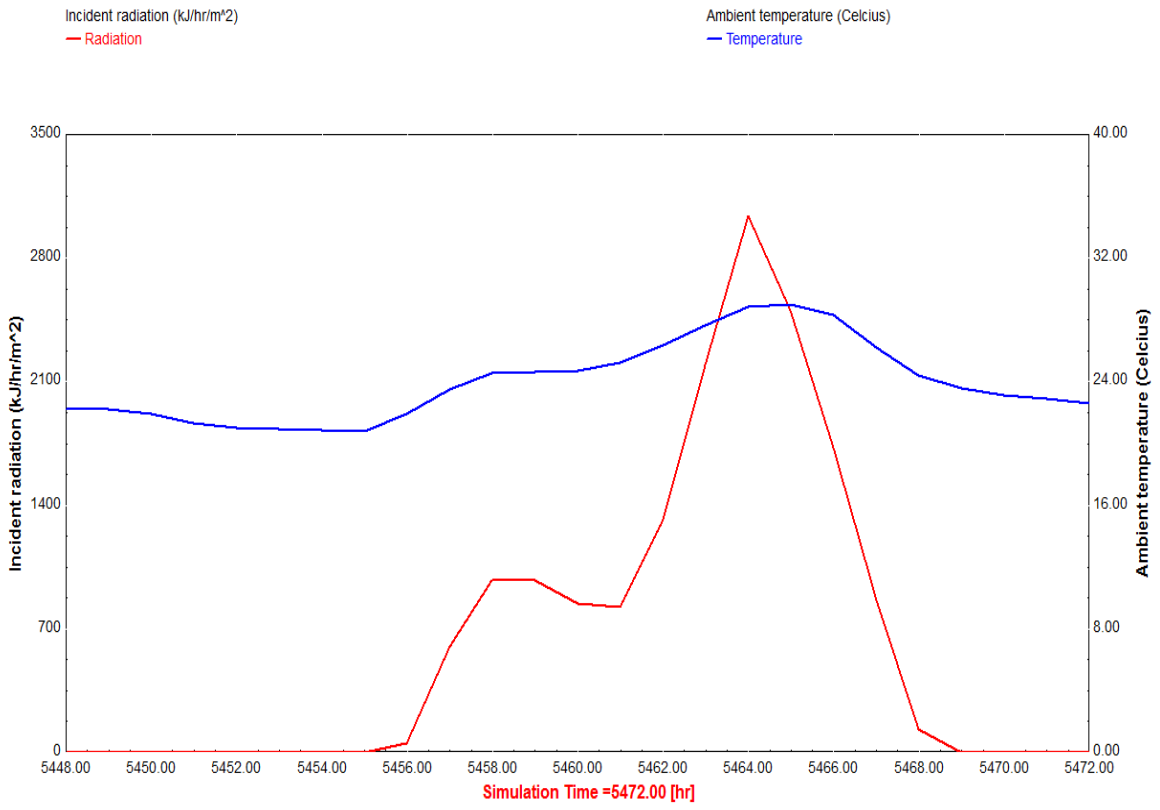

Figure 4.15: Solar radiation and ambient temperature variation for 16th August for Zaria.

4.1.4 Optimum collector area and insulation thickness

Figures 4.16 to 4.21 show the temperature profile of the solar oven at stagnation (no load) between 12pm and 4pm on 16th August for the different areas and insulation thicknesses.

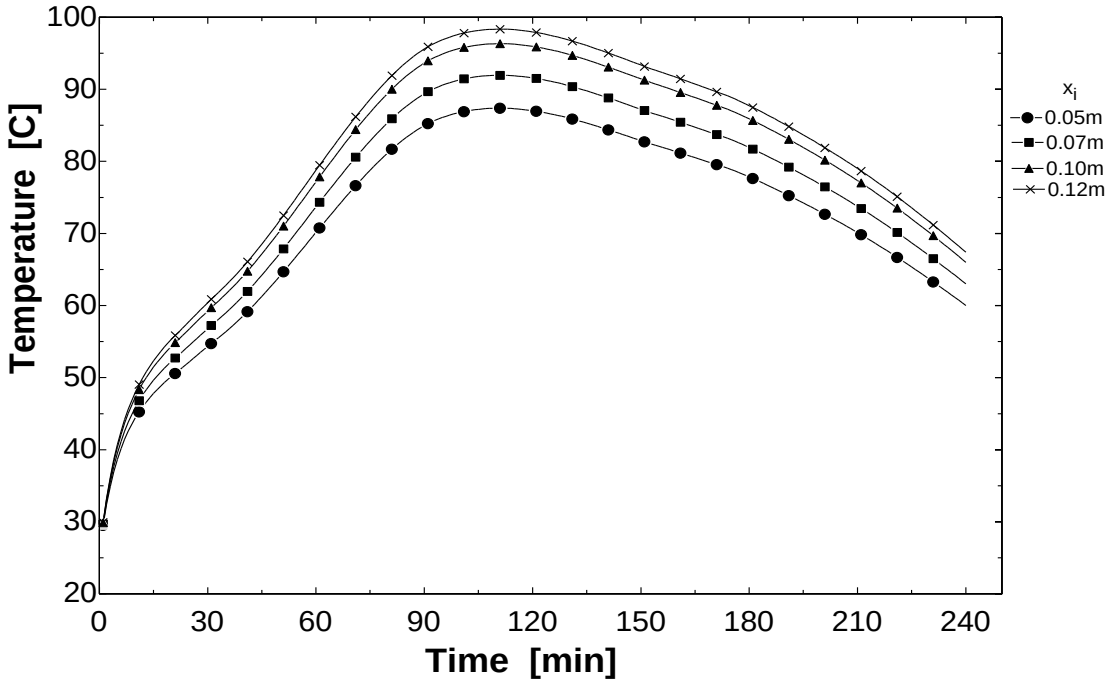

Figure 4.16: Temperature profile of oven box for collector area of 0.25m^2, with insulation thickness of 0.05m, 0.07m, 0.10m and 0.12m

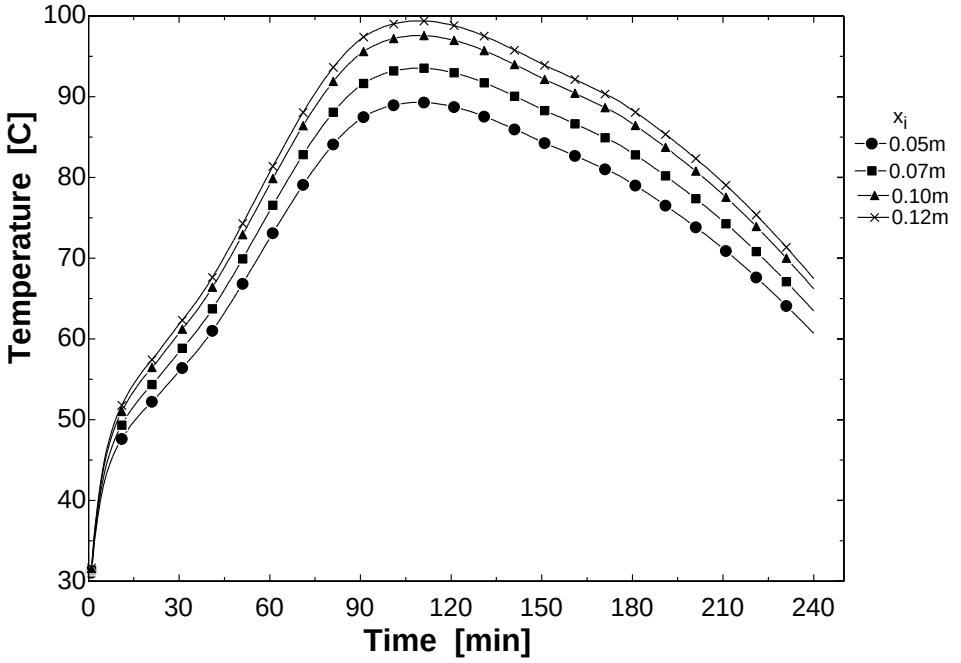

Figure 4.17: Temperature profile of oven box for collector area of 0.36m^2, with insulation thickness of 0.05m, 0.07m, 0.10m and 0.12m

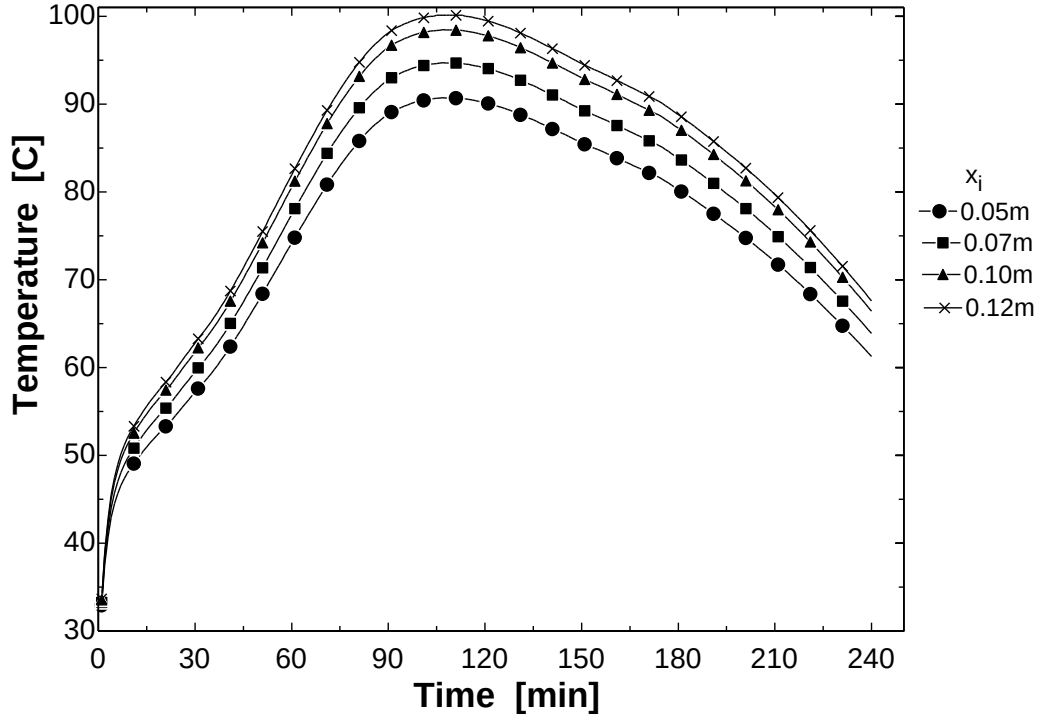

Figure 4.18: Temperature profile of oven box for collector area of 0.49m^2, with insulation thickness of 0.05m, 0.07m, 0.10m and 0.12m

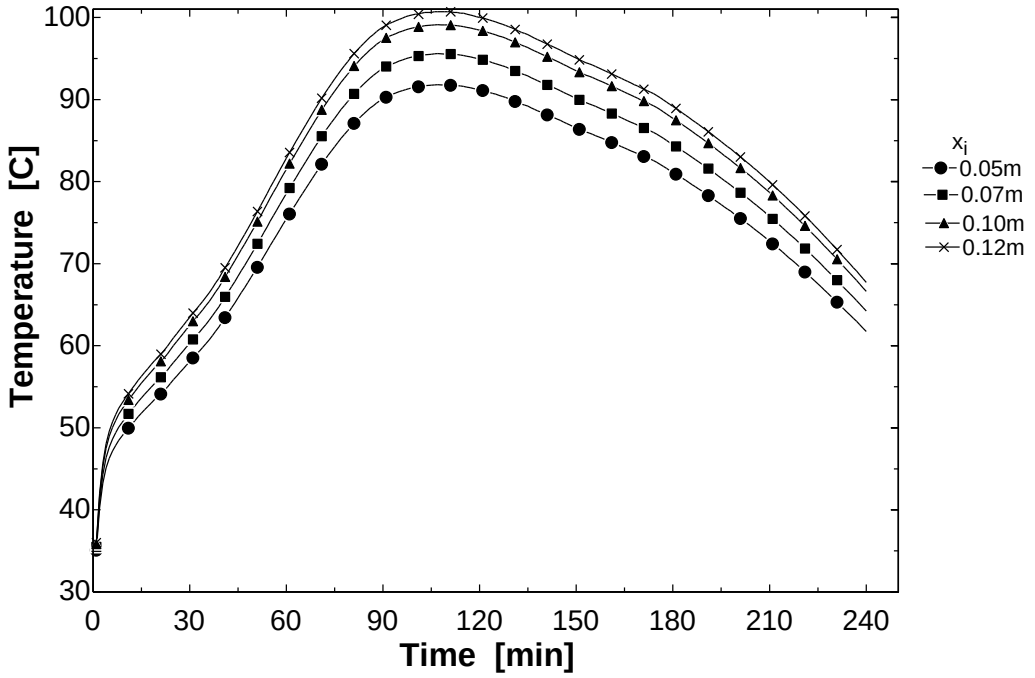

Figure 4.19: Temperature profile of oven box for collector area of 0.64m^2 with insulation thickness of 0.05m, 0.07m, 0.10m and 0.12m

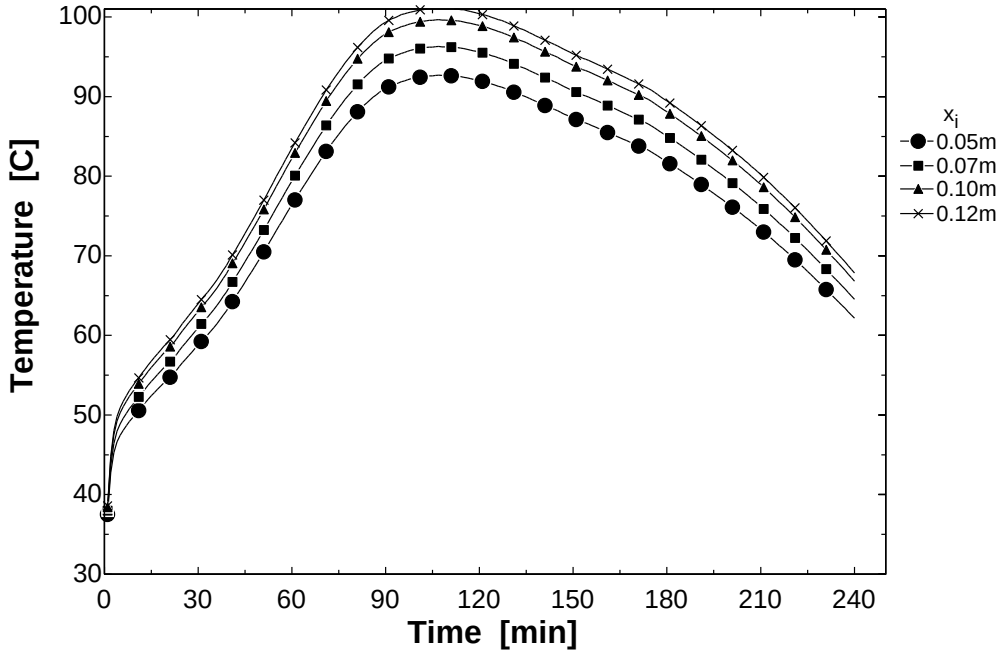

Figure 4.20: Temperature profile of oven box for collector area of 0.81m^2 with insulation thickness of 0.05m, 0.07m, 0.10m, and 0.12m.

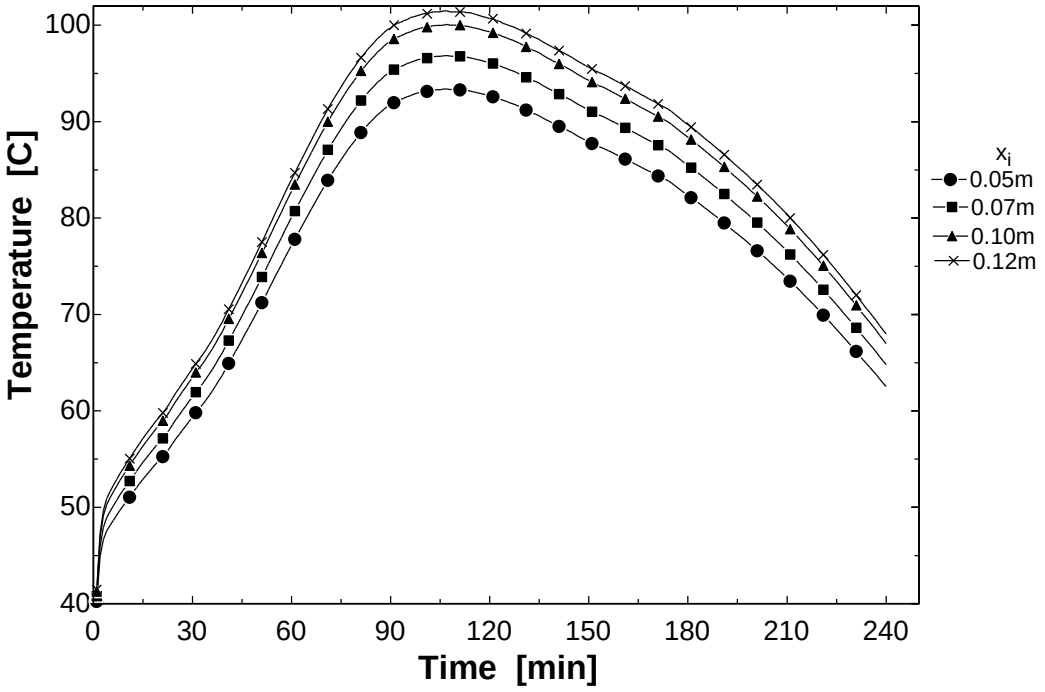

Figure 4.21: Temperature profile of oven box for collector area of 1.00m^2, with insulation thickness of 0.05m, 0.07m, 0.10m and 0.12m

From Figures 4.16 through 4.21, it is observed that: for collector areas of 0.36m^2 and below, the stagnation temperature is less than 100□C. For collector area of 0.49m^2 and insulation thickness of 0.12m, the stagnation temperature is 100□C. Further increase in area (0.64m^2, 0.81m^2, 1.00m^2) does not yield any significant increase in stagnation temperature, therefore a collector area of 0.49m^2 and insulation thickness of 0.12m were selected for the oven box design.

4.2 Experimental Results

The results of the experiments and theoretical results are presented in figures 4.22 through 4.34. Temperatures as well as the solar radiation (on primary y-axis) are plotted with local time. The results obtained from experiments were compared with the simulated results. The aim was to obtain the trend and the level of agreement of the experimental results with the simulated ones.

The root mean square error (RMSE) statistical tool was used to analyse the predictive power of the simulation model.

4.2.1 Observations

Figure4.22shows the radiation incident on the collector surface on 3rd April, 2014. It can be observed that the experimental values fluctuate around the simulated values. This may be attributed to the intermittent cloud cover. However, the simulated values appear to be an average of the experimental values. On 5th April 2014, the actual incident radiation is underestimated from 9:00am to 11:50am as can be observed from figure 4.23, but the simulated radiation seems to be in close agreement with the actual radiation for the rest of the time.

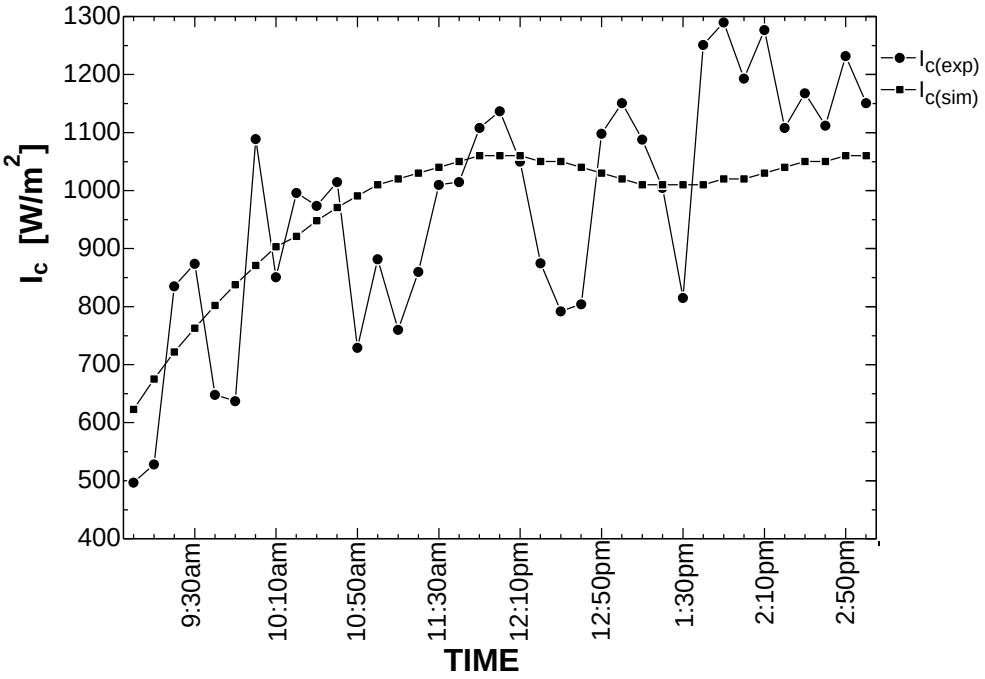

Figure 4.22: Experimental and simulated incident solar radiation with local time (3April, 2014).

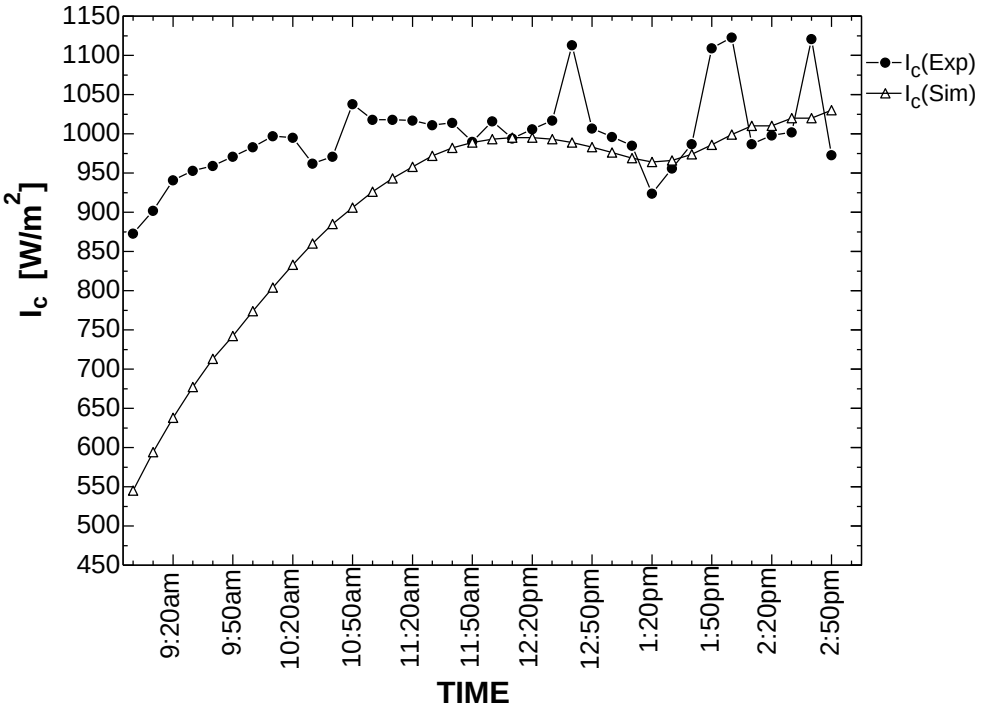

Figure 4.23: Experimental and simulated incident solar radiation with local time (5th April, 2014).

The actual and predicted values of ambient temperature for 3rd April follow a similar trend, with the actual values higher than the simulated values as observed from figure 4.24. This may be due to lower wind velocities on the experimental day. The experimental and simulated values of ambient temperature on 5th April seem to be in close agreement for most part of the time period.

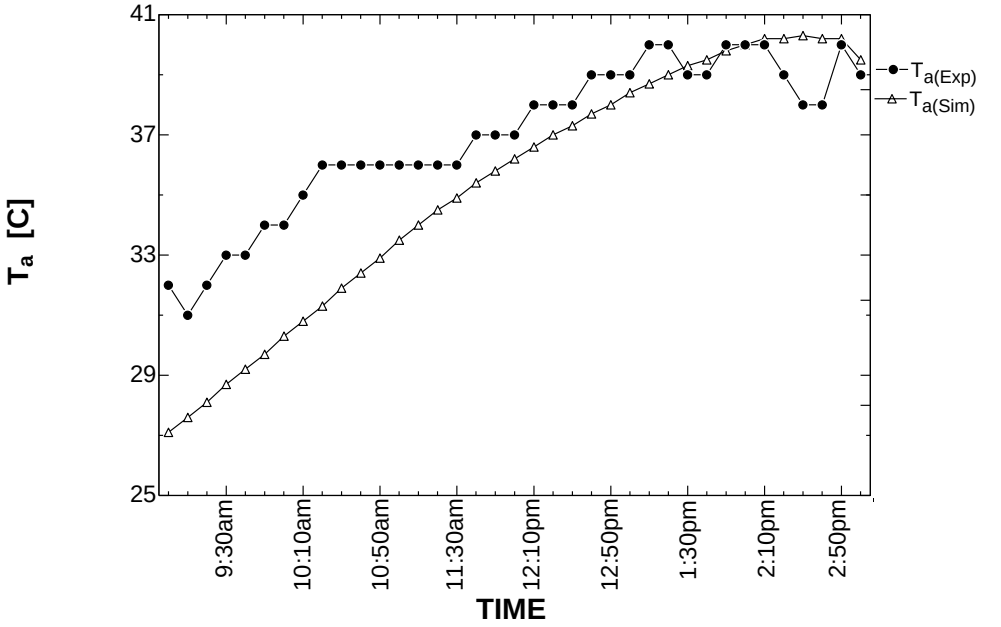

Figure 4.24: Experimental and simulated values of ambient temperature with local time (3rd April, 2014).

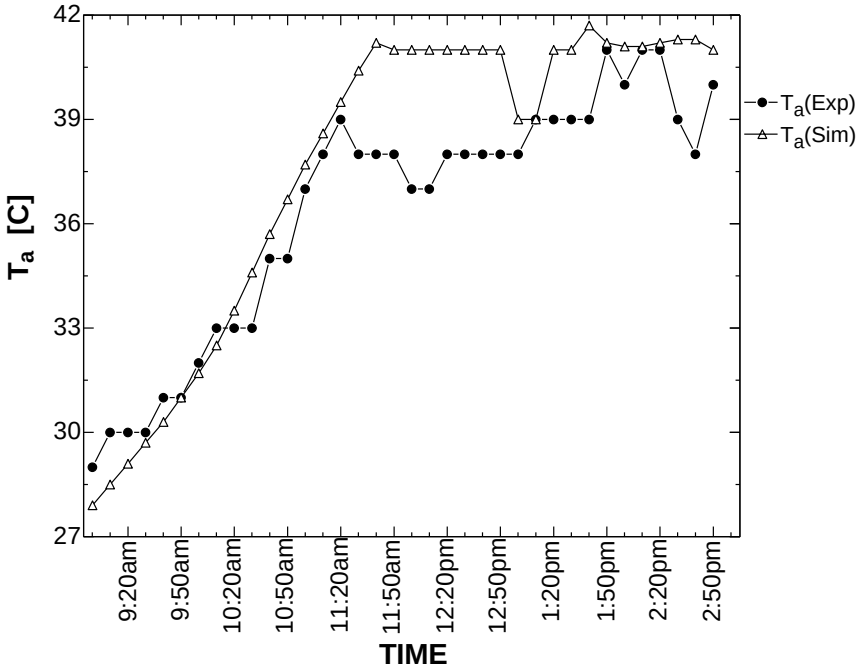

Figure 4.25: Experimental and simulated ambient temperature with local time (5th April, 2014).

Figure 4.25 shows the actual and simulated values of the stagnation temperature of the solar oven without load. Both values follow the same trend from 9am to 10:20am. From 10:20am

to 12:40pm, lower actual values are noticed, after which the actual temperatures become higher. However, both values are in close agreement for most time of the duration.

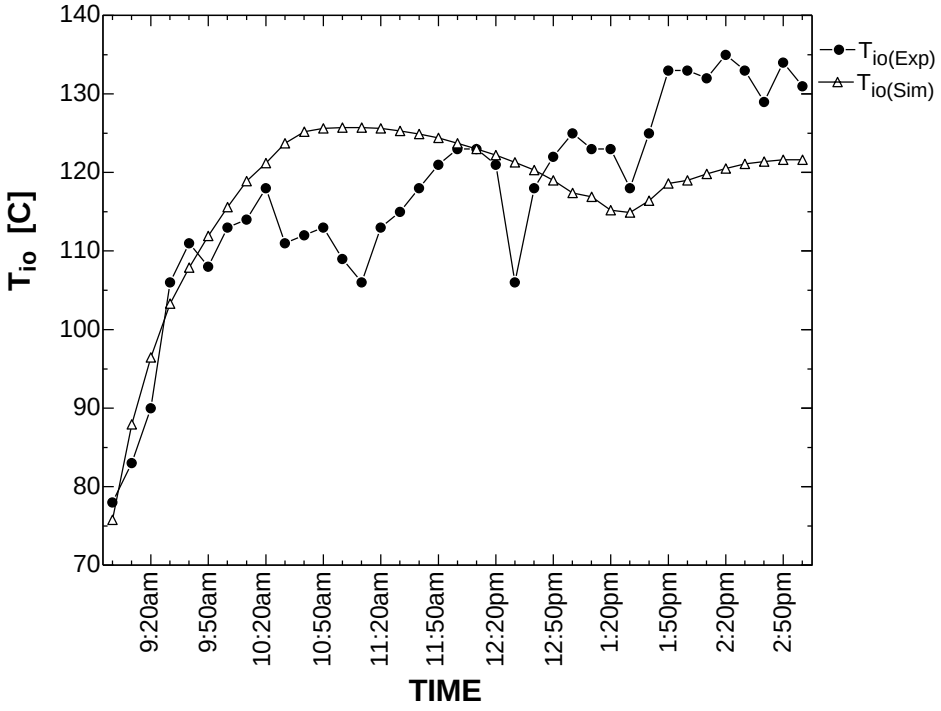

Figure 4.26: Experimental and simulated temperatures for oven chamber with local time (3 April, 2014).

The experimental and simulated temperature profiles of the cooking fluid (water) are shown in Figures 4.27 through 4.34. The results indicate that the solar oven was loaded eight times when the temperature reached 90□C. A summary of the duration of each stage of loading and final temperature at the end of each stage is presented in Table 4.1. Although the experimental results show higher temperatures, the simulated values are in close agreement with the actual values.

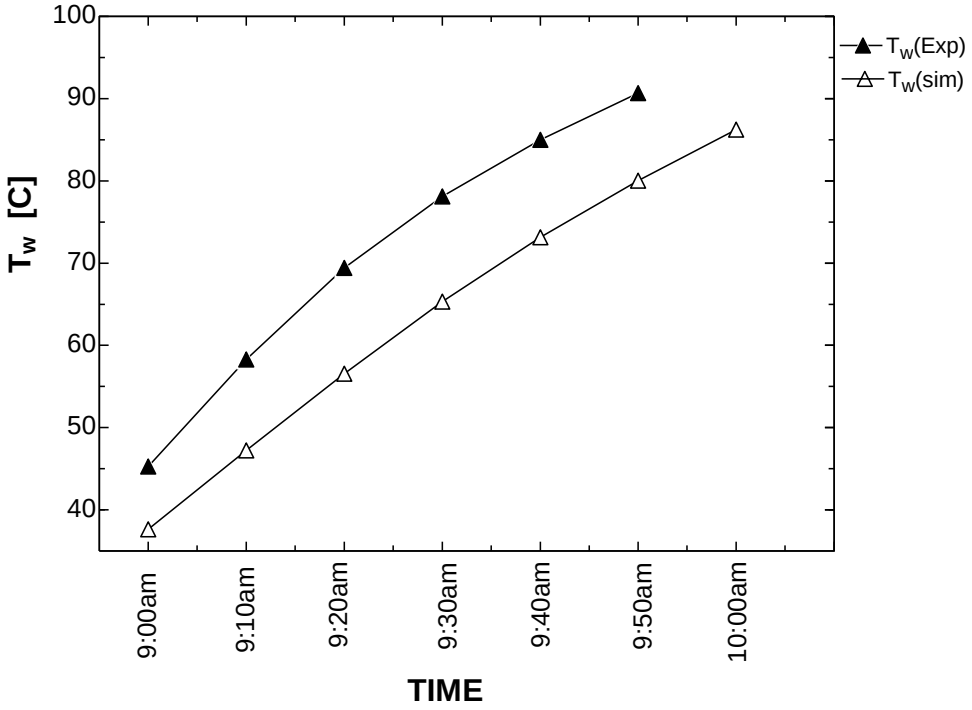

Figure 4.27: Experimental and simulated temperature profile of water from 9:00am to 10:00am (5th April, 2014).

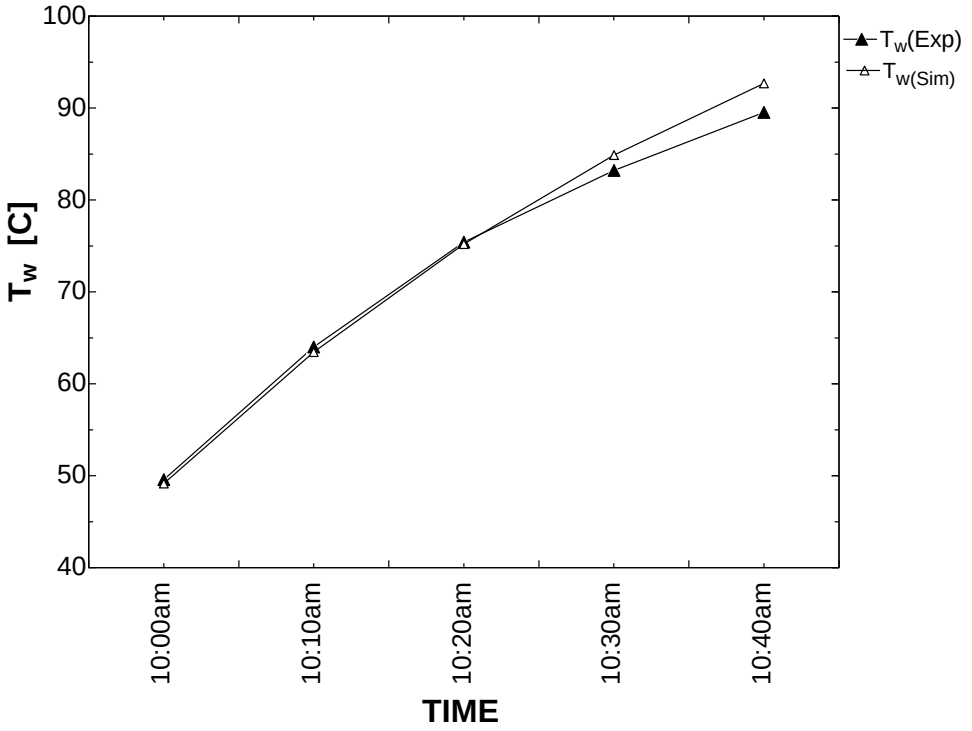

Figure 4.28: Experimental and simulated temperature profile of water from 10:00am to 10:40am (5th April, 2014).

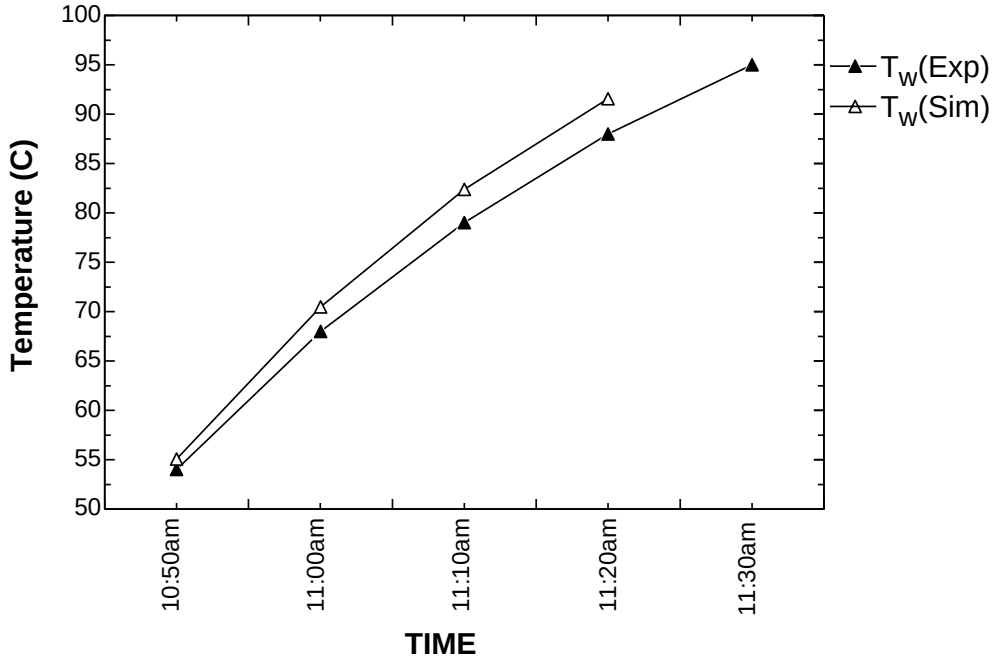

Figure 4.29: Experimental and simulated temperature profile water from 10:50am to 11:30am (5th April, 2014).

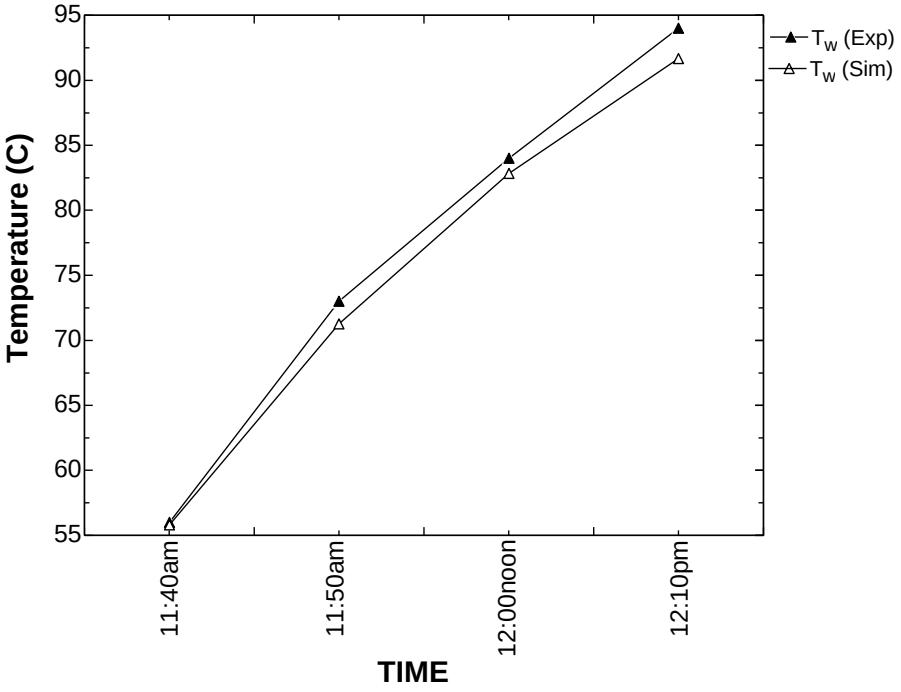

Figure 4.30: Experimental and simulated temperature profile of water from 11:40am to 12:10pm (5th April, 2014).

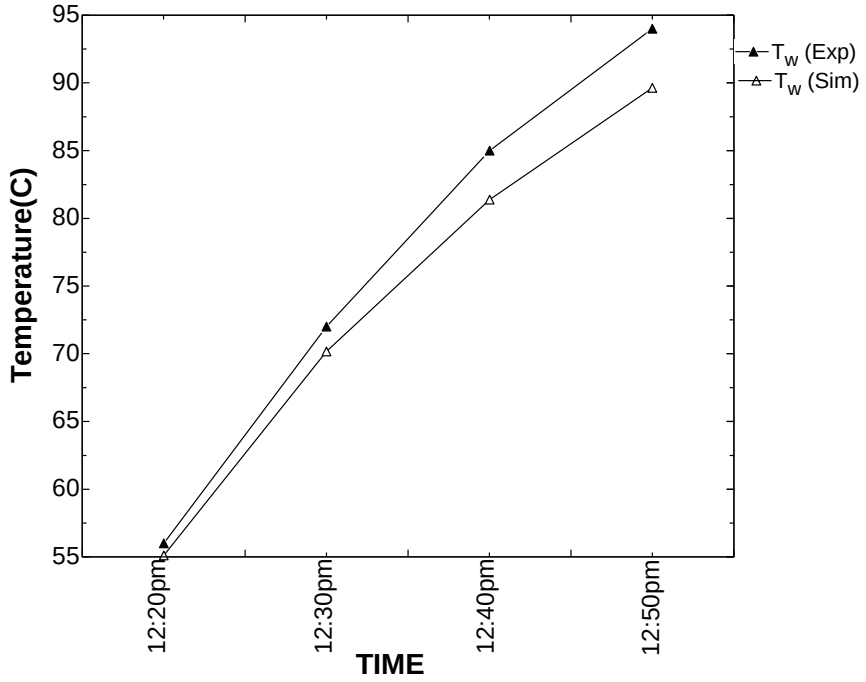

Figure 4.31: Experimental and simulated temperature profile of water from 12:20am to 12:50pm (5th April, 2014).

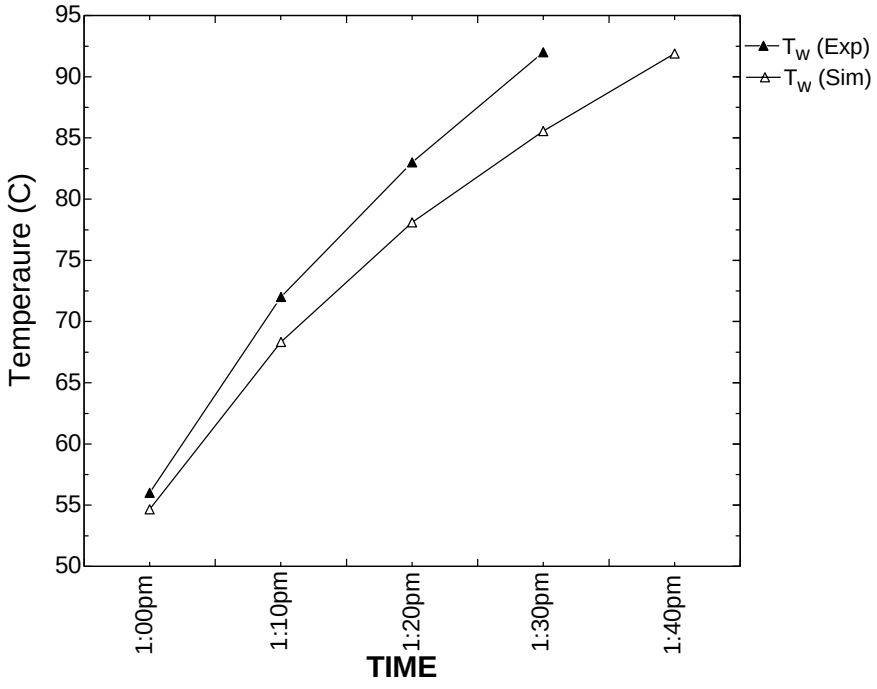

Figure 4.32: Experimental and simulated temperature profile of water from 1:00am to 1:40pm (5th April, 2014).

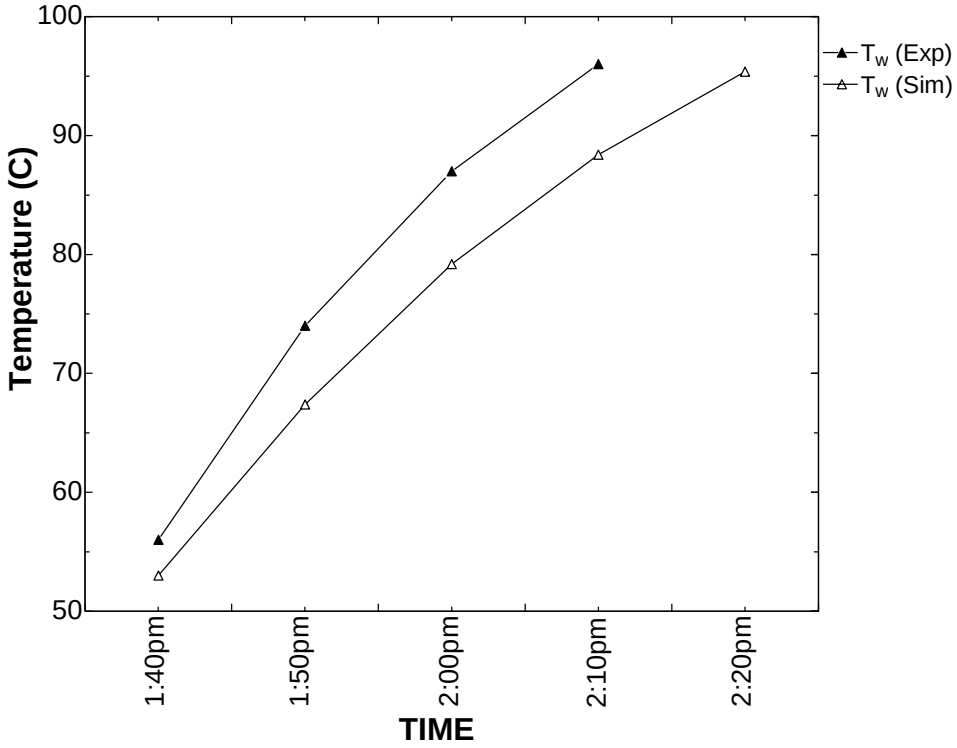

Figure 4.33: Experimental and simulated temperature profile of water from 1:40am to 2:20pm (5th April, 2014).

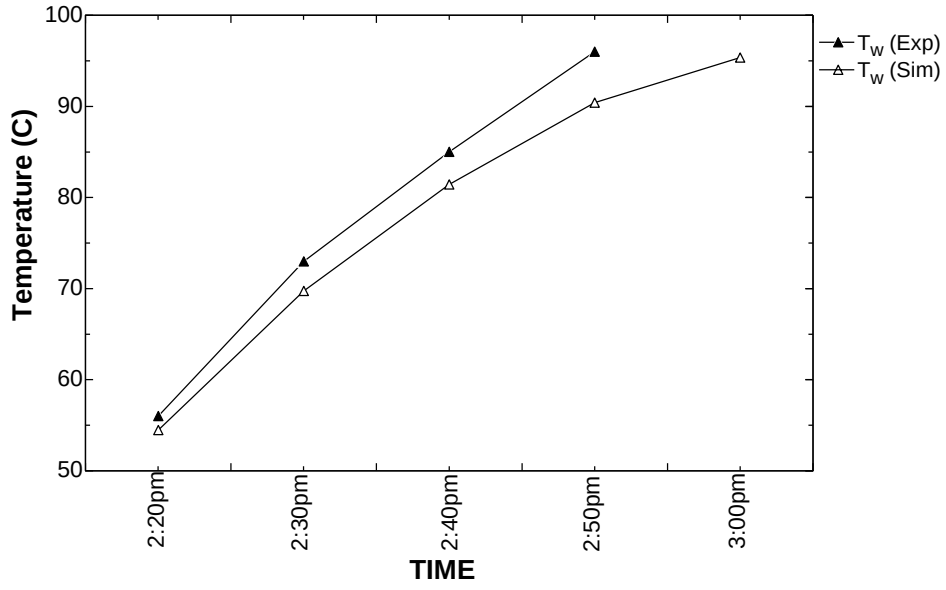

Figure 4.34: Experimental and simulated temperature profile of water from 2:20am to 3:00pm (5th April, 2014).

Table 4.3: Duration and final temperature of water at the end of each loading stage

TIME	Duration (min)	Final temperature(C)	
		Experiment	Simulation
9:10am-10:00am	60	91	80
10:10am-10:50am	50	90	92
11:00am-11:40am	40	95	92
11:50am-12:20pm	40	94	92
12:30pm-1:00pm	40	94	90
1:10pm-1:40pm	40	92	86
1:50pm-2:20pm	40	96	88
2:30pm-3:00pm	40	96	90

4.2.2 Error analysis

The RMSE and NSE analysis of the experimental and simulation based on the results for 3rd April 2014 and 5th April 2014 were obtained using the EES code shown in appendix E. The results are presented in appendix E. The experimental and simulation results of 3rd April (stagnation test) show a RMSE value of 8.75 C and NSE of 0.6. The results of 5th April (sensible heat test) show RMSE of 5.72 and NSE of 0.85. The outcomes of the analysis indicate minimal deviation of predicted result from the actual result and also a good quality of fit.

4.2.3 System performance measurement

Thesystemperformancewas evaluated from the experimental results of 5th April, 2014 using the ASAE standard. The temperature difference and the standardised cooking power

evaluated from the results of the experiment and simulation is presented in appendix E. The plotted results of the experiment and simulation together with the regression equation obtained using EES are shown in Figures 4.35 and 4.36 respectively. The coefficients of determination (R^2) for the results of experiment and simulation were found as 97.54% and 95.71% respectively which are within the limits recommended in the ASAE standard.

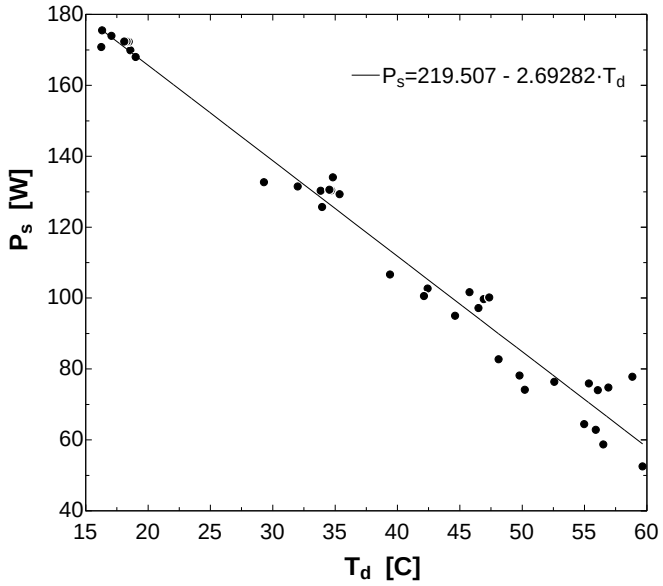

Figure 4.35: Adjusted cooking power plotted over temperature difference and the resulting regression line for experimental results.

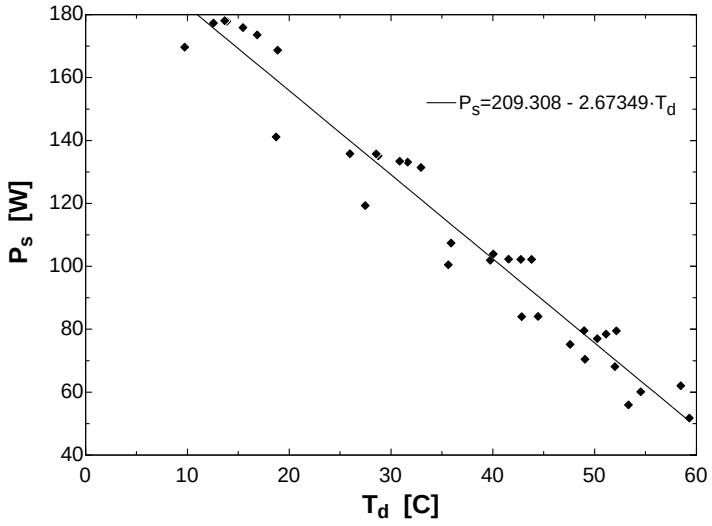

Figure 4.36: Adjusted cooking power plotted over temperature difference and the resulting regression line for simulation results.

The values of standardised cooking power for a temperature difference of 50°C are computed as 84.87W and 75.63W using the regression equations for the experimental and simulation results respectively.

4.2.4 Cost evaluation

Evaluation of the cost of oven was based on material, labour and overhead costs. The material cost involves the detailed breakdown of materials. Labour cost involves the expenses incurred during the manufacturing process. Overhead cost entails the transportation and miscellaneous expenses. Table 4.4 and 4.5 give details of the system cost.

Table4.4**:** Materialcost

	COMPONENT	**MATERIAL**	**COST(Naira)**
1	Inner and outer box	Plywood	8 000
2	Insulation	Saw dust	300
3	Inner chamber	Aluminium sheet	1 800
4	Glazing	Glass	1 400
5	Reflectors	Back-silvered glass	2 000
6	Frame stand	Mild steel	1 000
7	Bolts, nuts and washers	Grade 4.8 steel	80
8	Paint	Oil paint	900
9	Levelling tray	Mild steel	600

Subtotal=N16 080

Table 4.5: Labour and Overhead Cost

	TYPE OF LABOUR	**COST (NAIRA)**
1	Cost of producing the collector with reflectors, insulation, glazing etc	2 500
2	Cost of cutting the frame and producing the stand	1 800
3	Cost of transportation and miscellaneous expenses	1 200

Subtotal= N5 500

Grand total=N21 580

CHAPTER FIVE

SUMMARY, CONCLUSIONS AND RECOMMENDATIONS

5.1 Summary

A solar oven with reflectors was designed, simulated and constructed at Ahmadu Bello University Zaria, Nigeria. The system design was modelled using TRNSYS, Microsoft Excel, and EES. The design was modelled in four parts;

First, the typical meteorological year (TMY) solar data of Zaria obtained from www.solaranalytical.com was processed to obtain the monthly average daily solar resources of Zaria using the solar radiation and weather data processor TYPE 109 component of TRNSYS 16 software. Since solar radiation varies randomly with time, the month with the least average daily solar radiation was considered as the design month. The result showed that the month of August has the least solar radiation and therefore, considered as the design month.

Second, the enhancement of radiation by the plane reflectors on the collector at any hour of the day for random tilt angles and azimuth angles of collector and reflectors was modelled. Shadowing effect of the reflector on the collector was also taken care of.

Third, the energy absorbed by the collector was modelled in TRNSYS studio as a function of the design parameters.

Finally, the mechanism of heat transfer within the oven chamber and the heat loss to ambient air was modelled in EES. The model therefore calculates the temperature of the different components of the system after a time interval specified in the EES codes.

Optimisation of the system was carried out based on long term solar data for Zaria latitude 11.2^{o}N and longitude 7.8^{o} E) by:

i. Determining the collector slope and reflector tilts required for optimum interception of solar radiation.

ii. Continuously varying the collector design parameters (Area and insulation thickness) until a desired outcome was observed.

A summary of the tilt angles of reflectors R_1, R_2 and collector obtained for optimum collection of solar energy is given in table 5.1. The optimum collector area and insulation thickness based on the design month (August) was found to be $0.49m^2$ and 0.1m respectively.

The designed components of the oven were carefully constructed using available methods and materials. The system was coupled and tested in the workshop of mechanical engineering department of Ahmadu Bello University, Zaria. The oven model was also simulated for the days on which the tests were performed. The results were analysed and the performance of the oven was evaluated using the ASAE standard. A cost evaluation of the system was carried out.

5.2 CONCLUSIONS

The modelling, simulation, optimisation, construction and testing of a solar box oven with plane reflectors were carried out and the following outcomes were obtained.

i. Monthly optimum tilt angles for the collector and reflectors.

ii. The optimum collector area and insulation thickness, based on a stagnation temperature of $100^{\circ}C$ were $0.49m^2$ and 0.12m respectively.

iii. The solar oven was tested and simulated in accordance to the ASAE standard. The regression line for the experiment and simulation was obtained and used to compute

the cooking power of the oven. The experimental and simulated cooking powers are 84W and 75W respectively.

iv. The test results were used to analyse the predictive power of the solar oven model with the aid of the RMSE and NSE statistical tools. The RMSE values were 8.75°C and 5.72°C, while the NSE values were 0.6 and 0.85 for the stagnation temperature test and sensible heat test respectively. The results show little deviation of predicted values from actual values and also a good level of fit, thereby validating the model used for simulating the solar oven.

5.3 RECOMMENDATIONS

The following recommendations would help to improve and ease further research in solar oven design and construction:

1. Alternative methods of heat retention in the collector should be explored. Most of the heat is lost by convection from the glass cover. Top loss from the collector could be reduced by using multiple glazings. The side and bottom loss could also be reduced by using alternative insulating materials.
2. Tracking devices could be used to enhance solar radiation collection. Solar panels may be used to power such devices.
3. Alternative construction materials should be explored with a view to reducing the size and weight of the oven for easy handling and transportation.
4. The use of various oven cavity geometries should be investigated in collector design, in order to study the effect of various geometries on the performance.

References

Abdulrahim A. T., Diso I. S.,and Oumarou M. B. (2011). Development Of A Solar Tracking Bi-Focal Collectors. Continental J. *Renewable Energy 2 (2): 19 – 33.* Retrieved June 2013 from http://www.wiloludjournal.com/../135

A.S.A.E. S580, testing and reporting solar cooker performance (2003). American society of Agricultural Engineers. Retrieved March 2014 from http://solarcooking.org/asae_test_std.pdf.

Balogun O.A (2006). Design and Construction of a Solar Box Oven. Unpublished Undergraduate Project, Department of Mechanical Engineering, Ahmadu Bello University, Zaria.

Dasin D. Y., Asere A. A. and Habou D. (2011). Parabolic Solar Cooker Dish: Design And Simulation. Nigeria Journal of Solar Energy, Vol. 22, 52-61.

Duffie J. A. and Beckman W. A. (2001). Solar engineering of thermal processes. JohnWiley and Sons, New York.

Ekechukwu O.V. (2001). Design And Measured Performances Of A Plane Reflector Augmented Box-Type Solar-Energy Cooker. Department of Mechanical Engineering, University of Nigeria, Nsukka, Nigeria.

Essam A. Mohammed A., Ali A., and Salah A. (2010). Cylindrical Solar Cooker with Automatic Two Axes Sun Tracking System. *Jordan Journal of Mechanical and Industrial Engineering. Vol 4, No 4,. 477-486*. Retrieved April 2012 from http://jjmie.hu.jo/files/v4n4/jjmie-43...

Etiosa U., Mattew A. And Agharese E. (2008). National dialogue to Promote Renewable Energy and Energy Efficiency in Nigeria. *TheReport of a national dialogue to promote renewable energy and energy efficiency in Nigeria.Parkview Hotels, Abuja.*

Fayadh M. Abed (2011). Experimental Investigation of Thermal Performance of Solar Cooker with Reflector. Mechanical Department, College of Engineering University of Tikrit, Tikrit, Iraq. Retrieved june 2013 from http://www.eurojournals.com

Garg H.P. and Prakash J. (2000). Solar Energy: Fundamentals and applications. Tata McGraw-Hill Education.

Gwani A (2010). Design, Fabrication, and Testing of Solar Cooker. Unpublished Undergraduate Project, Department of Mechanical Engineering, Ahmadu Bello University, Zaria.

Harnessing the sun to benefit people and the environment. (2012, January 13). Retrieved from http://www.solarcookers.org.

Huseyn O.H, Serder O and Ali B (2010). Evaluation of efficiency for solar cooker using energy and exergy analyses. Retrieved April 2012 from http://www.tslcalgary.com/exergy1.html

Ishan P., Pallav P., and Negi B. (2007). Instrumentation error analysis of a box type solar cooker. *Energy conversion and management, 50(2), 365-375.* Retrieved June 2012 from http://www.solar cooking.wikia.com/wiki/pallav

Julien G. A, Emmanuel L., Clément A., Rufin O. A., & Brice A. S. (2013). Modelling solar energy transfer through roof material in Africa Sub-Saharan Regions. *ISRN Renewable Energy 34(7), 632-645* .

Kalogirou S.A (2004). Solar thermal collectors and applications. *Progress in Energy and Combustion Science 30 (2004) 231–295*. Retrieved April 2012 from http://serials.unibo.it/cgi-ser/start/en

Kimambo C.Z (2007). Development and performance testing of solar cookers. Department of Energy, University of Dar es Salaam, Tanzania. Retrieved May 2013 http://www.erc.uct.ac.za/jesa/volume18/18

Mahavar S., Sengar N., Rajawat P., Verma M., and Dashora P., (2012). Design development and performance studies of a novel single family solar cooker. *Renewable energy 47, 67-76.* Retrieved December 19, 2013 from www.elsevier.com/locate/renene.

Nahar N. M. (2009) Design and Development of a Large Size Non-tracking Solar Cooker. *Journal of Engineering Science and Technology Vol. 4, No. 3. 264 – 271*. Retrieved july 2013 from http://jestec.taylors.edu.my/vol%25204%252.

Neil, J. S. (2010).*Encyclopedia of Research Design*. Online ISBN**:** 9781412961288 | Publisher**:**SAGE Publications, Inc.

Oleg D. and Ralph C. (1999). Trends in Consumption and Production: Household energy consumption. *Discussion Paper of the United Nations Department of Economic and social affairs ET/ESA/1999/DP. 6*. Retrieved November 2012 from http://sustainabledevelopment.un.org/index

Ogumwole O.A (2006). Flat Plate Collector Solar Cooker. Department of Mechanical Engineering, Federal University of Technology Minna, Niger State, Nigeria

Pejack E. (2003). Solar cooker technology. Retrieved from http://www.static2.wikia.nocookie.net/_cb2007

Popoola O.I., and Ayanda J.D. (2005). Design Construction and Study of the Performance of a Conical Solar Concentrator. Nigerian journal of physics. 17(5). 275-284

Rakesh K., Kaushik S.C., and Garg H.P. (1994). Analytical study of collector solar gain enhancement by multiple reflectors. Centre for energy studies, Indian institute of technology, India. Retrieved November 2012 from http://eprint.iitd.ac.in/../kumana95.pdf.

Sanusi Y.S., Suleiman R.B.O and Amber I. (2011). Estimation of global solar radiation on the horizontal surface for Zaria, Northern Nigeria. Nigeria Journal of Solar Energy Vol 22, 71-78

Suleiman R.B.O (2011). Modelling and simulation of a solar powered absorption refrigeration system (PhD thesis). Department of Mechanical Engineering, Ahmadu Bello University, Zaria.

Shawn Shaw (2003). Development of a Comparative Framework for Evaluating the Performance of Solar Cooking Devices. Retrieved April 2012 from http://solarcooking.org/evaluating-solar-cookers.doc

Sambo A.S (2009). Strategic Developments In Renewable Energy In Nigeria. International Association for Energy Economics 3rd quarter 2009.

Taura L. S. and Musa A.O (2012). Design, Construction, and Testing of a Single-Glazed SolarCooker for Two Weather Situations. *European journal of scientific research, 73(4), 489-496*. Retrieved April 2012 from http://www.europeanjournalofscientificresearch.com

TemiladeSesan (2008). Status of Renewable Energy Policy and Implementation in Nigeria. Institute for Science and Society, University of Nottingham, United Kingdom. Retrieved May 2012 from http://www.gbengasesan.com/temidocs/repstatusnigeria.pdf

Uhuegbu C.C (2011). Design and Construction of a Wooden Solar Box Cooker with Performance and Efficiency Test. Department of Physics, Covenant University Ota Nigeria.

APPENDIX A

FLOW CHART FOR THE OVEN BOX OPTIMISATION PROCESS

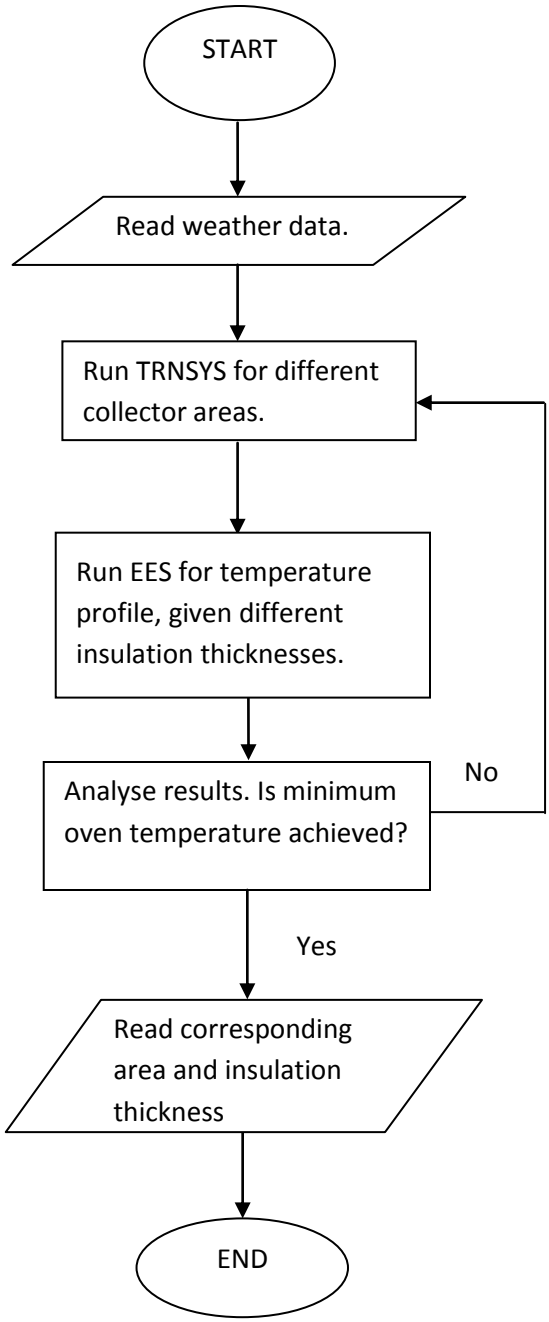

APPENDIX B

TRNSYS DECK FILE: ENERGY ABSORBED BY SOLAR OVEN

```
VERSION 16.1
**********************************************************************
*
*** TRNSYS input file (deck) generated by TrnsysStudio
*** on Saturday, August 09, 2014 at 10:27
*** fromTrnsysStudio project:
C:\Users\SHEIK\AppData\Local\VirtualStore\Program
Files\Trnsys16_1\MyProjects\Project12\Project12.tpf
***
*** If you edit this file, use the File/Import TRNSYS Input File function in
*** TrnsysStudio to update the project.
***
*** If you have problems, questions or suggestions please contact your local
*** TRNSYS distributor or mailto:software@cstb.fr
*** Units
*** Control cards
**********************************************************************
* START, STOP and STEP
CONSTANTS 3
START=2256
STOP=2280
STEP=0.016666666
* User defined CONSTANTS

SIMULATION   START       STOP  STEP ! Start time      End time    Time step
TOLERANCES 0.001 0.001             ! Integration      Convergence
LIMITS 30 30 30                    ! Max iterations  Max warnings      Trace
limit
DFQ 1                         ! TRNSYS numerical integration solver method
WIDTH 80                      ! TRNSYS output file width, number of characters
LIST                          ! NOLIST statement
                              ! MAP statement
SOLVER 0 1 1                        ! Solver statement      Minimum relaxation
factor      Maximum relaxation factor
```

```
NAN_CHECK 0                    ! Nan DEBUG statement
OVERWRITE_CHECK 0              ! Overwrite DEBUG statement
TIME_REPORT 0                  ! disable time report
EQSOLVER 0                     ! EQUATION SOLVER statement

* EQUATIONS "Tilt angles"
*
EQUATIONS 5
gamma_r2 = [5,11]+180
beta_c = 30
beta_r1 = 100
beta_r2 = 30
a = 1
*$UNIT_NAME Tilt angles
*$LAYER Main
*$POSITION 263 488
*------------------------------------------------------------------------------
-
* Model "Exchange factor" (Type 62)
*
UNIT 3 TYPE 62     Exchange factor
*$UNIT_NAME Exchange factor
*$MODEL .\Utility\Calling External Programs\Excel\Type62.tmf
*$POSITION 451 420
*$LAYER Main #
PARAMETERS 4
0           ! 1 Mode
8           ! 2 Nb of inputs
4           ! 3 Nb of outputs
1           ! 4 Show Excel
INPUTS 8
6,11        ! Zaria weather-2:solar azimuth angle ->input-1
a           ! Tilt angles:a ->input-2
6,22        ! Zaria weather-2:angle of incidence for tilted surface -1 -
>input-3
6,34        ! Zaria weather-2:angle of incidence for tilted surface -3 -
>input-4
6,10        ! Zaria weather-2:solar zenith angle ->input-5
```

```
6,23        ! Zaria weather-2:slope of tilted surface-1 ->input-6
6,29        ! Zaria weather-2:slope of tilted surface-2 ->input-7
6,35        ! Zaria weather-2:slope of tilted surface-3 ->input-8
*** INITIAL INPUT VALUES
0 0 0 0 0 0 0 0
LABELS 1
"C:\Users\SHEIK\Desktop\facing north.xls"
*------------------------------------------------------------------------------
-
* Model "Shading factor" (Type 62)
*
UNIT 4 TYPE 62     Shading factor
*$UNIT_NAME Shading factor
*$MODEL .\Utility\Calling External Programs\Excel\Type62.tmf
*$POSITION 457 207
*$LAYER Main #
PARAMETERS 4
0           ! 1 Mode
8           ! 2 Nb of inputs
4           ! 3 Nb of outputs
1           ! 4 Show Excel
INPUTS 8
6,11        ! Zaria weather-2:solar azimuth angle ->input-1
a           ! Tilt angles:a ->input-2
6,28        ! Zaria weather-2:angle of incidence for tilted surface -2 -
>input-3
0,0         ! [unconnected] input-4
6,10        ! Zaria weather-2:solar zenith angle ->input-5
6,23        ! Zaria weather-2:slope of tilted surface-1 ->input-6
6,29        ! Zaria weather-2:slope of tilted surface-2 ->input-7
6,35        ! Zaria weather-2:slope of tilted surface-3 ->input-8
*** INITIAL INPUT VALUES
0 0 0 0 0 0 0 0
LABELS 1
"C:\Users\SHEIK\Desktop\facing south.xls"
*------------------------------------------------------------------------------
-
* Model "Zaria weather" (Type 109)
```

```
*
UNIT 5 TYPE 109    Zaria weather
*$UNIT_NAME Zaria weather
*$MODEL .\Weather Data Reading and Processing\Standard Format\TMY2\Type109-
TMY2.tmf
*$POSITION 188 296
*$LAYER Main #
PARAMETERS 4
2           ! 1 Data Reader Mode
36          ! 2 Logical unit
4           ! 3 Sky model for diffuse radiation
1           ! 4 Tracking mode
INPUTS 3
0,0         ! [unconnected] Ground reflectance
0,0         ! [unconnected] Slope of surface
0,0         ! [unconnected] Azimuth of surface
*** INITIAL INPUT VALUES
0.2 30 0.0
*** External files
ASSIGN "C:\Users\SHEIK\Desktop\Solar Oven\SOLAR
LIB\Zaria_Nigeria_SPtMasterTable_472122_19790101_20100101_tmy2.tm2" 36
*|? Weather data file |1000
*------------------------------------------------------------------------
* Model "Zaria weather-2" (Type 109)
*
UNIT 6 TYPE 109    Zaria weather-2
*$UNIT_NAME Zaria weather-2
*$MODEL .\Weather Data Reading and Processing\Standard Format\TMY2\Type109-
TMY2.tmf
*$POSITION 332 307
*$LAYER Main #
PARAMETERS 4
2           ! 1 Data Reader Mode
37          ! 2 Logical unit
4           ! 3 Sky model for diffuse radiation
1           ! 4 Tracking mode
INPUTS 7
0,0         ! [unconnected] Ground reflectance
```

```
beta_r1           ! Tilt angles:beta_r1 ->Slope of surface-1
5,11        ! Zaria weather:solar azimuth angle ->Azimuth of surface-1
beta_c            ! Tilt angles:beta_c ->Slope of surface-2
5,11        ! Zaria weather:solar azimuth angle ->Azimuth of surface-2
beta_r2           ! Tilt angles:beta_r2 ->Slope of surface-3
gamma_r2          ! Tilt angles:gamma_r2 ->Azimuth of surface-3
*** INITIAL INPUT VALUES
0.2 0.0 0.0 0.0 0.0 0.0 0.0
*** External files
ASSIGN "C:\Users\SHEIK\Desktop\Solar Oven\SOLAR
LIB\Zaria_Nigeria_SPtMasterTable_472122_19790101_20100101_tmy2.tm2" 37
*|? Weather data file |1000
*------------------------------------------------------------------------------
* EQUATIONS "Absorbed energy"
*
EQUATIONS 16
alpha_eff = alpha_i/(alpha_i+(1+alpha_i)*[9,7]*A_c/A_sb)
alpha_i = 0.93*alpha_n
alpha_n = 0.9
I_r1 = [6,19]*cos([3,1])*[3,3]
I_r2 = [6,31]*cos([3,2])*[3,4]
rho = 0.9
A_c = a*a
A_sb = A_c+4*a*d
Trc1 = [3,1]
Trc2 = [3,2]
Tc = [6,28]
I_tc = [6,24]*(1000/3600)*A_c
d = 0.3
Q_ab = A_c*(1-
S_c)*([6,24]*[9,5]*alpha_eff+rho*([6,19]*[8,6]*alpha_eff*[3,3]*cos([3,1])+[6,3
1]*[10,6]*alpha_eff*[3,4]*cos([3,2])))*(1000/3600)
S_c = [4,1]+[4,2]
T_amb = [6,1]
*$UNIT_NAME Absorbed energy
*$LAYER Main
*$POSITION 558 306
*------------------------------------------------------------------------------
```

```
* Model "theta_rc1" (Type 35)
*
UNIT 8 TYPE 35     theta_rc1
*$UNIT_NAME theta_rc1
*$MODEL .\Loads and Structures\Window\Theoretical\Type35b.tmf
*$POSITION 590 189
*$LAYER Main #
PARAMETERS 5
2           ! 1 Window mode
1.50        ! 2 Area
1           ! 3 Number of glazings
0.037       ! 4 Extinction
1.526       ! 5 Refractive index
INPUTS 6
0,0         ! [unconnected] Room temperature
0,0         ! [unconnected] Ambient temperature
0,0         ! [unconnected] Loss coefficient
I_r1        ! Absorbed energy:I_r1 ->Total solar radiation
I_r1        ! Absorbed energy:I_r1 ->Beam radiation
Trc1        ! Absorbed energy:Trc1 ->Incidence angle
*** INITIAL INPUT VALUES
22.0 10.0 3.0 0.0 0.0 20.0
*------------------------------------------------------------------------------
* Model "theta_c" (Type 35)
*
UNIT 9 TYPE 35    theta_c
*$UNIT_NAME theta_c
*$MODEL .\Loads and Structures\Window\Theoretical\Type35b.tmf
*$POSITION 713 189
*$LAYER Main #
PARAMETERS 5
2           ! 1 Window mode
1.50        ! 2 Area
1           ! 3 Number of glazings
0.037       ! 4 Extinction
1.526       ! 5 Refractive index
INPUTS 6
0,0         ! [unconnected] Room temperature
```

```
0,0         ! [unconnected] Ambient temperature
0,0         ! [unconnected] Loss coefficient
I_tc        ! Absorbed energy:I_tc ->Total solar radiation
0,0         ! [unconnected] Beam radiation
Tc          ! Absorbed energy:Tc ->Incidence angle
*** INITIAL INPUT VALUES
22.0 10.0 3.0 0.0 0.0 20.0
*-------------------------------------------------------------------------
* Model "theta_rc2-2" (Type 35)
*
UNIT 10 TYPE 35    theta_rc2-2
*$UNIT_NAME theta_rc2-2
*$MODEL .\Loads and Structures\Window\Theoretical\Type35b.tmf
*$POSITION 813 184
*$LAYER Main #
PARAMETERS 5
2           ! 1 Window mode
1.50        ! 2 Area
1           ! 3 Number of glazings
0.037       ! 4 Extinction
1.526       ! 5 Refractive index
INPUTS 6
0,0         ! [unconnected] Room temperature
0,0         ! [unconnected] Ambient temperature
0,0         ! [unconnected] Loss coefficient
I_r2        ! Absorbed energy:I_r2 ->Total solar radiation
I_r2        ! Absorbed energy:I_r2 ->Beam radiation
Trc2        ! Absorbed energy:Trc2 ->Incidence angle
*** INITIAL INPUT VALUES
22.0 10.0 3.0 0.0 0.0 20.0
*-------------------------------------------------------------------------
* Model "Type55" (Type 55)
*
UNIT 11 TYPE 55    Type55
*$UNIT_NAME Type55
*$MODEL .\Utility\Integrators\Periodic Integrator\Type55.tmf
*$POSITION 684 307
*$LAYER Main #
```

```
PARAMETERS 21
1           ! 1 Integrate or sum input-1
8           ! 2 Relative starting hour for input-1
9           ! 3 Duration for input-1
24          ! 4 Cycle repeat time for input-1
0.016667          ! 5 Reset time for input-1
0           ! 6 Absolute starting hour for input-1
8760        ! 7 Absolute stopping hour for input -1
1           ! 8 Integrate or sum input-2
8           ! 9 Relative starting hour for input-2
9           ! 10 Duration for input-2
24          ! 11 Cycle repeat time for input-2
0.016667          ! 12 Reset time for input-2
0           ! 13 Absolute starting hour for input-2
8760        ! 14 Absolute stopping hour for input -2
1           ! 15 Integrate or sum input-3
8           ! 16 Relative starting hour for input-3
9           ! 17 Duration for input-3
24          ! 18 Cycle repeat time for input-3
0.016667          ! 19 Reset time for input-3
0           ! 20 Absolute starting hour for input-3
8760        ! 21 Absolute stopping hour for input -3
INPUTS 3
Q_ab        ! Absorbed energy:Q_ab ->Input-1
I_tc        ! Absorbed energy:I_tc ->Input-2
T_amb       ! Absorbed energy:T_amb ->Input-3
*** INITIAL INPUT VALUES
0. 0. 0.
*-------------------------------------------------------------------------------
* Model "Type25c" (Type 25)
*
UNIT 12 TYPE 25    Type25c
*$UNIT_NAME Type25c
*$MODEL .\Output\Printer\Unformatted\No Units\Type25c.tmf
*$POSITION 684 136
*$LAYER Main #
PARAMETERS 10
0.016667          ! 1 Printing interval
```

```
2265        ! 2 Start time
2271        ! 3 Stop time
38          ! 4 Logical unit
0           ! 5 Units printing mode
0           ! 6 Relative or absolute start time
-1          ! 7 Overwrite or Append
-1          ! 8 Print header
0           ! 9 Delimiter
1           ! 10 Print labels
INPUTS 5
beta_r1           ! Tilt angles:beta_r1 ->Input to be printed-1
beta_r2           ! Tilt angles:beta_r2 ->Input to be printed-2
11,3        ! Type55:Mean value of input-1 ->Input to be printed-3
11,13       ! Type55:Mean value of input-2 ->Input to be printed-4
11,23       ! Type55:Mean value of input-3 ->Input to be printed-5
*** INITIAL INPUT VALUES
beta_r1 beta_r2 Q_abI_cT_a
*** External files
ASSIGN "C:\Users\SHEIK\Desktop\Solar Oven\New folder\TOTAL1.txt" 38
*|? Output file for printed results |1000
*-------------------------------------------------------------------------------
END
```

APPENDIX C

ASSEMBLY AND WORKING DRAWINGS

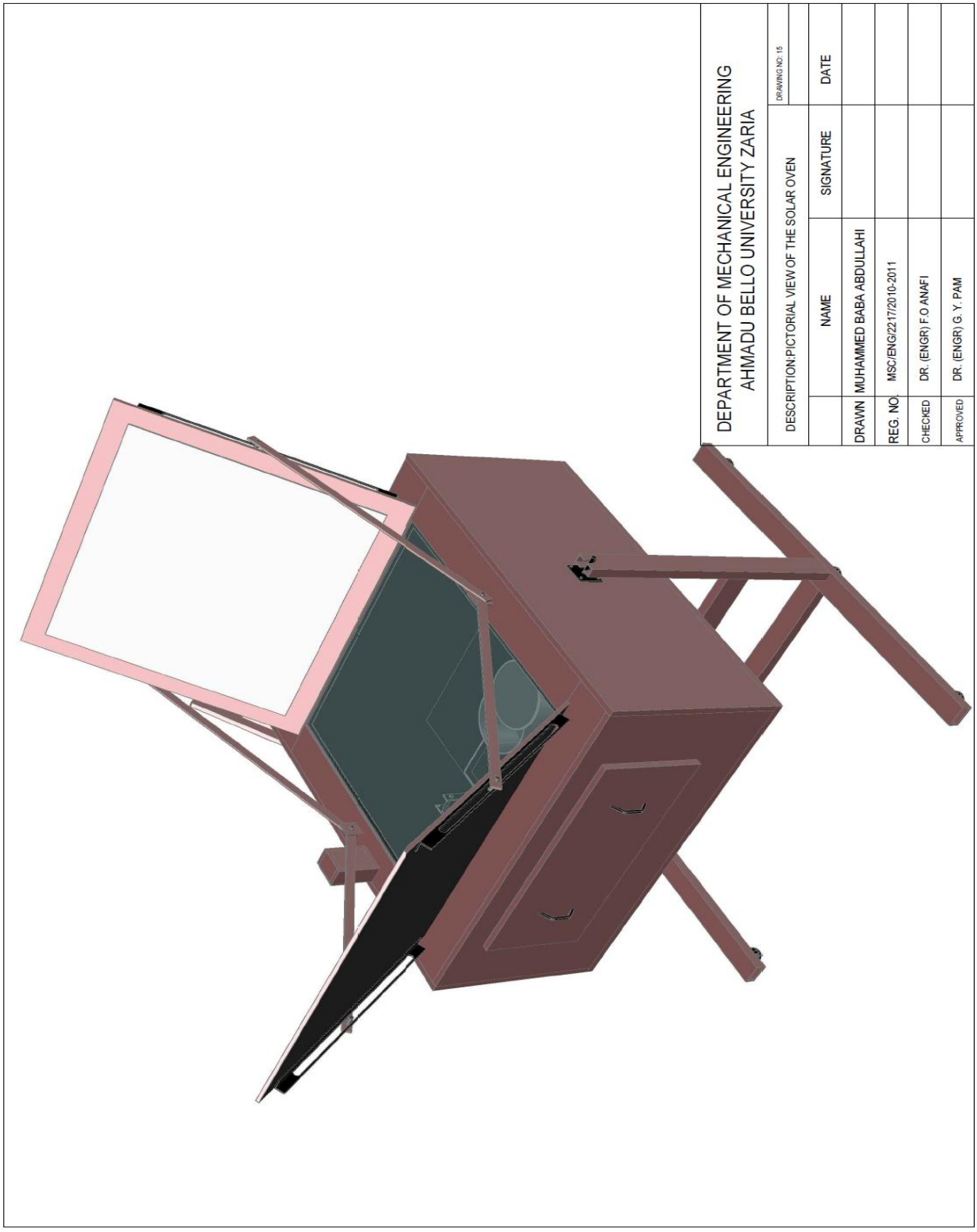

APPENDIX D

PICTURES OF THE SOLAR OVEN BOX

D1Thermocouple wires attached to glazing, Levelling tray and pot

D2 Pyranometer placed on collector

D3 Output meters for reading temperatures, and incident radiation.

D4 Overall set up with anemometer

APPENDIX E

(A) EES CODE: EVALUATION OF SOLAR OVEN TEMPERATURES

```
"Raleigh number (air)"
FUNCTION RA(T_s,T_infinity,L_x)

        T_fl=(T_s+T_infinity)/2

        beta=1/(T_fl+273)

        G_r=(L_x^3*9.81*beta*(DENSITY(Air,T=T_fl,P=101.320))^2*(T_s-
T_infinity))/(VISCOSITY(Air,T=T_fl))^2

        P_r=(CP(Air,T=T_fl)*1000*VISCOSITY(Air,T=T_fl))/CONDUCTIVITY(Air,T=T_fl)

        R_a=G_r*P_r

        RA=R_a
END RA

"Raliegh number (water)"

FUNCTION RA_w(T_s,T_infinity,L_x)

        T_fl=(T_s+T_infinity)/2

        beta=1/(T_fl+273)
```

```
        G_r=(L_x^3*9.81*beta*(DENSITY(Water,T=T_fl,P=101.320))^2*(T_s-
T_infinity))/(VISCOSITY(Water,T=T_fl,P=101.320))^2

        P_r=(CP(Water,T=T_fl,P=101.320)*1000*VISCOSITY(Water,T=T_fl,P=101.320))/CONDUCTIVITY
(Water,T=T_fl,P=101.320)

        R_a=G_r*P_r

        RA_w=R_a
END RA_w

FUNCTION TEMP(row, T_abt)
        IF row=1 then T_as:=T_abt ELSE T_as=TableValue('Table 1',row-1,2)
        TEMP:=T_as
END

"Temperature of water"
T_io_old=TEMP(row, T_a)

row=Time/delta+1

delta=600

"HEAT BALANCE EQUATIONS"

U_t*(T_a-T_c)+h_r*(T_p-T_c)+h_a*(T_io-T_c)=0  "cover"

A_c*S+A_sb*U_sb*(T_a-T_p)+(A_sb*h_a)*(T_io-T_p)+A_c*h_r*(T_c-T_p)=0 "absorber"
```

A_c*h_a*(T_c-T_io)+(A_sb*h_a)*(T_p-T_io)+0.24*h_t*(T_t-T_io)+0.12426*h_pt*(T_pt-T_io)=0 "air"

0.24*h_t*(T_io-T_t)+6300*(T_pt-T_t)=0 "tray"

6300*(T_t-T_pt)+0.12426*h_pt*(T_io-T_pt)+0.06*h_wt*(T_f-T_pt)=0 "pot"

q_u=0.06*h_wt*(T_pt-T_f) "water"

q_u=m*c*(T_f-T_io_old)/t

t=600;

“Area of side and bottom”

A_sb=A_c+4*d*sqrt(A_c);

m=1.5; c=4190;A_c=0.49;d=0.3;

"Convective heat transfer coefficient of water (h_wt)"

N_u_wt=0.68+0.67*R_a_wt^(1/4)/(1+(0.492/P_r_wt)^(9/16))^(4/9)

P_r_wt=(CP(Water,T=(T_f+T_io)/2,P=101.320)*1000*VISCOSITY(Water,T=T_f,P=101.320))/CONDUCTIV
ITY(Water,T=T_f,P=101.320)

R_a_wt=RA_w(T_io,T_f,0.3)

h_wt=N_u_wt*CONDUCTIVITY(Water,T=T_f,P=101.320)/0.3

"Convective heat transfer coefficient of air (h_a)"

N_u_a=0.52*(RA_a)^(1/4)

h_a=(N_u_a*CONDUCTIVITY(Air,T=T_io))/1.3

"h_a=(0.061*CONDUCTIVITY(Air,T=T_io)*(RA_a)^(1/3))/d"

RA_a=RA(T_p,T_io,1.3)

"Radiative heat transfer coefficient of air (h_r)"

h_r=(4*sigma#*(T_io+273)^3)/((1/e_1)+(1/e_2)-1)

e_1=0.88; e_2=0.95;

"Radiation coefficient of cover to air (h_c_r_a)"

h_r_c_a=e_1*sigma#*((T_c+273)^2+(T_a+273)^2)*(T_c+T_a+546)

"Wind heat transfer coefficient (h_w)"

h_w=5.7+3.8*V

" Top loss coefficient (U_t)"

U_t=h_w+h_r_c_a ; V=0.2

" Side and bottom loss coefficient (U_sb)"

U_sb=1/(x_1/k_1+x_i/k_i+x_2/k_2)

"Convective heat transfer coefficient of tray (h_t)"

N_u_t=0.52*(RA_t)^(1/4)

h_t=(N_u_t*CONDUCTIVITY(Air,T=T_io))/0.6

"h_a=(0.061*CONDUCTIVITY(Air,T=T_io)*(RA_a)^(1/3))/d"

RA_t=RA(T_io,T_t,0.6)

"Convective heat transfer coefficient of pot (h_pt)"

```
N_u_pt=0.52*(RA_pt)^(1/4)
h_pt=(N_u_pt*CONDUCTIVITY(Air,T=T_io))/0.1
"h_a=(0.061*CONDUCTIVITY(Air,T=T_io)*(RA_a)^(1/3))/d"
RA_pt=RA(T_io,T_pt,0.1)

x_1=0.015; x_2=0.015; x_i=0.1; k_1=0.2; k_2=0.2; k_i=0.06
```

(B) EES SIMULATION CODE: DETREMINATION OF RMSE AND NSE

```
N=35

DUPLICATE i=1,N                    {Set T_sim[i] and T_exp[i] to values in Lookup table}
T_sim[i]=lookup(i,#T_sim)
T_exp[i]=lookup(i,#T_exp)
END
sigma=sqrt(sum((T_sim[i]-T_exp[i])^2,i=1,N)/N)   {sigma is the Root mean square error(RMSE)}

A=sum((T_exp[i]-T_sim[i])^2,i=1,N)

B=sum((T_exp[i]-(AvgLookup('Lookup 1','T_exp')))^2,i=1,N)

C=AvgLookup('Lookup 1','T_exp')

alpha=1-(A/B)       {alpha is the Sutcliffe Coefficient of Efficiency (NSE) }
```

APPENDIX F

EXPERIMENTAL AND SIMULATION RESULTS

Table1. Experimental results of 5th April, 2014 with corresponding values of the temperature difference and standardised power for each interval.

TIME	T_w (C)	T_a (C)	T_d (C)	P_s (W)
9:00am	45	29	16	170.8
9:10am	58	29	29	132.7
9:20am	69	30	39	106.7
9:30am	78	30	48	82.74
9:40am	85	30	55	64.48
9:50am	91	31	60	52.58
10:00am	50	31	19	169.9
10:10am	64	32	32	131.5
10:20am	75	33	42	102.7
10:30am	83	33	50	74.16
10:40am	90	33	57	58.76
10:50am	54	35	19	168
11:00am	68	34	34	125.7
11:10am	79	37	42	100.6
11:20am	88	38	50	78.17
11:30am	95	39	56	62.89

TIME	T_w (C)	T_a (C)	T_d (C)	P_s (W)
11:40am	56	38	18	172.3
11:50am	73	38	35	130.4
12:00noon	84	38	47	97.21
12:10pm	94	37	57	74.8
12:20pm	56	38	18	172.4
12:30pm	72	37	35	129.3
12:40pm	85	38	47	99.71
12:50pm	94	38	56	74.04
1:00pm	56	38	18	172.4
1:10pm	72	38	34	130.3
1:20pm	83	38	45	95.03
1:30pm	92	39	53	76.38
1:40pm	56	39	17	174
1:50pm	74	39	35	134.1
2:00pm	87	41	46	101.7
2:10pm	96	41	55	75.94

Table 2. Simulation results of 5th April, 2014 with corresponding values of the temperature difference and standardised power for each interval.

TIME	T_w (C)	T_a (C)	T_d (C)	P_s (W)
9:00am	37.62	27.9	9.719	169.7
9:10am	47.21	28.5	18.71	141.1
9:20am	56.57	29.1	27.47	119.3
9:30am	65.32	29.7	35.62	100.5
9:40am	73.14	30.3	42.84	84.01
9:50am	80.04	31	49.04	70.48
10:00am	86.23	31.7	54.53	60.11
10:10am	91.8	32.5	59.3	51.79
10:20am	52.36	33.5	18.86	168.7
10:30am	67.54	34.6	32.94	131.4
10:40am	79.5	35.7	43.8	102.2
10:50am	88.84	36.7	52.14	79.49
11:00am	96.15	37.7	58.45	62.06
11:10am	55.45	38.6	16.85	173.6
11:20am	71.12	39.5	31.62	133.1
11:30am	83.14	40.4	42.74	102.2
11:40am	92.32	41.2	51.12	78.47
11:50am	55.46	40	15.46	175.9

TIME	T_w (C)	T_a (C)	T_d (C)	P_s (W)
12:00noon	70.85	40	30.85	133.4
12:10pm	82.54	41	41.54	102.3
12:20pm	91.25	41	50.25	77.02
12:30pm	54.87	41	13.87	177.9
12:40pm	69.73	41	28.73	135.1
12:50pm	80.75	41	39.75	101.9
1:00pm	88.6	41	47.6	75.17
1:10pm	94.32	41	53.32	55.93
1:20pm	52.55	40	12.55	177.3
1:30pm	65.96	40	25.96	135.8
1:40pm	76.89	41	35.89	107.4
1:50pm	85.63	41.2	44.43	84.04
2:00pm	93.08	41.1	51.98	68.15
2:10pm	54.75	41.1	13.65	178.1
2:20pm	69.75	41.2	28.55	135.7
2:30pm	81.34	41.3	40.04	103.9
2:40pm	90.27	41.3	48.97	79.53

Table3. Experimental and simulation results of stagnation temperature test (3rd April 2014).

TIME	$T_{io(Exp)}$ (C)	$T_{io(Sim)}$ (C)	TIME	$T_{io(Exp)}$ (C)	$T_{io(Sim)}$ (C)
9:00am	78	75.76	12:10pm	123	123
9:10am	83	87.92	12:20pm	121	122.2
9:20am	90	96.44	12:30pm	106	121.3
9:30am	106	103.3	12:40pm	118	120.3
9:40am	111	107.9	12:50pm	122	119
9:50am	108	111.9	1:00pm	125	117.4
10:00am	113	115.6	1:10pm	123	116.9
10:10am	114	118.9	1:20pm	123	115.2
10:20am	118	121.2	1:30pm	118	114.9
10:30am	111	123.7	1:40pm	125	116.4
10:40am	112	125.2	1:50pm	133	118.6
10:50am	113	125.6	2:00pm	133	119
11:00am	109	125.7	2:10pm	132	119.8
11:10am	106	125.7	2:20pm	135	120.5
11:20am	113	125.6	2:30pm	133	121.1
11:30am	115	125.3	2:40pm	129	121.4
11:40am	118	124.9	2:50pm	134	121.6
11:50am	121	124.4	3:00pm	131	121.6
12:00noon	123	123.7			